

**BIOCOMPOSITE FROM POLY(LACTIC ACID)
AND OIL PALM EMPTY FRUIT BUNCH/
COTTON HYBRID FIBERS**



**A Thesis Submitted in Partial Fulfillment of the Requirements for the
Degree of Master of Engineering in Polymer Engineering
Suranaree University of Technology
Academic Year 2011**

พอลิเมอร์เชิงประกอบชีวภาพจากพอลิแลคติกแอซิด และ เส้นใยผสมระหว่าง
เส้นใยเปลือกผลปาล์มน้ำมันกับเส้นใยฝ้าย



วิทยานิพนธ์นี้เป็นส่วนหนึ่งของการศึกษาตามหลักสูตรปริญญาวิศวกรรมศาสตรมหาบัณฑิต
สาขาวิชาวิศวกรรมพอลิเมอร์
มหาวิทยาลัยเทคโนโลยีสุรนารี
ปีการศึกษา 2554

**BIOCOMPOSITE FROM POLY(LACTIC ACID) AND OIL PALM
EMPTY FRUIT BUNCH/COTTON HYBRID FIBERS**

Suranaree University of Technology has approved this thesis submitted in partial fulfillments of the requirement for a Master's Degree.

Thesis Examining Committee

Nitinat Suppakarn

(Asst. Prof. Dr. Nitinat Suppakarn)

Chairperson

M. Utai

(Asst. Prof. Dr. Utai Meekum)

Member (Thesis Advisor)

Pranee Chumsamrong

(Asst. Prof. Dr. Pranee Chumsamrong)

Member

Sukit Limpijumnong

(Prof. Dr. Sukit Limpijumnong)

Vice Rector for Academic Affairs

Kontorn Chamniprasart

(Assoc. Prof. Flt. Lt. Dr. Kontorn Chamniprasart)

Dean of Institute of Engineering

พันธทิพย์ กิ่งช้าง : พอลิเมอร์เชิงประกอบชีวภาพจากพอลิแลคติกแอซิด และ เส้นใยผสมระหว่างเส้นใยเปลือกผลปาล์มน้ำมันกับเส้นใยฝ้าย (BIOCOMPOSITE FROM POLY(LACTIC ACID) AND OIL PALM EMPTY FRUIT BUNCH/COTTON HYBRID FIBERS) อาจารย์ที่ปรึกษา : ผู้ช่วยศาสตราจารย์ ดร.อุทัย มีคำ, 177 หน้า.

จากการออกแบบการทดลองเชิงสถิติแบบพหุคูณ(2⁴) ทำให้ได้สูตรเบื้องต้นของพอลิเมอร์เชิงประกอบของพอลิแลคติกแอซิดเสริมแรงด้วยเส้นใยเปลือกผลปาล์มน้ำมัน ในการขยายผลการศึกษาทดลองต่อไปพบว่าพอลิแลคติกแอซิดเสริมแรงด้วยเส้นใยผสมระหว่างเส้นใยฝ้ายกับเส้นใยเปลือกผลปาล์มน้ำมัน ทำให้สมบัติเชิงความร้อน และ สมบัติเชิงกลของพอลิเมอร์เชิงประกอบดีขึ้นได้ แต่ความสามารถทางการไหลจะลดต่ำลงเมื่อเพิ่มปริมาณสัดส่วนเส้นใยฝ้าย โดยที่พอลิเมอร์เชิงประกอบที่เตรียมได้สามารถย่อยสลายตัวเชิงชีวภาพได้ การเติมทาลค์กัมในส่วนผสมพอลิเมอร์เชิงประกอบเพิ่มค่าดัชนีการไหลของพอลิเมอร์เชิงประกอบได้ ผลของความขึ้นคั่งค้างในตัวอย่างจากการอบบ่มไอน้ำ เปรียบเทียบกับชิ้นงานที่อบแห้งในตู้อบสูญญากาศ ไม่มีผลต่อค่าคุณสมบัติของชิ้นงานทดสอบของพอลิเมอร์เชิงประกอบที่เตรียมได้

การเติมระบบสารก่อร่างแหของไวนิลไซเลนกับไดควิมิตเปอร์ออกไซด์ทำให้เกิดโซ่ร่างแหของพอลิแลคติกแอซิด ในพอลิเมอร์เชิงประกอบพบว่าค่าอุณหภูมิการบิดงอเพิ่มขึ้นตามปริมาณของไวนิลไซเลนที่เติมลงไป ส่วนความแข็งแรงเหนียวมีแนวโน้มลดลงเมื่อเพิ่มปริมาณไวนิลไซเลน วิธีการผสมไดควิมิตเปอร์ออกไซด์และไวนิลไซเลน ไปบนยางธรรมชาติดัดแปลงอีพ็อกซิไดซ์จำนวนร้อยละ 50 โดยจำนวนโมล โดยตรง พบว่าจะให้คุณสมบัติของพอลิเมอร์เชิงประกอบที่เตรียมได้ ดีกว่า วิธีการเตรียมสูตรการผสมพอลิเมอร์เชิงประกอบ โดยการคลุกผสมสารก่อร่างแหกับเม็ดพอลิแลคติกแอซิด

จากผลการศึกษาวิจัยทำให้ได้พอลิเมอร์เชิงประกอบของพอลิแลคติกแอซิดเสริมแรงด้วยเส้นใยผสมระหว่างเส้นใยปาล์มน้ำมันกับเส้นใยฝ้ายจำนวน 2 สูตร โดยวัสดุเชิงประกอบทั้ง 2 สูตรนี้จะมีคุณสมบัติที่ดีมาก

สาขาวิชา วิศวกรรมพอลิเมอร์

ปีการศึกษา 2554

ลายมือชื่อนักศึกษา พันธทิพย์ กิ่งช้าง

ลายมือชื่ออาจารย์ที่ปรึกษา [ลายมือ]

PANTIP KINGCHANG : BIOCOMPOSITE FROM POLY(LACTIC ACID)
AND OIL PALM EMPTY FRUIT BUNCH/COTTON HYBRID FIBERS.
THESIS ADVISOR : ASST. PROF. UTAI MEEKUM, Ph.D., 177 PP.

BIOCOMPOSITE/POLY(LACTIC ACID)/OIL PALM EMPTY FRUIT BUNCH/
COTTON/HYBRID FIBERS

The statistical approach, 2^k factorial design of experiment (DOE), initially used to the oil palm empty fruit bunch (EFB)/poly(lactic acid) (PLA) biocomposite formula. Further exploring, cotton and EFB hybrid fibers were employed as reinforcement in the PLA based composite. The thermal and mechanical properties of the material were improved but the flow ability of the material became restriction by increasing the fraction of cotton fiber. The biologically degradability of the hybrid composite was observed. Adding talc into the composite ingredient improved the melt flow index (MFI) of the hybrid biocomposite. For the effect of moisture residual existed in the sample via the sauna incubation, it concluded that there was no differentiate between the normal and vacuum dried samples.

The crosslink system using vinyltrimethoxysilane (VTMS)/dicumyl peroxide (DCP) was introduced into the PLA matrix of the hybrid biocomposite. The heat deflection temperature (HDT) of the sauna cured sample was enhanced by VTMS. The toughness was likely to decrease with increasing the VTMS. Direct incorporating the crosslink agents into the epoxidized natural rubber (ENR50) was given rise to the better properties than adding into the PLA matrix.

According to this research study, two main EFB/cotton hybrid reinforced biocomposite formulae were derived. The biocomposite materials obtained from these two formulae showed the superior properties.



School of Polymer Engineering

Academic Year 2011

Student's Signature Pantip Kingchang

Advisor's Signature M. Utai

ACKNOWLEDGEMENTS

First of all, I would like to express my deep sense of gratitude to my advisor Asst. Prof. Dr.Utai Meekum for his consistent supervision, advice and support throughout this project. In addition, I wish to express my gratitude to Asst. Prof. Dr.Nitinat Suppakarn and Asst. Prof. Dr.Pranee Chumsamrong for their valuable suggestions and guidance given as committee members.

I wish to acknowledgement the financial supports from Center of Excellence on Petrochemical and Materials Technology directly related to my course of study at the Suranaree University of Technology.

The author is also grateful to all the my friends and staffs of the School of Polymer Engineering for their help and assistance throughout the period of this study.

Finally, my graduation will not be accomplish if I do not acquire best chance from my parents who support and encourage in everything throughout my life.

Pantip Kingchang

TABLE OF CONTENTS

	Page
ABSTRACT (THAI)	I
ABSTRACT (ENGLISH)	II
ACKNOWLEDGEMENTS	IV
TABLE OF CONTENTS	V
LIST OF TABLES	X
LIST OF FIGURES	XIV
SYMBOLS AND ABBREVIATIONS	XX
CHAPTER	
I INTRODUCTION	1
1.1 General introduction	1
1.2 Natural fibers and composites	2
1.3 Research objectives	7
1.4 Scope and limitation of the study	7
II LITERATURE REVIEW	8
2.1 Biocomposites	8
2.1.1 Synthetic polymer and natural fibers composites	8
2.1.2 Biopolymer and synthetic fibers composites	10

TABLE OF CONTENTS (Continued)

	Page
2.1.3 Biopolymer and natural fibers composites	11
2.2 Natural fibers treatment	13
2.2.1 Chemical treatment	13
2.2.2 Thermal treatment.....	16
2.3 Toughening of polymer.....	17
2.3.1 Rubber toughened polymer.....	17
2.3.2 Filler toughened polymer.....	18
2.4 Crosslinking of polymer	20
III EXPERIMENTAL.....	26
3.1 Materials	26
3.2 Preparation of fiber	32
3.3 Composite compounding	33
3.4 Specimen preparation.....	34
3.5 Performance testing and characterization	35
3.5.1 Melt flow index (MFI).....	35
3.5.2 Heat deflection temperature (HDT).....	35
3.5.3 Izod impact testing.....	35
3.5.4 Flexural testing.....	36
3.5.5 Morphological properties.....	36
3.5.6 Biodegradability.....	36

TABLE OF CONTENTS (Continued)

	Page
3.6 Analysis of DOE using Design Expert™	37
VI RESULTS AND DISCUSSION	41
4.1 Design of experiment#1: Effect of fiber, silane and solid epoxy	41
4.1.1 The MFI analysis	44
4.1.2 Analysis of HDT	46
4.1.3 Impact strength of biocomposite.....	51
4.1.4 Flexural properties	60
4.1.5 Scanning electron microscopy (SEM)	69
4.2 Effect of solid epoxy on biocomposite	72
4.2.1 MFI of composite versus epoxy contents	75
4.2.2 HDT and epoxy contents	76
4.2.3 Impact strength and epoxy contents.....	76
4.2.4 Flexural properties and epoxy contents	78
4.2.5 Scanning electron microscopy (SEM)	79
4.3 Effect of cotton fiber.....	81
4.3.1 MFI of composite versus cotton fraction.....	84
4.3.2 HDT of composites versus cotton fraction	84
4.3.3 Impact properties and cotton fraction	86
4.3.4 Flexural properties versus cotton fraction.....	87

TABLE OF CONTENTS (Continued)

	Page
4.3.6 Biodegradability testing	91
4.4 Effect of talc.....	93
4.4.1 Flow ability of hybrid composite.....	96
4.4.2 HDT of the talc filled hybrid composite	97
4.4.3 Impact properties of the talc filled hybrid composite.....	98
4.4.4 Flexural properties of the talc filled hybrid composite.....	100
4.4.5 Scanning electron microscopy (SEM)	102
4.5 Design of experiment#2: Hybrid biocomposite from crosslinked PLA using peroxide/silane system.....	104
4.5.1 Flow ability of hybrid biocomposite.....	108
4.5.2 HDT of hybrid biocomposite	109
4.5.3 Impact strengths of hybrid biocomposite.....	114
4.5.4 Flexural properties of hybrid biocomposite.....	123
4.6 Comparison of peroxide/silane ratios and mixing procedures.....	134
4.6.1 Flow ability of hybrid biocomposite versus VTMS contents.....	139
4.6.2 HDT of hybrid biocomposite versus VTMS contents and mixing procedures	141

TABLE OF CONTENTS (Continued)

	Page
4.6.3 Impact properties of hybrid biocomposite versus VTMS contents and mixing procedures	142
4.6.4 Flexural properties of hybrid biocomposite versus VTMS contents and mixing procedures	145
4.6.5 Scanning electron microscopy (SEM)	148
V CONCLUSIONS	151
REFERENCES	154
APPENDICES	
APPENDIX A. CUMULATIVE PROBABILITIES TABLE.....	162
APPENDIX B. PUBLICATION.....	169
BIOGRAPHY	177

LIST OF TABLES

Table	Page
1.1	Properties of natural and synthetic fibers..... 5
3.1	Summarization of materials and their function in biocomposite manufacturing 27
3.2	The properties of the commercial poly(lactic acid) 28
3.3	The properties of the silanes 28
3.4	Proximate chemical composition of EFB and cotton fibers 29
3.5	The properties of solid epoxy resin..... 29
3.6	The properties of polyester polyols..... 30
3.7	The properties of tris(2,4-di-tert-butylphenyl) phosphate 31
3.8	The properties of octadecyl 3-(3,5-di-tert-butyl-4-hydroxyphenyl) propionate 32
3.9	The 2 ³ factorial design matrix..... 38
3.10	Calculation method for the standard effect values..... 40
4.1	The parameters and level for DOE 42
4.2	The 2 ³ factorial design matrix..... 42
4.3	Results of the designed responds 43
4.4	ANOVA results obtained from the MFI 46
4.5	ANOVA results obtained from the HDT (original)..... 49
4.6	ANOVA results obtained from the HDT (cured) 51

LIST OF TABLES (Continued)

Table	Page
4.7 ANOVA results obtained from the notched impact strength (original).....	54
4.8 ANOVA results obtained from the notched impact strength (cured)	55
4.9 ANOVA results obtained from the unnotched impact strength (original).....	57
4.10 ANOVA results obtained from the unnotched impact strength (cured)	59
4.11 ANOVA results obtained from the flexural strength (original).....	62
4.12 ANOVA results obtained from the flexural strength (cured)	64
4.13 ANOVA results obtained from the flexural modulus (original).....	66
4.14 ANOVA results obtained from the flexural modulus (cured)	68
4.15 The predicted regression model of the biocomposite derived from DOE	69
4.16 Composition of the composites.....	73
4.17 Material testing results.....	74
4.18 The hybrid composite formula.....	82
4.19 Material testing results.....	83
4.20 Formulation of the talc filled hybrid composite	94
4.21 Test results of the talc filled hybrid composite	95
4.22 The parameters and level for DOE	106
4.23 The 2 ² factorial design matrix.....	106
4.24 Results of the designed responds	107
4.25 ANOVA results obtained from the MFI	109
4.26 ANOVA results obtained from the HDT (original).....	111
4.27 ANOVA results obtained from the HDT (cured)	112

LIST OF TABLES (Continued)

Table	Page
4.28 ANOVA results obtained from the HDT (cured/dried)	114
4.29 ANOVA results obtained from the notched impact strength (original).....	115
4.30 ANOVA results obtained from the notched impact strength (cured)	117
4.31 ANOVA results obtained from notched impact strength (cured/dried).....	118
4.32 ANOVA results obtained from the unnotched impact strength (original).....	120
4.33 ANOVA results obtained from the unnotched impact strength (cured)	121
4.34 ANOVA results obtained from the unnotched impact strength (cured/dried).....	123
4.35 ANOVA results obtained from the flexural strength (original).....	125
4.36 ANOVA results obtained from the flexural strength (cured)	126
4.37 ANOVA results obtained from the flexural strength (cured/dried).....	128
4.38 ANOVA results obtained from the flexural modulus (original).....	129
4.39 ANOVA results obtained from the flexural modulus (cured)	131
4.40 ANOVA results obtained from the flexural modulus (cured/dried).....	132
4.41 DOE conclusions	133
4.42 Experimental formulation for manufacturing the hybrid composite with increasing VTMS content	135
4.43 The MFI and HDT result of sample#Is and sample#IIs	137
4.44 The mechanical properties of sample#Is and sample#IIs	138
5.1 Hybrid composite formulations	153

LIST OF TABLES (Continued)

Table	Page
A.1 Cumulative probabilities for negative Z-values table.....	163
A.2 Cumulative probabilities for positive Z-values table.....	166



LIST OF FIGURES

Figure	Page
1.1	Classification of plant fibers 3
2.1	Schematic reactions of maleic anhydride treated EFB fibers 14
2.2	Reaction schematic illustration of surface treatments 15
2.3	Schematic illustration of crosslinking reaction mechanism for wood fiber/polymer metrics 21
2.4	Schematic illustration of silane-grafting and water-crosslinking processes 23
2.5	Schematic illustration of chemical crosslinking of TAIC between two PLA molecules 25
3.1	Origin of (a) EFB and (b) cotton fiber 29
3.2	Chemical structure of dicumyl peroxide (DCP) 30
3.3	Chemical structure of the epoxidized natural rubber 30
3.4	Normal distribution curve 39
4.1	The normal plot of the standard effect obtained from the MFI 45
4.2	The pareto chart of MFI 46
4.3	The normal plot of the standard effect obtained from the HDT (original) 48
4.4	The pareto chart of the HDT (original) 49
4.5	The normal plot of the standard effect obtained from the HDT (cured) 50
4.6	The pareto chart of the HDT (cured) 50

LIST OF FIGURES (Continued)

Figure	Page
4.7	The normal plot of the standard effect obtained from the notched impact strength (original)..... 53
4.8	The pareto chart of notched impact strength (original) 53
4.9	The normal plot of the standard effect obtained from the notched impact strength (cured) 54
4.10	The pareto chart of the notched impact strength (cured) 55
4.11	The normal plot of the standard effect obtained from the unnotched impact strength (original)..... 56
4.12	The pareto chart of the unnotched impact strength (original)..... 57
4.13	The normal plot of the standard effect obtained from the unnotched impact strength (cured) 58
4.14	The pareto chart of the unnotched impact strength (cured) 59
4.15	The normal plot of the standard effect obtained from the flexural strength (original)..... 61
4.16	The pareto chart of the flexural strength (original)..... 62
4.17	The normal plot of the standard effect obtained from the flexural strength (cured) 63
4.18	The pareto chart of the flexural strength (cured) 63
4.19	The normal plot of the standard effect obtained from the flexural modulus (original)..... 65
4.20	The pareto chart of the flexural modulus (original)..... 66

LIST OF FIGURES (Continued)

Figure	Page
4.21	The normal plot of the standard effect obtained from the flexural modulus (cured) 67
4.22	The pareto chart of the flexural modulus (cured) 67
4.23	SEM micrograph of biocomposites; (a) run#2 (original), (b) run#2 (cured), (c) run#5 (original), and (d) run#5 (cured)..... 71
4.24	The plot of HDT and MFI with of epoxy contents 75
4.25	The plot of impact properties with epoxy contents..... 77
4.26	The plot of flexural properties with epoxy contents 79
4.27	SEM of the biocomposite with; (a) 0.4 phr (original), (b) 0.4 phr (cured), (c) 1.2 phr (original), and (d) 1.2 phr (cured) of epoxy contents 80
4.28	Plot of HDT and MFI of the hybrid biocomposite as a function of EFB and cotton fiber ratios 85
4.29	Plot of impact properties of the hybrid biocomposite as a function of EFB and cotton fiber ratios 87
4.30	Plot of flexural properties of the hybrid biocomposite as a function of EFB and cotton fiber ratios 88
4.31	SEM micrograph of the biocomposites reinforced with; (a) 100:0 (original), (b) 100:0 (cured), (c) 50:50 (original) (d) 50:50 (cured), (e) 0:100 (original), and (f) 0:100 (cured) of EFB/cotton ratios 91

LIST OF FIGURES (Continued)

Figure	Page
4.32 Relationship between weight loss and the composting time of hybrid composite at 50:50 EFB/cotton and neat PLA.....	92
4.33 MFI of biocomposite as a function of talc and the hybrid fiber contents	96
4.34 HDT of biocomposite as a function of talc and the hybrid fiber contents.....	98
4.35 Notched impact strength of biocomposite as a function of talc and the hybrid fiber contents.....	99
4.36 Unnotched impact strength of biocomposite as a function of talc and the hybrid fiber contents.....	100
4.37 Flexural strength of biocomposite as a function of talc and the hybrid fiber contents	101
4.38 Flexural modulus of biocomposite as a function of talc and the hybrid fiber contents	102
4.39 SEM micrograph of the hybrid biocomposite with; (a) 0:65 (original), (b) 0:65 (cured), (c) 0:65 (cured/dried), (d) 50:20 (original), (e) 50:20 (cured), and (f) 50:20 (cured/dried) of talc and hybrid fiber ratios.....	103
4.40 (a) normal plot and (b) pareto chart of the MFI.....	109
4.41 (a) normal plot and (b) pareto chart of the HDT (original).....	110
4.42 (a) normal plot and (b) pareto chart of the HDT (cured).....	112
4.43 (a) normal plot and (b) pareto chart of the HDT (cured/dried).....	113

LIST OF FIGURES (Continued)

Figure		Page
4.44	(a) normal plot and (b) pareto chart of the notched impact strength (original)	115
4.45	(a) normal plot and (b) pareto chart of the notched impact strength (cured)	116
4.46	(a) normal plot and (b) pareto chart of the notched impact strength (cured/dried)	118
4.47	(a) normal plot and (b) pareto chart of the unnotched impact strength (original)	119
4.48	(a) normal plot and (b) pareto chart of the unnotched impact strength (cured)	121
4.49	(a) normal plot and (b) pareto chart of the unnotched impact strength (cured/dried)	122
4.50	(a) normal plot and (b) pareto chart of the flexural strength (original)	124
4.51	(a) normal plot and (b) pareto chart of the flexural strength (cured)	126
4.52	(a) normal plot and (b) pareto chart of the flexural strength (cured/dried) ...	127
4.53	(a) normal plot and (b) pareto chart of the flexural modulus (original)	129
4.54	(a) normal plot and (b) pareto chart of the flexural modulus (cured)	130
4.55	(a) normal plot and (b) pareto chart of the flexural modulus (cured/dried) ...	132
4.56	Flow chart of compounding process of method#I	136
4.57	Flow chart of compounding process of method#II	136
4.58	MFI of the hybrid composite with VTMS contents	140

LIST OF FIGURES (Continued)

Figure		Page
4.59	HDT of the hybrid composite with VTMS contents.....	142
4.60	Notched impact strength of the hybrid composite with VTMS contents.....	143
4.61	Unnotched impact strength of the hybrid composite with VTMS contents...	145
4.62	Flexural strength of the hybrid composite with VTMS contents.....	146
4.63	Flexural modulus of the hybrid composite with VTMS contents.....	147
4.64	SEM micrograph of the hybrid biocomposite having 5.0 phr of VTMS (a) sample#I (original), (b) sample#II (original), (c) sample#I (cured), and (d) sample#II (cured).....	149

SYMBOLS AND ABBREVIATIONS

%	=	Percent
°C	=	Degree celsius
mol	=	Mole
wt%	=	Percent by weight
phr	=	Part per hundred of resin
rpm	=	Revolution per minute
min	=	Minute
wt/wt	=	Weight by weight
wt/v	=	Weight by volume
mm	=	Millimeter
μm	=	Micrometer
g	=	Gram
kg	=	Kilogram
cm ³	=	Cubic centrimeter
MPa	=	Mega pascal
GPa	=	Giga pacal
J	=	Joule
kN	=	Kilo newton
kJ/m ²	=	Kilo joule per meter square

CHAPTER I

INTRODUCTION

1.1 General introduction

In recent years, as a result of growing environmental awareness, natural fibers have been increasingly used as reinforcement in thermoplastic composite materials. Natural fibers, such as sisal, kenaf, bamboo, and jute, are composed of cellulosic and lignocellulosic materials. Thermoplastic polymers derived from petroleum based, such as polypropylene (PP), high-density polyethylene (HDPE), low-density polyethylene (LDPE), and polystyrene (PS), have generally been used as matrix polymers. However, these polymers do not degrade easily in the natural environment, resulting in various forms of environmental pollution. To overcome this problem, the use of the environmental friendly and degradable polymers is considered as an alternative to conventional plastic materials. Among the biodegradable polymers, poly (lactic acid) (PLA) is a very interesting material. PLA is a polymer obtained from renewable agricultural raw material, which are fermented into lactic acid (Cheng, Lau, Liu, Zhao, Lam, and Yin, 2009) and then polymerized into long chain molecule. It is degraded by micro organism and it is a thermoplastic polymer with excellent mechanical properties. PLA provides good aesthetics, strength and easily to process in most equipments. But commercial application of pure PLA is limited because of its inherent weakness, such as low impact strength and high brittleness. The most significant weakness of pure PLA is its low heat resistance. HDT of pure PLA is less

than 60°C. So it needs modification step for most practical applications. More research effort is being directed toward finding methods of addressing the weakness of PLA without compromising its biodegradability (Nyambo, Mohanty, and Misra, 2010).

1.2 Natural fibers and composites

The properties of biodegradable polymer can also be improved by reinforcing it with fiber(s), which enhances mechanical and thermal stability. Some properties of natural fibers and synthetic fibers are presented in Table 1.1 (Taylor, 2004). The Natural fibers are normally lighter in specific weight than the synthetic ones. Natural fibers are subdivided based on their origins, coming from plants, animals or minerals. All plant fibers are composed of cellulose while animal fibers consist of proteins (hair, silk, and wool) (John and Thomas, 2008).

Plant fibers such as hemp, jute and flax can be a substitute for synthetic fibers i.e. glass and carbon fibers in composites material. Although the tensile strength and tensile modulus of natural fibers are remarkably lower than those of synthetic fibers. The advantages of natural fibers are low-density with high specific properties (properties per unit weight), abundance and inexpensive. Furthermore, the natural fibers are recyclable, biodegradable, renewable, and locally abundant. On the contrary, the synthetic fibers have serious drawbacks in manners of high cost, non-recycle, non-renewable and non-biodegradable. So, there is much research on natural fibers reinforced composites. The many studies have investigated the biodegradable polymers filled with natural fibers, such as kenaf, bamboo, ramie and the polymer matrix commonly used is PLA.

Plant fibers can be classified into five groups according to the part of the plant from which they are extracted as shown in Figure 1.1.

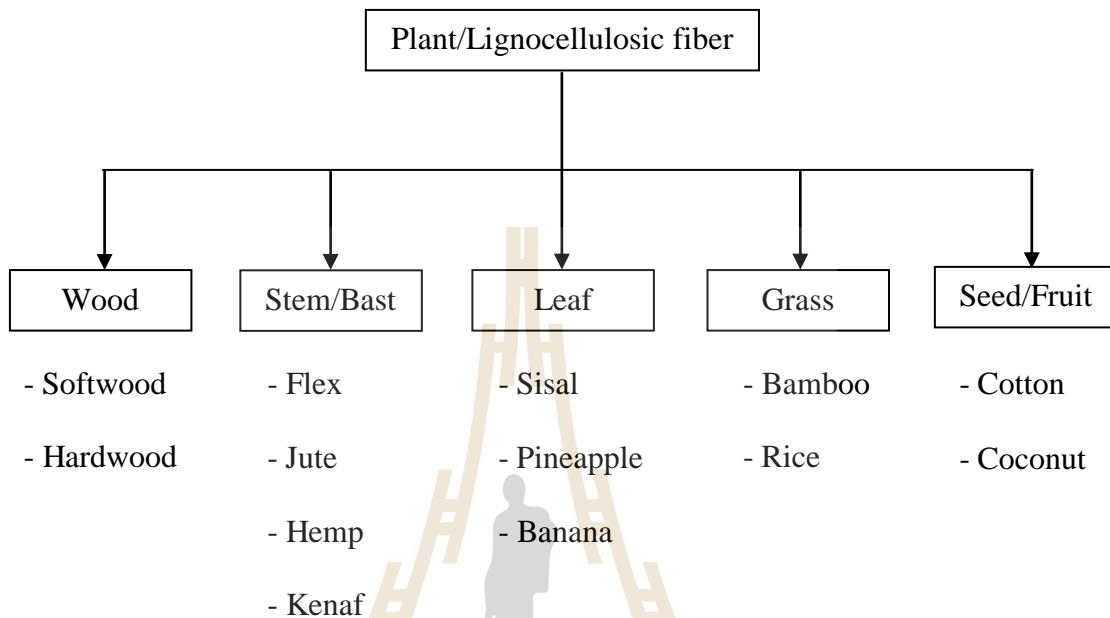


Figure 1.1 Classification of plant fibers (Schuh, 2004).

The reinforcing efficiency of natural fibers is related to the nature of cellulose and its crystallinity. The major components of natural fibers are mainly composed of cellulose, hemicelluloses, and lignin binder. In order to expand the use of agro-fibers for composites, it is useful to have the information on fiber characteristics and the factors, which affect performance of the fiber (Rowell, Hun, and Rowell, 2000).

In this study, oil palm empty fruit bunch (EFB) and cotton fibers will be used as reinforcement for PLA matrix. Cotton fibers consist of cellulose about 80 - 90 %wt (Hegde, Dahiya, and Kamath, 2004). The EFB is the fiber mass discarded after separating the hard shell from fresh fruits bunch. EFB fiber consist of about 65 - 77 %wt of cellulose (Khalid, Ratnam, Chuah, Ali, and Choong, 2008; Rozman, Lai, Ismail,

and Ishak, 2000). In addition, the amount of EFB fiber is the by-product of oil palm industry is dramatically increased as the consumption of oil palm as biodiesel is rapidly increased. Thus, considerable research and development efforts have to be undertaken to find usefulness applications for the EFB.

However, the main drawback of natural fibers may be their hydrophilic in nature, which decreases the compatibility with hydrophobic polymeric matrix. This will lead to a very poor interfacial bonding between fibers and matrix. To overcome these incompetency, various fiber surface treatments like mercerization, isocyanate treatment, maleic anhydride treatment and silane treatment have been set up which may result in improving interfacial between the polymer matrix and natural fibers in order to enhance the physical and mechanical properties of the end products (Lee and Wang, 2006).

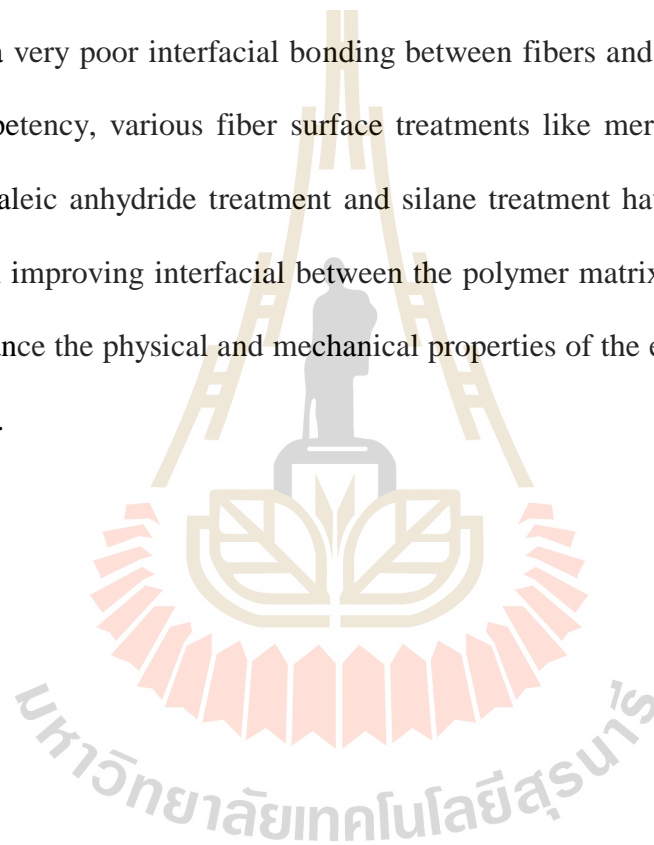


Table 1.1 Properties of natural and synthetic fibers (Taylor, 2004).

Type	Fibers	Density (g/cm ³)	Tensile strength (MPa)	Tensile modulus (GPa)	Elongation at break (%)	Decomposition temperature (°C)	Price (Euros/kg)
Natural	Oil palm	0.9	130 - 248	6.7	9.7 - 14	-	0.1
	Cotton	1.5 - 1.6	350	11	2 - 10	-	0.35
	Jute	1.3 - 1.5	187 - 540	3 - 55	1.4 - 3.1	270	0.7
	Ramie	-	585 - 900	33	2.0 - 3.5	260	-
	Hemp	1.4 - 1.5	580 - 1,110	3 - 90	1.3 - 4.7	258	-
	Bamboo	-	-	1.7 - 29	3.2	-	-
	Flax	1.4	250 - 1,000	12 - 100	1.3 - 40	280	0.15 - 0.76
	Sisal	1.4	507 - 855	24	2.9	270	0.7 - 1.02
	Banana	1.3	791	30	2.10	-	0.7 - 0.9
	Kenaf	1.4	930	53	-	270	-
	Coconut	-	544	14	-	-	0.36 - 0.45

Table 1.1 Properties of natural and synthetic fibers (continued).

Type	Fibers	Density (g/cm ³)	Tensile strength (MPa)	Tensile modulus (GPa)	Elongation at break (%)	Decomposition temperature (°C)	Price (Euros/kg)
Synthetic	E-glass	2.5	1,625 - 3,400	72	2 - 5	756	1.6 - 2.0
	C-glass	2.5	2,800	69	-	756	9.3 - 16
	S-glass	2.5	4,600	87	-	946	8.3 - 20
	A-glass	2.5	2,400	68	-	696	2.5
	Aramid	1.4	2,380 - 3,100	124	-	496	16.67
	Carbon	1.8 - 1.9	2,090 - 5,200	525	-	3,647	33 - 166
	Zirconia	5.6	700	100	-	2,497	41.7
	Alumina	2.8	1,000	100	-	1,997	-



1.3 Research objectives

The main objectives of this research can be classified as followings:

- (i) To study the mechanical properties of biocomposite derived from PLA reinforced with oil palm empty fruit bunch and cotton hybrid fibers.
- (ii) To evaluate the effect of composite constituents on the properties.
- (iii) To investigate the influence of silane treatment and crosslink on the properties of the biocomposite.

1.4 Scope and limitation of the study

The main study of this research was to produce natural fibers reinforced PLA composites for superior mechanical properties and high temperature. The commercially available PLA was used. The thermal, mercerization and silane treated oil palm empty fruit bunch and cotton fibers were used as reinforcement. Solid epoxy was used as compatibilizer. Viscous polyester polyols was used as active plasticizer. Epoxidized natural rubber with epoxide content of 50% was employed as impact enhancer. Talc was obtained as filler for cost reduction, mechanical improver and provides the aesthetic appearance of the composites. The mechanical properties by means of flexural, impact strength and morphological properties of the composites were investigated. Also, the heat deflection temperature (HDT) was evaluated.

CHAPTER II

LITERLATURE REVIEW

2.1 Biocomposites

2.1.1 Synthetic polymer and natural fibers composites

Thermoplastic polymers devised from petroleum base synthetic resources, such as polypropylene (PP), high-density polyethylene (HDPE), low density polyethylene (LDPE), poly(vinyl chloride) (PVC) and polystyrene (PS) do not degrades easily in natural environment. So it has effort to combine the petroleum and bioresources to produce biocomposites. For example, sisal fibers were studied for fiber reinforcement in LDPE, PS, PVC and HDPE by Joseph, Thomas, and Pavithran (1996); Manikandan Nair, Thomas, and Groeninckx (2001); Fávvaro, Ganzerli, de Carvalho Neto, da Silva, and Radovanovic (2010); Djidjelli, Boukerrou, Founas, Rabouhi, Kaci, and Farenc (2007), respectively.

Khalid, Ratnam, Chuah, Ali, and Choong (2008) studied the comparative of PP composites reinforced with oil palm empty fruit bunch fiber (EFB) and oil palm derived cellulose. The composites were prepared by extrusion and compression molding. The cellulose and EFB fibers were blended in different ratio up to 50 wt%. The results found that the flexural modulus increased with increasing filler content and PP/cellulose composites exhibited higher modulus than PP/EFB composites. However, increasing percentage of EFB reduced the flexural strength and elongation at break. Scanning electron microscope (SEM) showed that cellulose had

an effective interaction with PP matrix when compared with PP/EFB. It showed the cellulose was covered by the layer of matrix. But the PP/EFB showed some deep holes and fiber pull-out.

Rozman, Tay, Kumar, Abusamah, Ismail, and Mohd (2001) prepared polypropylene hybrid composites from oil palm empty fruit branch fiber and glass fibers (GF). The fibers and PP were mixed into different loading content at 10 - 40 wt% of overall fiber content. The proportion of EFB and GF loading were at 0, 25, 50, 75 and 100% of EFB fibers. From the results found that the flexural strength and tensile strength decreased as the amount of EFB fibers in composites increased, that the significant reduction of occur for 25% EFB fiber content.

The effect of fiber size on the mechanical properties of EFB filled polyurethane (PU) foam was studied by Badri, Othman, and Razali (2005). Higher compressive stress was observed for 45 - 56 μm fiber particulate. This was due to the higher surface area of the fibers in powder form, which may produce better hindrance to stress-impact propagation. The SEM indicated that small size fibers got embedded in the matrix well comparing to large size fibers. However, the flexural strength of EFB filled PU composites decreased with decreasing in filler size.

Ratnam, Raju, and Yunus (2007) prepared EFB fibers and poly(methyl acrylate) grafted EFB for adding into poly(vinyl chloride) (PVC)/epoxidized natural rubber (ENR) blends by varied EFB loading from 0 to 30 wt%. They reported the reduction in tensile strength of composites at higher EFB fiber loading. Other mechanical properties; tensile modulus and flexural modulus increased with increasing EFB content. However, the impact strength and elongation at break of the composites were found to decrease with the increase in fiber loading.

Kim, Moon, Kim, and Ha (2008) found that the tensile strength depends on the interfacial interaction between PP and wood fibers. The tensile strength of the PP/wood fibers composites decreased with increasing wt% of wood fibers. However, the tensile strength of the PP/cotton fibers composites displayed different behavior. With the addition of 10 wt% cotton fibers, the tensile strength decreased. But with the addition of 20 and 30 wt% cotton fibers, the tensile strength increased because of the entanglement of the cotton fibers, as confirmed by the SEM micrographs.

Mwaikambo, Martuscelli, and Avella (2000) prepared polypropylene composites using kapok/cotton fiber together as reinforcement. Treating the reinforcement with acetic anhydride and sodium hydroxide (NaOH) was the fiber modification. They found that fiber modification gave a significant improvement to the thermal properties.

2.1.2 Biopolymer and synthetic fibers composites

Many researches explore about synthetic fibers reinforced biodegradable polymer. Khan, Parsons, Jones, Walker, and Rudd (2010) prepared the polycaprolactone (PCL) reinforced with phosphate glass fibers. They found that the mechanical properties of the composites were improved. Neppalli, Marega, Marigo, Bajgai, Kim, and Causin (2010) filled nylon 6 fibers to PCL composites it was found that at very low filler contents, 3%, material exhibited and improved stiffness with a simultaneous increase in ductility.

Huda, Drzal, Mohanty, and Misra (2006) prepared PLA/glass fibers composites. The amount of 30 wt% of glass fiber was constituted to produce the composites by twin screw extruder and an injection molding. From the mechanical

properties showed that PLA/glass fibers composites had the tensile strength, tensile modulus and impact strength better than that neat PLA. Moreover, the flexural modulus and strength of composites increased significantly with the addition of the glass fiber. From the thermal analysis found that the shifting of T_g and HDT of PLA/glass fibers composite to higher temperatures when compared to neat PLA sample. SEM observations of PLA/glass composites indicated that glass fiber was well dispersed in the PLA matrix. The glass fiber was covered with a thin layer of matrix linking the fiber surface to the matrix.

Parsons, Ahmed, Haque, Fitzpatrick, Niazi, and Walker (2009) manufactured composites comprising of PLA matrix reinforced with phosphate glass fibers. They made composites using a variety of fibers architectures, from non-woven random mats to unidirectional fiber. The fibers in these structures provide the improvement of creep resistance.

Wan, Wang, Li, and Dong (2001) studied PLA/carbon fibers composites with different fiber surface treatment conditions, untreated and with nitric acid oxidation for 4 hours and 8 hours, were performed to determine the influence of surface treatment on the interfacial adhesion strength and mechanical properties of the composites. They found that the treated composites exhibited stronger interface adhesion and better mechanical properties in comparison to those untreated counterparts. There was a greater percentage of improvement in interfacial adhesion strength than in the mechanical properties.

2.1.3 Biopolymer polymer and natural fibers composites

Many researchers have been currently being harness in developing a new class of fully biodegradable composites by combining natural fibers with

biodegradable resins. PLA was reinforced with natural fibers such as kenaf, flax and cotton. Moreover, PLA reinforced by animal fibers such as silk and chicken feather fibers were published by Zhao, Cheung, Lau, Xu, Zhao, and Li (2008); Cheng, Lau, Liu, Zhao, Lam, and Yin (2009).

Bax and Mëssig (2008) fabricated composite specimens consisting of PLA reinforced with cordenka and flax fibers, respectively. Samples with three different fiber proportions, 10, 20 and 30 wt%, for PLA/flax composites and samples with four different proportions, 10, 20, 30 and 40 wt%, for PLA/cordenka composites were prepared. The results showed that the highest impact strength and tensile strength were found for cordenka reinforced PLA at 30 wt% fibers content. The highest Young's modulus was found for the composites made from PLA and flax. SEM reviewed that poor adhesion between the matrix and fibers for both composites.

Yussuf, Massoumi, and Hassan (2010) studied and compared performance of PLA/kenaf and PLA/rice husk composites with the fibers content of 20 wt%. From the result found that flexural modulus of the material was increased drastically when filled with both kenaf and rice husk fibers. The flexural strength decreased by addition natural fibers. The PLA/kenaf composites showed better mechanical properties compare to PLA/rice husk composites. The poor performances of rice husk compare to kenaf fibers could be attributed from the difference of chemical composition of fibers and also the aspect ratio of the fibers, the higher of aspect ratio lead to the higher of mechanical properties.

The PLA/cotton composites by adding lignin for adhesion promoter were studied by Graupner (2008). The composites with fiber mass proportion of 40 wt% were produced by compression molding. The results of the composites

investigations showed that the addition of lignin had an influence on the composites performance. The tensile and Young's modulus of composites increased when adding lignin. However, the PLA/cotton/lignin composite had a tensile and Young's modulus lower than PLA/kenaf composites.

Kamath, Bhat, Parikh, and Mueller (2005) studied nonwoven composites with cotton reinforced PLA. The results showed that adding cotton help in increasing the tensile elongation of the composites. Interfacial bonding between cotton fibers and the polymer was very good. Moreover, the tensile results for samples with PLA/cotton when adding flax fibers showed the strength and modulus improvement more than adding kenaf to PLA/cotton composites. Also, adding cotton to PLA/kenaf or PLA/flax composites found that cotton help in increasing the tensile elongation of the composites.

2.2 Natural fibers treatment

2.2.1 Chemical Treatment

Currently, many research projects are devoted to the utilization of cellulose based fibers as reinforcement for polymer. The chemical treatment on natural fibers can commonly improve the interfacial adhesion and hence the mechanical performance.

According to the study by Rozman, Saad, and Ishak (2003), EFB were modified and added into PP composites. EFB fibers had been chemically modified with maleic anhydride (MAH). MAH was dissolved in dimethylformamide (DMF). The fibers were added into solution at 90°C for 1 hour. The polymer and fibers were mixed by twin screw extrusion. Dicumyl peroxide was added during the compounding

process. The composites with MAH treated EFB showed higher flexural and impact strength than those with untreated EFB. This may be attributed to the enhanced adhesion between the MAH treated EFB and PP matrix. The improvement of the properties was explained by the crosslink reaction between the treated fiber and polymer matrix as shown in Figure 2.1.

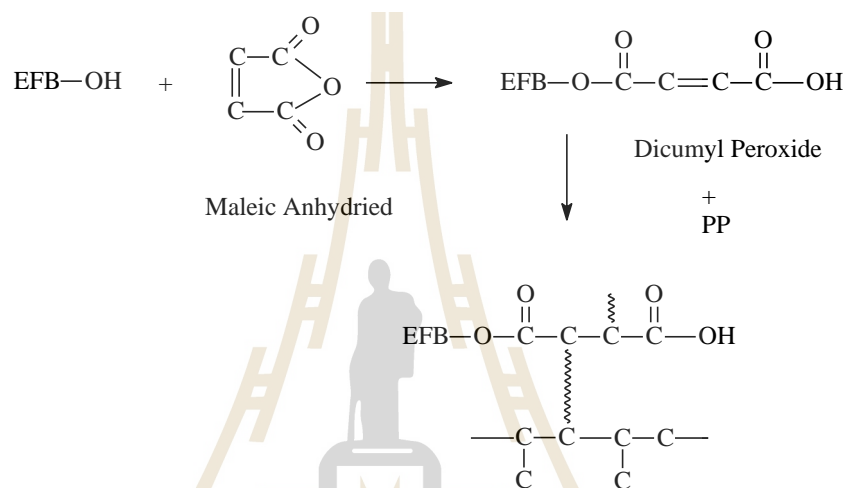
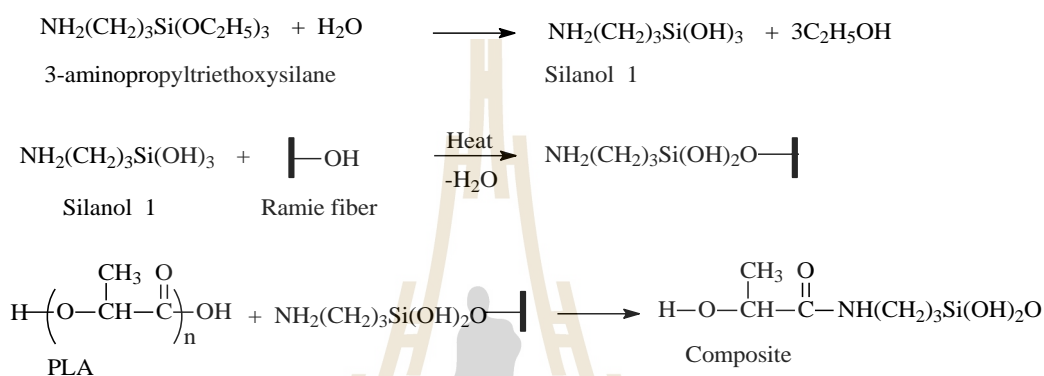


Figure 2.1 Schematic reactions of maleic anhydride treated EFB fibers.

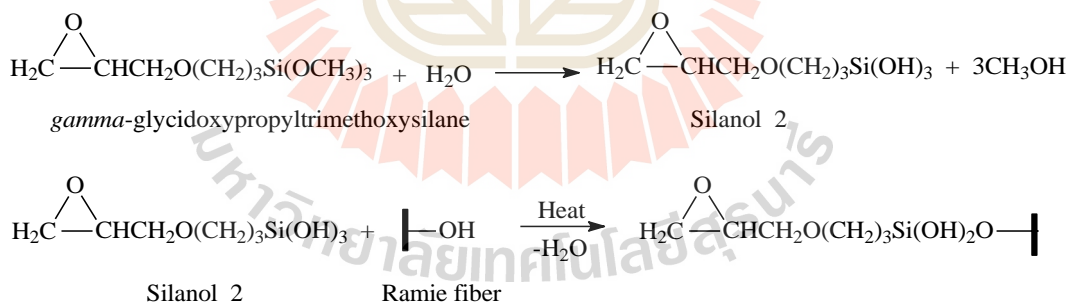
Yu, Ren, Li, Yuan, and Li (2010) used ramie fibers that were treated by alkali and silane, 3-aminopropyltriethoxysilane (APS) and *gamma*-glycidoxypropyltrimethoxysilane (GPS). For treatment process, silane was diluted to 6% concentration in acetone. The fibers were immersed into silane solution for 24 hours. For alkali treatment, fibers were immersed in sodium hydroxide solution at 5 cw/v for 3 hours at room temperature. The results of this study showed that surface treatment improved the compatibility between the PLA matrix and fibers. The mechanical properties and the thermo-mechanical properties of the composites with treated fibers were better than that of neat PLA and the composites with untreated fibers. These improvements

were due to the enhanced interfacial adhesion between the PLA matrix and the fibers. The following schematic diagrams show, Figure 2.2, the reaction between silanes and alkaline and fibers, respectively;

3-aminopropyltriethox silane:



gamma-glycidoxypropyltrimethoxysilane:



Alkali treatment:

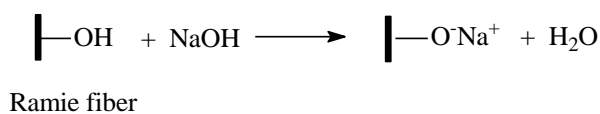


Figure 2.2 Reaction schematic illustration of surface treatments.

Huda, Drzal, Mohanty, and Misra (2008) investigated the effect of fiber surfaces treatments. In the study, the alkali treatment was succeeded by immersion kenaf fibers in sodium hydroxide solution, 5% wt/v, for 2 hours. The silane treatment using 3-aminopropyltriethoxysilane (APS) was performed by coupling the kenaf fibers with the agent. The reinforcements were classified into untreated, alkali, silane, and alkali/silane treated fibers. The results indicated that both silane treated and alkali treated fibers reinforced composite offered superior mechanical properties compared to untreated samples. The alkali and followed by silane treatment fibers reinforced composite also manifested the significantly improved in mechanical properties.

Lee, Kim, Lee, Kim, and Dorgan (2009) employed the *gamma*-glycidoxypropyltrimethoxy-silane (GPS) for PLA/kenaf fibers composites by varying the content of GPS from 1, 3 and 5 wt%. From the result, it reviewed that silane had improved the mechanical properties. The composites with low loading level of silane provided significant benefit to the mechanical properties. The 3 wt% of GPS material exhibited the most significant effect between treated and untreated composites.

Hornsby, Hinrichsen, and Tarverdi (1997) studied the effect of modified fibers and modified matrix of wheat or flax straw as fiber reinforcement for polypropylene. The samples were prepared from modified fibers and PP. For fibers modification, the fibers were treated with 2 wt% of different chemical agent; 3-aminopropyl-triethoxysilane (APS), *gamma*-glycidoxypropyltrimethoxysilane (GPS) and vinyl-trimethoxysilane (VTMS). From the results found that the composites with treated fibers showed higher mechanical properties than those with untreated fibers.

2.2.2 Thermal treatment

Heating cellulose fiber at higher temperatures than normal drying conditions, such as above 170°C, has been shown to appreciably reduce the swelling, shrinking and/or degradation of the lingo-cellulosic material. The thermal modifications of wood resulting in the changes of lignin and hemicelluloses, while the crystallinity of fiber increases. Rusche (1973) studied the strength properties of dried wood fiber after thermal treatment. Wood fibers were heated at temperature range from 100 to 200°C. The decrease in the strength properties was related to the rate of thermal degradation. The modulus of elasticity was decreased significantly only when the losses of substance caused by the thermal treatment.

Hakkou, Pétrissans, Zoulalian, and Gérardin (2005) investigated the change of wettability of wood during thermal treatment. Wood blocks were treated by thermal treatment in an oven at different temperatures for 8 hours under nitrogen atmosphere. The temperature was increased by the rate 20°C/min from 20 to 240°C. Fourier transform infrared spectroscopy (FTIR) results showed that thermal treatment led to an important decrease of the carbonyl band at 1730 cm⁻¹ indicating hemicelluloses degradation. Wood, which is naturally hydrophilic, becomes rather hydrophobic after heat treatment in the range of temperatures between 130 and 160°C.

Van Den Oever, Beck, and Mëssig (2010) studied the effect of water content in undried and dried natural fibers on PLA degradation during processing as well as on the composite's mechanical performance. The fibers evaluated were ramie, flax and cotton, containing of 6 - 9% moisture in the undried state and 0.2 - 0.4% in the dried condition. Intrinsic viscosity and melt flow index analysis indicated that the effect of the different levels of moisture in the fibers have a similar and small effect

on PLA degradation. Morphology, flexural strength and charpy impact of the composites were not significantly affected by the water present in the undried fibers.

2.3 Toughening of polymer

2.3.1 Rubber toughened polymer

Chuayjuljit, Soatthiyanon, and Potiyaraj (2006) studied the improving toughness of epoxy matrix by blending with epoxidized natural rubber (ENR). They used ENR that contained epoxide group at 25, 40, 50, 60, 70 and 80% by mol. Bisphenol type epoxy resin was mixed with ENR at 2, 5, 7 and 10 phr, and polyamide resin was used as curing agent. From the results, it was found that the impact strength of epoxy resin can be improved by blending with ENR. The tensile strength and Young's modulus were found to be decreased with an increasing amount of epoxide groups in ENR and also with an increasing the amount of ENR blends. Specimens exhibited lower flexural strength and flexural modulus when the amount of the modified rubber increased.

The effect of ENR as a compatibilizer on properties of high density polyethylene (HDPE)/soya powder (SP) blends was studied by Ismail and Ooi (2010). The ENR50, 50% by mol of epoxidation, was used at 2.5, 5.0, 7.5 and 10.0 phr. They found that at 2.5 phr of ENR50 was the optimal content to significantly increase the tensile properties of HDPE/SP blends, which attributed to the good compatibilization effect of ENR50 as verified by the morphologies and Fourier Transform Infrared (FTIR) results.

Phinyocheep, Saelao, and Buzaré (2007) examined the melt blending of poly(ethylene terephthalate) (PET) and natural rubber (NR) in a twin screw

extruder. They found that the toughness of the PET/NR blend was increased as the amount of NR increased. This should come from the interaction between the carbonyl group of PET with the abnormal groups such as hydroxyl function in NR, resulting in improving the compatibility of the blends, hence increasing in the toughness.

2.3.2 Filler toughened polymer

Raghu, Bose, and Mahanwar (2006) investigated effect of the contents and sizes of talc. Tensile strength, flexural strength, flexural modulus, percent elongation at break and impact strength behavior of the talc filled HDPE was prepared at loading ranging from 0 to 30 wt% and the particle size of 5 to 10 μm of talc filler were employed. The result showed that the tensile strength and flexural modulus increased whereas impact strength and percent elongation at break decreased as the filler loading increases. Also, flexural strength, flexural modulus and tensile strength increased with decreased in the particle size.

Lapcik, Jindrova, Lapcikova, Tamblyn, Greenwood, and Rowson (2008) published the effect of the talc filler on the physicochemical and mechanical properties of polypropylene and polypropylene copolymer with ethylene-propylene-diene monomer (EPDM) elastomer. Talc filled samples with different talc contents from 5, 10, 15, 20, 25 and 30% by wt were designed. The composites were mixed by extruder and then injected by injection molding. From the results found that increasing filler content led to the increasing mechanical strength and toughness.

Shelesh-Nezhad and Taghizadeh (2007) investigated the influences of adding talc mineral particles of 10 μm on the mechanical properties of injection molded PP/talc composites. The talc and PP were mixed into different loading; 10, 20 and 30 wt%. The results of experiments indicated that the maximum flexural strength

and maximum impact strength were achieved by adding 10 and 20 wt% of talc, respectively. With addition of 10 wt% of talc to the PP matrix, the tensile strength was slightly affected.

Singh, Mohanty, and Misra (2010) presented the development of hybrid composites from wood fibers, talc and polyhydroxybutyrate-co-valerate (PHBV). The weight proportions of PHBV/wood/talc were 60/40/0, 70/30/10, 80/20/20 and 90/10/30, respectively. The highest flexural modulus and flexural strength was observed with at 40% of talc, but flexural modulus and flexural strength decreased with replacement of talc by wood. From the SEM found that the better interfacial interaction and dispersion of talc with PHBV than the wood fibers. The HDT of the hybrid composite was not much affected by the presence of talc, but largely significant by the wood fiber.

2.4 Crosslinking of polymer

Crosslinking is one of the important methods to improve the thermal and chemical resistance of polymers. In general, there are three crosslink methods, *i.e.* radiation, peroxide and silane crosslinking. Among the crosslinking methods, the silane process is cost effective and easily to operate.

Kuan, Kuan, Ma, and Huang (2006) studied wood fibers reinforced linear low density polyethylene (LLDPE). Water crosslink technique was used to improve the physical properties of wood composite. Composites were compounded in twin screw extruder and treated with vinylalkoxysilane (VTMS) and dicumyl peroxide (DCP). The samples were placed in the isothermal water bath at 70°C for 0.5, 1, 2, 4 hours to pursue water crosslink reaction. Tensile strength, flexural strength and flexural

modulus were significantly increased with increasing water crosslink time. However, tensile elongation and impact strength decreased with the increasing of water crosslink time. From the SEM indicated that the composites treated with silane modifiers and water crosslink process exhibited much better bonding between fiber and matrix. The heat deflection temperature of the composite increased with the increasing of wood fiber content and water crosslink time. The reaction mechanism for silane/water crosslink was established as demonstrate in Figure 2.3.

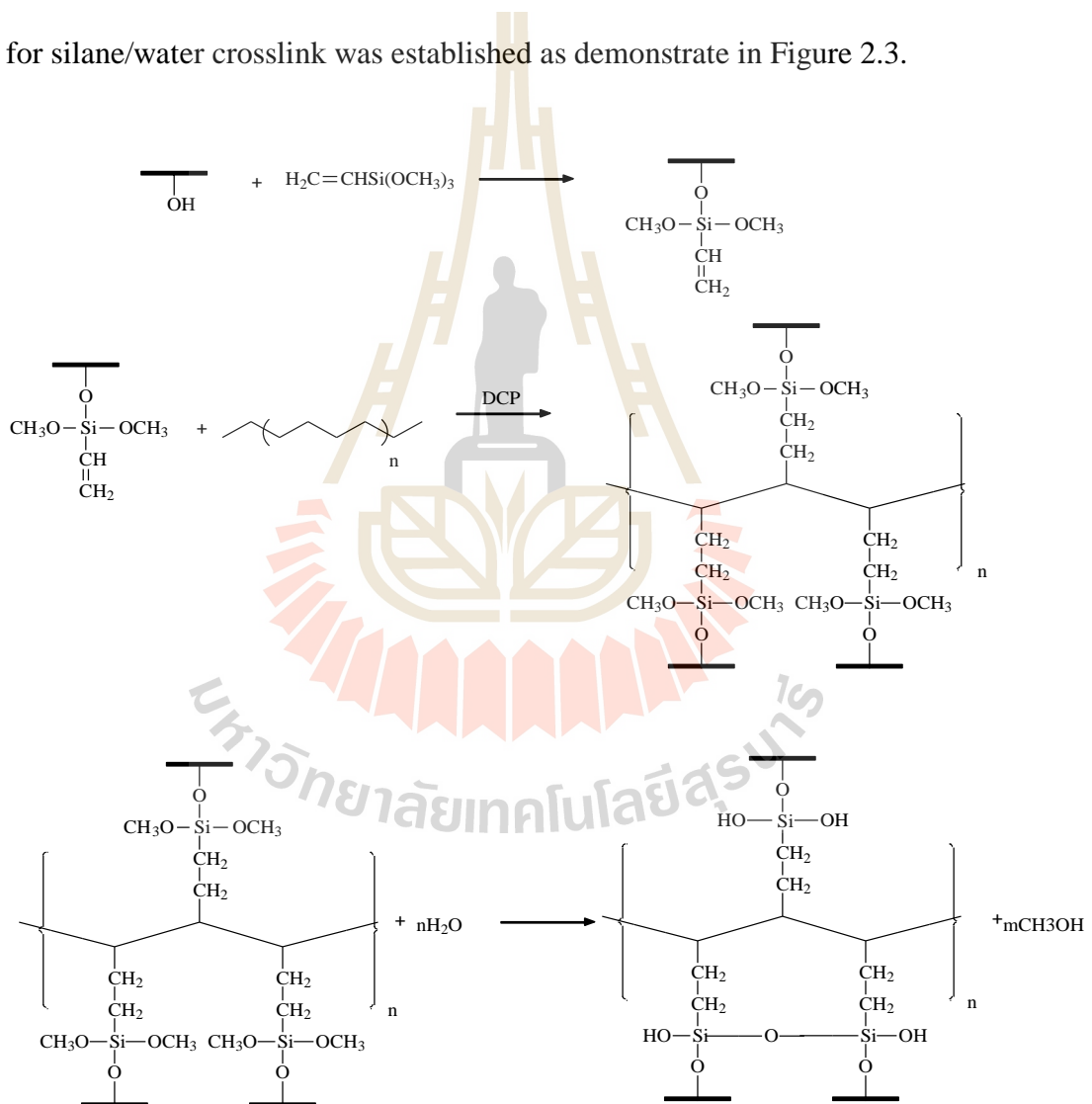


Figure 2.3 Schematic illustration of crosslinking reaction mechanism for wood fiber/polymer matrix.

Zhou, Wang, and Hu (2009) studied the melt grafting of VTMS onto PP/ethylene propylene diene terpolymer (EPDM) blend. The compounds were added with 2 and 4 phr of VTMS with four different DCP contents, 0.1, 0.2, 0.3 and 0.4 phr. The mechanical properties of the samples were improved by the incorporation of relatively higher DCP and VTMS concentration. It had been found that thermal stability of the blend was improved. The gel percentage of the crosslinked polymer increased with increasing DCP, EPDM and VTMS concentration.

Grubbström and Oksman (2009) studied of silane-crosslink of wood/HDPE composite. The composites were prepared in a compounding extruder. A solution of VTMS and DCP (12:1 wt/wt) was prepared and added into the composition at 4 wt%. The wood plastic composite was extruded as a profile and immediately pressed in a hot press. The crosslinked composites were achieved by storing in either room temperature at 20°C or in a sauna at 90°C. The rest of the crosslinked composites were stored for 3, 6 or 12 hours, 1, 2, 3, 4, 6, 9 or 13 days. The results showed that all crosslinked composites displayed higher strengths compared with noncrosslinked controlled samples. Tensile strength improved in comparison with the noncrosslinked sample.

Bengtsson and Oksman (2006) had established the silane crosslinked wood/LDPE composites. Silane crosslinked composites with different amounts of VTMS were produced in the compounding process using co-rotating twin screw extruder. The composite specimens were stored in a sauna oven at 100% RH and 90°C for 48 hours and at room temperature to study the effect of humidity on the degree of crosslink. Gel content and swelling experiments showed that the highest degree of crosslink was found in the composites obtained from sauna incubation. The

crosslinked composites showed toughness and impact strength superior to those composites to which no silane added. The flexural modulus, on the other hand, was lower in the crosslinked samples than in those no crosslinked ones.

Han, Bian, Liu, Han, Wang, Dong et al. (2009) developed the crosslinked poly(L-lactide) (PLLA) by grafting VTMS onto PLLA using DCP, followed by silane hydrolysis to form siloxane linkages between PLLA chain. The compounds were added with VTMS, 3 to 8 phr, and DCP, 0.1 to 0.5 phr. Crosslinked PLLA were obtained by curing of silane grafted PLLA on hot water. The proposed mechanism of the silane grafting and water crosslinking processes for PLLA is schematically shown in Figure 2.4. They found that, this method had improved the thermal stability, mechanical properties and hydrolysis resistance of PLLA. The T_g of silane water crosslinked PLLA increased with increased in crosslinking density.

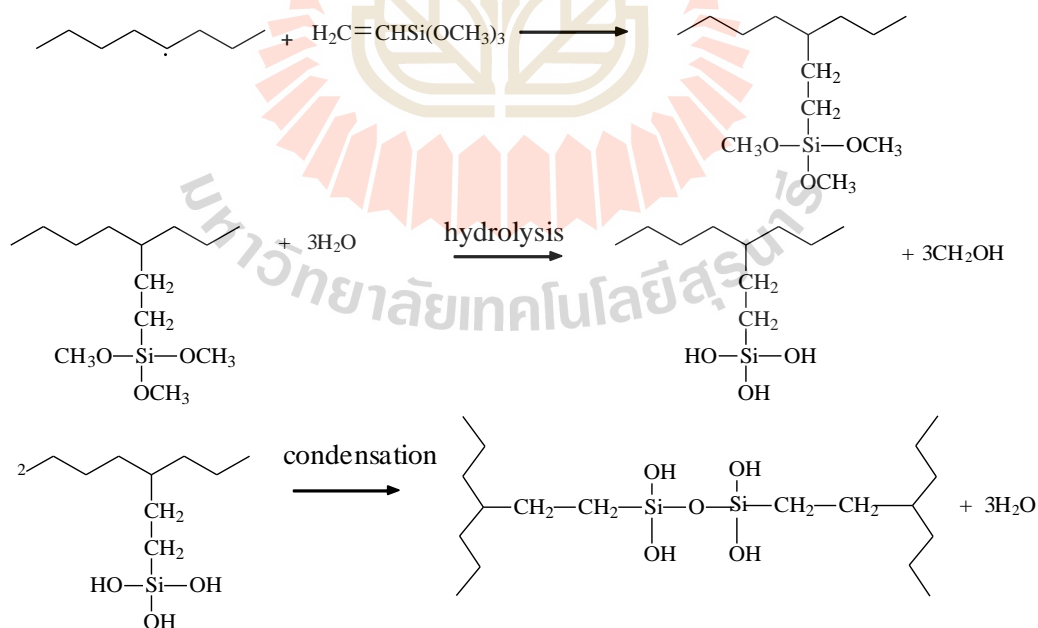


Figure 2.4 Schematic illustration of silane-grafting and water-crosslinking processes.

Sirsinha and Meksawat (2004) studied the silane/water crosslink of metallocene ethylene-octane copolymer (EOR). The EOR was first grafted with VTMS at 5 phr using 0.1 phr of DCP as initiator in twin screw extruder. To complete crosslink reaction, the samples were immersed in water at 70°C. The effect of time for crosslink reaction was investigated. They found that the rate of crosslink was very fast in the early stage and decreased thereafter. The maximum gel content of 77% was reached after 60 hours of treatment time. Increasing the immersing time beyond 60 hours, the gel content did not increase further. Tensile strength and elongation at break decreased, whereas modulus at intermediate and high strains increased with increased of crosslink time.

Yang, Wu, Yang, and Yang (2008) studied the improvement of the thermal stability and mechanical properties of PLA. The crosslinking was introduced via chemical treatment of the melt by adding small amounts of crosslinking agents; triallyl isocyanurate (TAIC) and DCP. PLA samples containing different concentrations of TAIC, 0.15 to 3.0% and DCP of 0.2 to 1.5% were mixed. The crosslink reaction was purposed as shown in Figure 2.5. From the results found that crosslinked structures could be effectively introduced into PLA by the initiation of DCP in the presence of a small amount of TAIC. Crosslinked chain was also responsible for the improved tensile modulus and tensile strength. The thermal stability was also improved which indicated by TGA and DMA results. However, the brittleness increased with the introduction of a highly crosslinked structure.

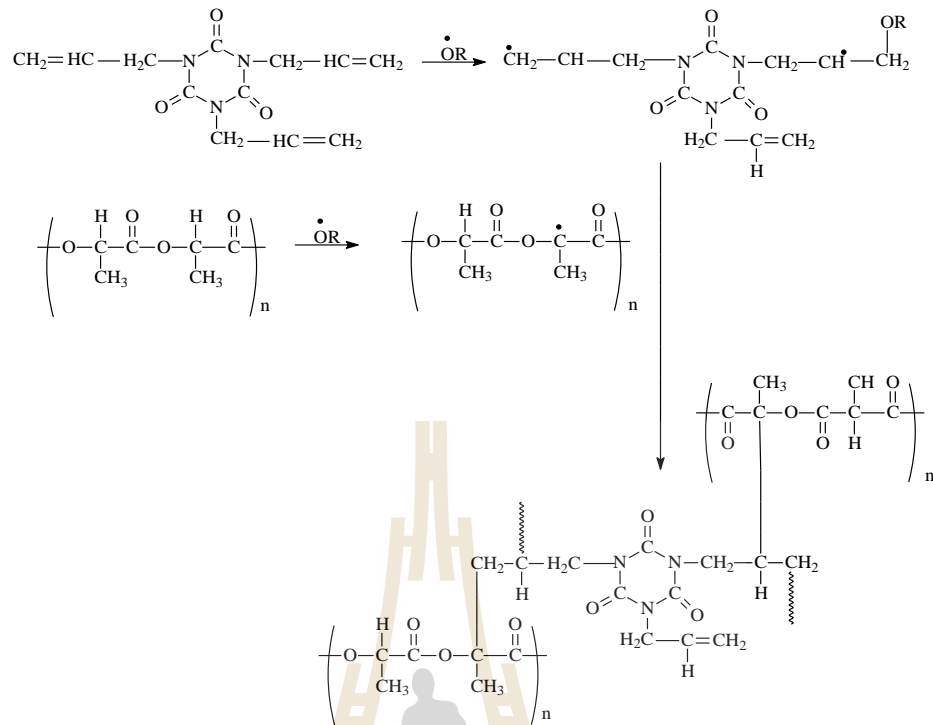


Figure 2.5 Schematic illustration of chemical crosslinking of TAIC between two PLA molecules.

CHAPTER III

EXPERIMENTAL

3.1 Materials

Table 3.1 summarizes the reagents used and their function in compounding process. Poly(lactic acid) grade 2002D was purchased from Nature Works[®] and used as the polymer matrix. The silanes, 3-aminopropyltriethoxysilane (APS; A-1100), *gamma*-glycidoxypropyltrimethoxysilane (GPS; A-187) and vinyltrimethoxysilane (VTMS; A-171) from Crompton Osi Specialty were used as coupling agents. The commercially available dicumyl peroxide (DCP) were used as free radical initiator. The solid epoxy, diglycidyl ether of bisphenol A (DGEBA), Epotec YD-019, was obtained from Thai Epoxy & Allied Products Co., Ltd. and used as reactive compatibilizer. The epoxidized natural rubber (ENR50) having 50% by mol of epoxidation was supplied by San-Thap International Co.,Ltd. Talc, average particle size, reported by manufacturer, of 1.1 μm , was purchased from Luzenac company. Aliphatic polyester polyols, Rayelast[®] A8770, used as reactive plasticizer was purchased from IRPC Polyol Co., Ltd. The mixed between Tris(2,4-di-tert-butylphenyl) phosphate, Irgafos 168, and Octadecyl 3-(3,5-di-tert-butyl-4-hydroxyphenyl) propionate, Inganox 1076, at 1:1 by weight ratio was employed as heat/processing stabilizer and they were supplied from Ciba Specialty Chemicals Corporation. The oil palm empty fruit bunch (EFB) fiber from local palm oil refinery

was obtained. The cotton pulp as raw fiber form, USA grade, was kindly supplied from cotton yarn weaver. It will be as the individual and combination, as called hybrid fibers, with the other fiber. Properties of the materials used in this research work as given by manufacturers are show in Tables 3.2 to 3.8, respectively.

Table 3.1 Summarization of materials and their function in biocomposite manufacturing.

Chemical name	Trade name	Function
Diglycidyl ether of bisphenol A	Epotec YD-019	Reactive compatibilizer
3-aminopropyltriethoxysilane	A-1100	Coupling agents
<i>gamma</i> -glycidoxypropyltrimethoxy silane	A-187	Coupling agents
Vinyltrimethoxysilane	A-171	Coupling agents
Dicumyl peroxide	-	Free radical initiator
Polyester polyols	Rayelast [®] A 8770	Reactive plasticizer
Tris(2,4-di-tert-butylphenyl) phosphate	Irgafos 168	Heat/processing stabilizer
Octadecyl 3-(3,5-di-tert-butyl-4-hydroxyphenyl) propionate	Inganox 1076	Heat/processing stabilizer

Table 3.2 The properties of the commercial poly(lactic acid); PLA 2002D.

Properties	Value
Chemical structure	$\left[\text{O}-\underset{\text{CH}_3}{\text{CH}}-\overset{\text{O}}{\parallel}{\text{C}} \right]_n \text{O}-\underset{\text{CH}_3}{\text{CH}}-\overset{\text{O}}{\parallel}{\text{C}}-$
Specific gravity	1.24
Melt index, g/10 min (190°C/2.16 kg)	4 - 8
Tensile strength at break, psi (MPa)	7,700 (53)
Tensile yield strength, psi (MPa)	8,700 (60)
Tensile modulus, kpsi (GPa)	500 (3.5)
Notched Izod impact, ft-lb/in (J/m)	0.24 (12.81)

Table 3.3 The properties of silanes.

Properties	A-1100	A-187	A-171
Chemical name	3-aminopropyl triethoxysilane (APS)	<i>gamma</i> -glycidoxypropyl trimethoxysilane (GPS)	vinyl trimethoxysilane (VTMS)
Chemical structure	$\text{H}_2\text{N}-(\text{CH}_2)_3-\underset{\text{OCH}_2\text{CH}_3}{\overset{\text{OCH}_2\text{CH}_3}{\text{Si}}}-\text{OCH}_2\text{CH}_3$	$\text{H}_2\text{C}-\underset{\text{H}}{\overset{\text{O}}{\text{C}}}-\text{CH}_2\text{OCH}_2\text{CH}_2\text{CH}_2-\underset{\text{OCH}_3}{\overset{\text{OCH}_3}{\text{Si}}}-\text{OCH}_3$	$\text{CH}_2=\text{CH}-\underset{\text{OCH}_3}{\overset{\text{OCH}_3}{\text{Si}}}-\text{OCH}_3$
Appearance	Clear, colorless	Clear, colorless	Clear, colorless
Specific gravity at 25°C	1.069	0.950	0.97
Flash point (°C)	110	96	28
Boiling point (°C)	290	220	122

Table 3.4 Proximate chemical composition of EFB and cotton fibers

(Khalid et al., 2008; Rozman et al., 2000; Hegde et al., 2004).

Chemical composition	EFB fiber	Cotton fiber
Cellulose	65 - 77	80 - 90
Hemicellulose	35	4 - 6
Lignin	20 - 25	-

**Figure 3.1** Origin of (a) EFB and (b) cotton fiber**Table 3.5** The properties of solid epoxy resin; Epotec YD-019.

Properties	Value
Chemical name	Diglycidyl ether of bisphenol A
Chemical structure	$\text{H}_2\text{C}-\text{O}-\text{CH}-\text{CH}_2-\text{O}-\left\{ \text{C}_6\text{H}_4-\text{C}(\text{CH}_3)_2-\text{C}_6\text{H}_4-\text{O}-\text{CH}_2-\text{CH}(\text{OH})-\text{CH}_2-\text{O} \right\}_n-\text{CH}_2-\text{CH}-\text{O}-\text{CH}_2$
Epoxide equivalent weight (EEW. g/eq)	2,637
Softening point (°C)	130 - 145
Viscosity at 25°C (40% in butyl carbitol, cPs)	7,490

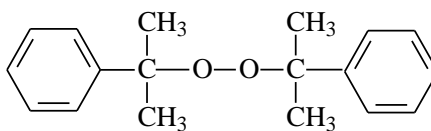


Figure 3.2 Chemical structure of dicumyl peroxide (DCP).

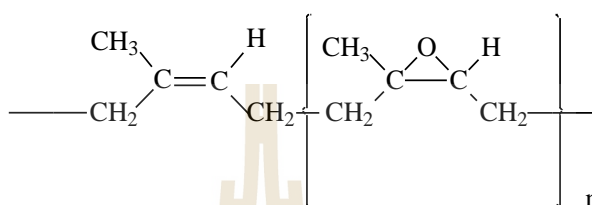


Figure 3.3 Chemical structure of the epoxidized natural rubber.

Table 3.6 The properties of polyester polyols; Rayelast[®] A 8770.

Properties	Value
Chemical structure	$\text{H}-\text{O}-\left[\text{CH}_2-\text{CH}_2-\text{O}-\underset{\text{m}}{\text{C}} \begin{array}{l} \text{O} \\ \parallel \end{array} \text{CH}_2-\text{CH}_2-\underset{\text{n}}{\text{C}} \begin{array}{l} \text{O} \\ \parallel \end{array} \text{O}-\left(\text{CH}_2-\text{CH}_2-\text{O} \right)_m \text{H}$
Appearance	Light yellow liquid
Viscosity at 60°C (cps)	1,500 - 1,800
Hydroxyl value (mg KOH/gm)	54 - 60
Acid number (mg KOH/gm, max.)	1.2 - 1.6
Water Content (max, %)	0.05
Color (Pt-Co, max.)	150

Table 3.7 The properties of tris(2,4-di-tert-butylphenyl) phosphate; Irgafos 168.

Properties	Value
Appearance	White powder
Purity (min, %)	99.0
Melting point (°C)	183 - 187
Volatility (%)	0.3
Clarity of solution	Clear
Acid value (mgKOH/g) (max, %)	0.3
Anti hydrolyze (90°C, water 14 hrs)	Qualified
Transmittance	(425nm) 96% min; (500nm) 98% min

Table 3.8 The properties of octadecyl 3-(3,5-di-tert-butyl-4-hydroxyphenyl) propionate; Inganox 1076.

Properties	Value
Appearance	White crystal powder
Purity (min, %)	98.0
Melting point (°C)	50 - 55
Volatility (max, %)	0.5
Flash point (°C)	110
Ash (max, %)	0.1
Transmittance	(425nm) 96% min; (500nm) 98% min

3.2 Preparation of fiber

For oil palm empty fruit bunch fibers preparation, the fiber was soaked in water for overnight. After that, fiber was compressed to remove excess water and then transferred into internal mixer chamber, Haake Rheomix 3000P Model 557-1306, at 170°C and ground by using Banbury rotors at the rotors speed of 100 rpm for 15 minutes. The heat treated fiber then was mercerized by constantly boil in 3% wt/v sodium hydroxide (NaOH) solution for 4 hours. Then the chemical treated fiber was then flooded with water several time until the natural stage was detected. The first time treated EFB fiber was then mercerized again in the same manner as described. The reason for doing the mercerization process twice is because there is a large amount of oil residue in the fiber. One time mercerization might not enough to remove the oil contamination. The heat/chemical treated fiber was finally dried in oven at 80°C for several hours until there is no major moisture detected.

For the cotton fiber, the heat and alkali treatment were performed in the same procedure as for EFB fiber except that the sodium hydroxide solution used in the mercerization step was decreased to 2% wt/v. The cotton fiber was treated for one time mercerization. The reason for reducing the concentration of the alkaline solution is due to the fact that cotton is less contaminated than the EFB. So, there is no need much of the alkaline in the reaction as for the oil palm fiber. Use less alkaline concentration mean less in capital cost and less environmental pollution.

Moisture depleted EBF and cotton fibers were eventually treated with silane before used to prepare the composite material. The treatment process was performed by reacting the silane and fiber in the internal mixer at 120°C and rotor speed of 100

rpm for 6 minutes, respectively. The treated fiber was sealed in plastic bag and allowed to rest at room temperature overnight.

3.3 Composite compounding

In two roll mill, Chachareon, with the rolls diameter of 60 mm, the ENR50 was plasticated for a few minutes and then the solid epoxy was incorporated until smooth milky mixture obtained. After that, the treated fiber and talc powder were gradually added into the rubber mixture. This fiber and filler cooperation process would last at least 15 minutes. The rubber compound was stored at temperature below 0°C in freezer for overnight. Then, solid hard rubber/fiber compound was immediately crushed into small pieces by using motor driven crusher. Temperature hardening assists the compound to be easily ground without sticking onto jaws crusher.

The co-rotating intermeshing twin screw extruder from Brabender Model PL2100 having the screws diameter of 25 mm and L/D ratio at 20, was established for mixing equipment. The mixer is consisted of 3 triple disks kneader zones. PLA and ground rubber/fiber compound pellets were evacuated in the oven at 80°C for 2 hours prior to mix. The dried PLA and rubber/fiber were dried blend with peroxide, high viscous liquid polyester polyols and heat/processing stabilizer powder in mixing bowl. The ingredients were manually and vigorously stirred using metal paddle. The pre blended materials was constantly fed into twin screw mixer through the pre calibrated single screw feeder to maintain the fill factor below 1.0. In the twin screw melt mixing process, temperature at 150, 160, 170, 180 and 190°C from feeding zone

to die zone, respectively, and the screw speed at 12 rpm was electronically controlled. The composite was then coarse ground in motor driven crusher.

3.4 Specimen preparation

The test specimen was prepared by injection molding. The composite pellets obtained from the above procedure were dried in vacuum oven at 80°C for at 2 hours to remove any residue moisture present before injection molding. The injection molding employed in the study was Chuan Lih Fa Machine Model CLF-80T with four cavities and edge gates two plats mold. The injection conditions were achieved at the barrel temperature for all zones at 190°C. The rectangular specimen with the dimension of 13×128×4 mm was obtained.

The composite test specimens were divided into 3 categories of samples. One was allowed to anneal at room temperature for at least 24 hours, and they were called as original sample. The second set of specimen was incubated in sauna simulated condition in which oven filled with saturated water vapor at 60°C. The incubation period was 12 hours and it was called as sauna treatment sample. This sauna process would accelerate the completion of crosslink reaction via the silane and water condensation reaction. The last group of sample was obtained by vacuum drying of sauna treated samples at 80°C for at least 2 hours. This type of sample was occasionally performed to verify the effect of residual moisture presented in the sauna cure step on the properties of the composite.

3.5 Performance testing and characterization

3.5.1 Melt flow index (MFI)

Melt flow index of the composites were performed as ASTM D1238 using the Kayeness melt flow indexer at 190°C with load of 2.16 kg and 10.00 kg assigned as 190/2.16 and 190/10.00, respectively.

3.5.2 Heat deflection temperature (HDT)

Regarding to ASTM D648, heat deflection temperature (HDT) was examined using Atlas Testing Machine, Model HDV1. The heating rate used at $2\pm 0.2^\circ\text{C}/\text{min}$. The samples were heated from ambient temperature to the desired value by using silicone oil as heating transfer media. The injected rectangular cross section specimen with 128 mm in length, 13 mm in depth, and 4 mm in width were tested. Three specimens were immersed under the calculated loading weight at the assigned standard load, 0.45 MPa, and span length of 100 mm. The HDT was recorded from the thermometer when the specimen had been deflected to 0.25 mm or 0.010 in.

3.5.3 Izod impact testing

Impact tests were conducted according to ASTM D256 using the Atlas Model BPI impact testing machine. The test specimens with 13 mm in thickness, 64 mm in length, and 4 mm in width were obtained by saw cutting from the injection molding sample. For the notched mode of impact test, the 5 specimens were V-notched by using standard notch machine, Union TSL. Notches 3.0 mm deep were cut into sample. The impact resistance testing for both unnotched and notched modes were performed at the striking energy of 2.7 J. The impact strength was calculated, averaged and reported as SI unit, kJ/m^2 . The figure was obtained from the failure energy divided by the cross section area of the sample.

3.5.4 Flexural testing

The flexural properties of samples were determined using a universal testing machine, Instron Model 5565, with load cell of 5 kN at 25°C. The standard test method, ASTM D790, with the three points bending test fixture was followed to determine flexural characteristic. The flexural strength and modulus were resolved. The test specimen was calculated and adjusted. The injected test specimen having the same dimensions as described for the HDT testing was employed.

3.5.5 Morphological properties

The morphology of fractured surface of the biocomposite specimens were taken from notched Izod impact testing were examined using scanning electron microscope (SEM) Jeol Model JSM 6400. The specimens were cut at the thickness of 5 mm below the fractured surface. It was placed on the sample holder and coated and adhered by silver paint. Fracture surface was again coated by electro deposition by gold ion sputtering for 5 minutes.

3.5.6 Biodegradability

The biodegradability testing of sample were conducted by using simulated landfill chamber. Within chamber, it was filled with composted soil at 60°C. The aerobic atmosphere was imitated by constantly feeding of oxygen gas or pumping the fresh air into the compost. The test specimens were immersed in water overnight and pre weighing before test. They were then buried in the soil at approximately 2 inches in depth. The samples were removed to monitor the weight loss every 2 weeks. The weight loss percentage was calculated by the following equation 3.1.

$$\text{Weight loss (\%)} = \frac{(W_0 - W_t)}{W_0} \times 100 \quad (3.1)$$

Where W_0 = Weight of test sample before burial

W_t = Weight of test sample after burial for given buried time(t)

3.6 Analysis of DOE using Design Expert™

The design of experimental (DOE) by mean statistical approach conducted in this research was 2^k factorial method. The k components are the interested design parameters. Each parameter (k) for each test is divided into two levels and arbitrarily called “low (-)” and “high (+)”. For example, mostly 3 parameter factors that was “ 2^3 ” factorial was designed. Then, the total of 8 conditions of experiments were conducted. Table 3.9 shows the example of the design matrix for $k = 3$. One or more responds are needed for analysis. It will be used to verify the effect of the given parameter on the individual respond. The interaction between the parameters, such as AB, ABC and so on, that affect to the respond will also be analyzed.

An alternative to the normal probability plot of factor effects is the half-normal plot. This is a plot of the absolute value of the effect estimates against their cumulative normal probabilities. The straight line on half normal plot always passes through the origin and should also pass close to fiftieth percentile data value.

The degree of significant (α) is given at 95% confidential for this study. The calculation of significant level of the experimental data is verified by using Design Expert™ version 7.0.0, which is the commercial statistical software analysis to assist the statistical figure calculation. The significant effects from half-normal plot can be

also confirmed by ANOVA testing. If p -value less than 0.05 indicate that the calculated effect(s) is/are significantly affected by the design parameter(s).

Table 3.9 The 2^3 factorial design matrix.

Condition	Factor			Interaction				Response
	A	B	C	AB	AC	BC	ABC	Y_i
1	+	+	+	+	+	+	+	
2	+	+	-	+	-	-	-	
3	+	-	+	-	+	-	-	
4	+	-	-	-	-	+	+	
5	-	+	+	-	-	+	-	
6	-	+	-	-	+	-	+	
7	-	-	+	+	-	-	+	
8	-	-	-	+	+	+	-	

The effects of factors are calculated by averaging the responses of each factor at the plus (+) level and subtracting the average at the minus (-) levels for same factor as show in equation 3.2. Then, the calculated effects were ranked, i , from minimum to maximum. The p -value is area under the normal distribution. According to the design of experiment method, p -value is calculated from equation 3.3 where i is the rank of effect $i(E_{f,i})$. Accordingly, Z -value as cumulative probability, as shown in Figure 3.4, is obtained from the conversion of p -value as summarized in Table A-1 and A-2 of the appendix A.

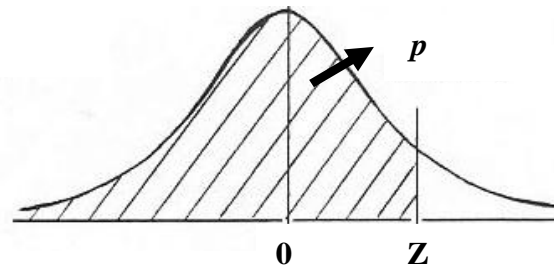


Figure 3.4 Normal distribution curve.

$$E_{f,i} = \frac{\sum Y_{(E+)}}{n/2} - \frac{\sum Y_{(E-)}}{n/2} \quad (3.2)$$

$$p = \frac{i-0.5}{2^k - 1} \quad (3.3)$$

Where

$E_{f,i}$ = The effect value of responses i

$Y_{(E+)}$ = The responses of high level factor

$Y_{(E-)}$ = The responses of low level factor

p = Probability

k = Number of factor are used design

i = Rank number of the effect, that order by followed effect value ($E_{f,i}$)

Table 3.10 Calculation method for the standard effect values.

Rank (<i>i</i>)	Effect value ($E_{f,i}$)	<i>p</i> -value	Z-value
1	$E_{f,1}$	$\frac{1-0.5}{2^k-1}$	
2	$E_{f,2}$	$\frac{2-0.5}{2^k-1}$	
3	$E_{f,3}$	$\frac{3-0.5}{2^k-1}$	
...	
...	
...	
2^k-1	$E_{f,2^k-1}$	$\frac{(2^k-1)-0.5}{2^k-1}$	

CHAPTER IV

RESULTS AND DISCUSSION

4.1 Design of Experiment#1: Effect of fiber, silane and solid epoxy

Attempting to manufacture the natural fiber reinforced composite based on PLA matrix, absolute green composite, optimization of the compound constituents was statistically performed by mean of 2^k factorial design of experiment (DOE). The thermal, rheological and mechanical, including flexural and impacts, properties were measured and used as the statistical response for analysis. In this section, the treated palm oil fiber, 3-aminopropyltriethoxysilane (APS; A-1100) and solid epoxy loading in the composite ingredients are investigated. They are statistically assigned as parameter A, B and C, respectively. Epoxidised rubber (ENR50) and heat and processing stabilizer were constantly added at 20, 2 phr, respectively (Meekum, 2010). The levels of the given parameters are shown in Table 4.1. According to the rule of design, $2^3 = 8$, eight combinations with difference in the parameters levels were designed and they are summarized in Table 4.2. The measures responses are also given in Table 4.3.

Roughly scanning the test results obtained, it is obviously seen that there are remarkable different between the original samples and the samples that underwent sauna treatment. It indicates that silane/moisture condensation reaction via sauna incubation generally shows the higher in test values than the atmospheric annealing ones. This observation suggests that the condensation reaction might trigger the macro

crosslinked polymer chain or the bonded between fiber and matrix phase and hence enhance the interfacial bonding. However, closer investigation by mean of statistical calculation using the DOE method as described above in order to verifying the main effect of the parameter(s) used on the properties of composite is necessarily at the degree of the analysis significant of 95% confidential. The DOE results include the normal plot, pareto chart and also the ANOVA conclusion of both original and cured samples are following.

Table 4.1 The parameters and levels for DOE.

Parameters	Low level (-1)		High level (+1)	
	EFB fiber (phr)	10	25	40
Silane (phr)	1.0	3.5	4.0	7.0
Solid epoxy (phr)	0.5	1.5	2.0	3.0

Table 4.2 The 2³ factorial design matrix.

Condition	Factor			Interaction				Composition (phr)					
	A	B	C	AB	AC	BC	ABC	(A) EFB fiber	(B) Silane (APS; A-1100)	(C) Solid epoxy	PLA	ENR50	Stabi- lizer
Run#1	+	+	+	+	+	+	+	(+)40	(+)4.0	(+)2.0	100	20	2
Run#2	+	+	-	+	-	-	-	(+)65	(+)7.0	(-)0.5	100	20	2
Run#3	+	-	+	-	+	-	-	(+)40	(-)1.0	(+)3.0	100	20	2
Run#4	+	-	-	-	-	+	+	(+)65	(-)3.5	(-)1.5	100	20	2
Run#5	-	+	+	-	-	+	-	(-)10	(+)7.0	(+)3.0	100	20	2
Run#6	-	+	-	-	+	-	+	(-)25	(+)4.0	(-)1.5	100	20	2
Run#7	-	-	+	+	-	-	+	(-)10	(-)1.0	(+)2.0	100	20	2
Run#8	-	-	-	+	+	+	-	(-)25	(-)3.5	(-)0.5	100	20	2

Table 4.3 Results of the designed responses.

Condition	Composition (phr)			MFI at 190/2.16 (g/10min)	HDT (°C)		Notched impact strength (kJ/m ²)		Unnotched impact strength (kJ/m ²)		Flexural strength (MPa)		Flexural modulus (GPa)	
	(A) EFB fiber	(B) Silane (APS; A-1100)	(C) Solid epoxy		original	cured	original	cured	original	cured	original	cured	original	cured
Neat PLA	0	0	0	5.531±0.372	53.7±0.6	53.5±0.5	2.19±0.21	2.03±0.12	20.54±1.26	24.47±1.11	111.65±1.25	111.86±2.78	3.07±0.05	2.93±0.12
Run#1	(+)40	(+)4.0	(+)2.0	49.915±1.562	55.0±0.0	59.3±4.0	4.27±0.42	5.00±0.38	10.24±0.41	9.19±1.09	42.84±2.10	47.33±2.69	2.28±0.24	2.65±0.04
Run#2	(+)65	(+)7.0	(-)0.5	38.483±2.629	53.5±1.5	60.7±5.5	3.85±0.21	4.09±0.45	5.94±0.21	8.51±0.79	31.72±1.88	33.04±7.11	2.56±0.31	2.50±0.29
Run#3	(+)40	(-)1.0	(+)3.0	20.842±1.777	54.0±1.0	58.0±0.0	4.20±0.37	4.96±0.26	11.49±1.21	13.02±1.05	55.72±5.02	52.54±4.76	2.54±0.16	2.71±0.04
Run#4	(+)65	(-)3.5	(-)1.5	21.276±2.527	55.5±0.5	65.3±3.1	4.60±0.32	4.88±0.31	10.55±1.23	12.49±0.75	42.12±6.91	47.37±1.20	2.65±0.15	2.66±0.17
Run#5	(-)10	(+)7.0	(+)3.0	79.023±3.079	55.0±0.0	54.0±1.0	5.20±0.76	6.47±0.37	15.62±2.10	15.21±0.79	66.69±5.53	66.76±0.94	2.49±0.17	2.45±0.05
Run#6	(-)25	(+)4.0	(-)1.5	69.810±6.033	56.1±0.3	55.0±0.0	5.39±0.39	6.13±0.09	13.99±2.23	12.74±0.29	59.34±0.97	60.01±2.47	2.52±0.04	2.49±0.06
Run#7	(-)10	(-)1.0	(+)2.0	49.796±1.623	54.3±0.3	53.0±0.0	4.60±0.67	6.09±0.28	12.25±1.88	16.17±1.65	66.67±2.66	67.58±1.57	2.54±0.11	2.41±0.19
Run#8	(-)25	(-)3.5	(-)0.5	45.534±1.677	54.7±0.6	55.7±0.6	5.49±0.22	6.18±0.26	12.30±0.86	14.99±0.44	59.09±3.17	58.63±4.62	2.55±0.07	2.49±0.17

4.1.1 The MFI analysis

Rheological properties by mean of the melt flow index obtained at 190/2.16 from run#1 to run#8 are illustrated in Table 4.3. Taken these responses into the standard effects calculation for the individual parameter and also the interacted parameters by assisting of Design ExpertTM computer program and then converting the values into normal probability are performed. Consequently, the plot between the normal % probability and their effects are constructed as illustrated in Figure 4.1. From the normal plot, it is obviously seen that the fiber (-A) and silane (+B) contents, which are negative and positive effects respectively, are excluded from the linear trend line. It is indicated that these two parameter are probably significant effect on the flowability of the green composites but others are not. Not only the normal plot is employed to conclude the effect of the parameter on the MFI of the composite but also the pareto chart is also presented as shown in Figure 4.2. The chart confirms that the calculated t -values derived from parameters A and B are higher than the critical t -value. It reviews that these two factors are significant effect to the flowability of the biocomposites. The ANOVA testing for the MFI response at the given degree of confidence are reported in Table 4.4. The test result conclude that the designed model; fiber, silane and epoxy contents and their levels, is significant as the calculated p -value, 0.0003, of the model lower the given critical value, 0.05. Furthermore, the fiber content (-A) and silane content (+B) are negatively and positively significant effects on MFI, correspondingly. As seen also from the calculated p -value of the parameters A and B, are 0.0005 and 0.0009 in which are lower the assigned value at 0.05. It is meant that the viscosity of the composite will be increased, lower MFI, with increasing the fiber content as it is usual phenomena for the rheological behavior of

fiber reinforced composite. For the addition of silane into the biocomposite ingredient, the MFI is increased, lower in viscosity, with increasing the silane content. However, if the reinforced material undergo sauna treatment the flow index of the material would perhaps be decreased because the addition of silane will induce bonding between the chains or with the surface of the fiber as seen in the crosslink process for the polyolefin (Beltran and Mijangos, 2000). Consequently, the viscosity of the polymeric material will be increased.

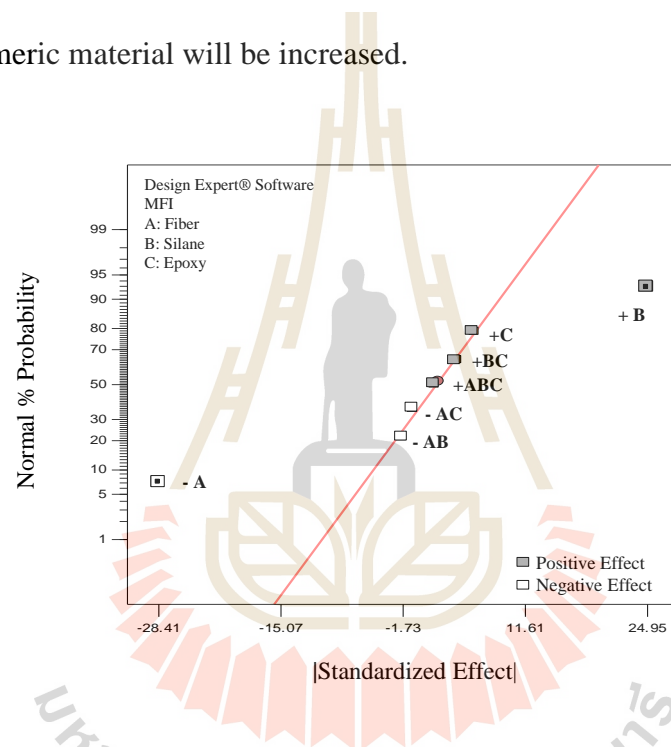


Figure 4.1 The normal plot of the standard effect obtained from the MFI.

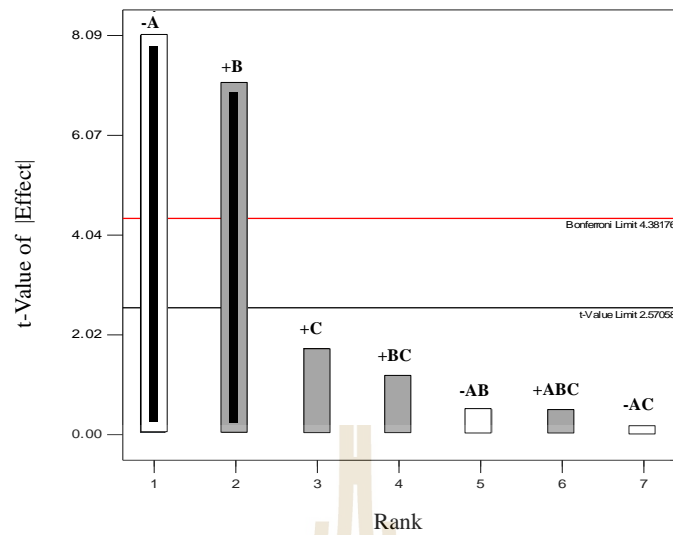


Figure 4.2 The pareto chart of the MFI.

Table 4.4 ANOVA results obtained from the MFI.

Source	Sum of squares	df	Mean square	<i>f</i> -value	<i>p</i> -value
Model	2859.296	2	1429.648	57.911	0.0003
A-Fiber	1614.540	1	1614.540	65.400	0.0005
B-Silane	1244.756	1	1244.756	50.422	0.0009
Residual	123.435	5	24.687		
Cor Total	2982.731	7			

4.1.2 Analysis of HDT

HDT as service temperature of the green composite derived from designed experiment are also presented as one of the analysis responses. It is seen that the HDT of original samples, as seen in the Table 4.3, are approximately at 55°C. They are roughly equal to the value obtained from neat PLA. However, after the sauna treatment some of the sample such as run#1, 2, 3 and 4, are risen and superior

than pure PLA. Within this designed experiment, run#4 samples, high fiber content but low silane and epoxy contents, shows the maximum HDT value at $65.3 \pm 3.1^\circ\text{C}$.

The statistical evaluation by mean of normal plot for the original samples as shown in Figure 4.3. The plot hints that the silane (+B), interaction of fiber and silane (-AB), and fiber and solid epoxy (+AC) are out of linear trend line. These parameters might be the significant effect to the HDT of the original sample. Together with the pareto chart provided in Figure 4.4 shows that HDT value is not significantly affected either by the designed model and parameters. According to the constructed chart, it reveals that the calculated t -values of B, AB and AC are below the limited t -value. The non significant of the parameters can be concluded. With the assisting of the ANOVA testing results at 95% of confidential, they are given in Table 4.5. From the statistical conclusion, they enlighten that the designed model with p -value equal to 0.6037 which is higher than the given critical value at 0.05. Therefore, the designed model, both parameter and level of contents, is not significant on the HDT. Hence, factor B, AC and AB are also non significant as indicated by higher in the calculated p -value than 0.05.

On the other hand for sauna incubated samples, the normal plot displays that fiber content (+A) and silane (-B) which are positive and negative effect on HDT are excluded from the linear line as shown in Figure 4.5. The potential to be the significant parameters are high. At the same time, the pareto chart in Figure 4.6 illustrates that only t -value of fiber (+A) is beyond the critical t -value but not for the silane (-B). Statistical confirmation by ANOVA, the test result summarizes in Table 4.6. It is seen that calculated p -value of the design model and fiber content are 0.0439 which are lower than that the critical value. But the Figure for silane is higher than the

critical value. The conclusion can be made that fiber content (+A) is positively and significantly effects on the biocomposite sample after sauna treatment. Meaning that if biocomposite with high HDT is required, the fiber loading will set at high level of loading, more than 40 phr. From the analysis, higher in heat resistance of the composite can be dissolved from the fact that EBF fiber, at high level of content, prevent the deformation of the polymer matrix in the composite. Hence, the material can withhold the rising of surrounding temperature without major deformation. The other important possibility in the superior in HDT of high fiber loading composite is that the chemical reaction via silane coupling agent during sauna treatment process provide the interfacial network bonding between the reinforcement and matrix. Therefore, if the structure is become stiffer then the thermal resistance of sample will be improved. SEM investigation will be discussed and used to strengthen this statement later on.

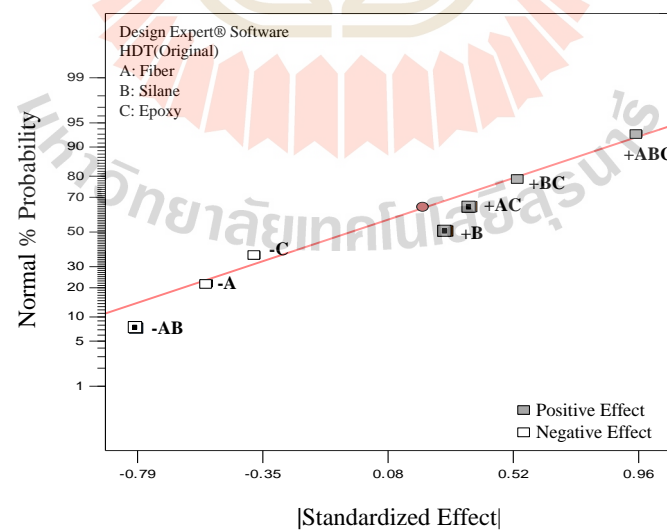


Figure 4.3 The normal plot of the standard effect obtained from the HDT (original)

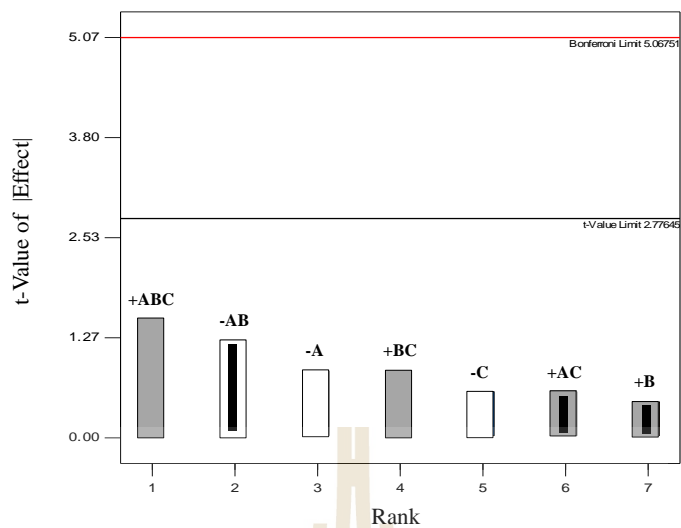


Figure 4.4 The pareto chart of the HDT (original).

Table 4.5 ANOVA results obtained from the HDT (original).

Source	Sum of squares	df	Mean square	<i>f</i> -value	<i>p</i> -value
Model	1.705	3	0.568	0.691	0.6037
B-Silane	0.170	1	0.170	0.207	0.6729
AB	1.253	1	1.253	1.523	0.2847
AC	0.281	1	0.281	0.342	0.5902
Residual	3.292	4	0.823		
Cor Total	4.997	7			

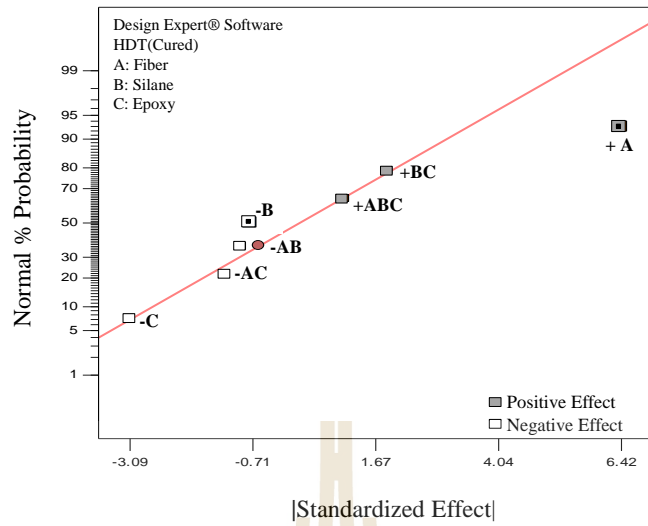


Figure 4.5 The normal plot of the standard effect obtained from the HDT (cured).

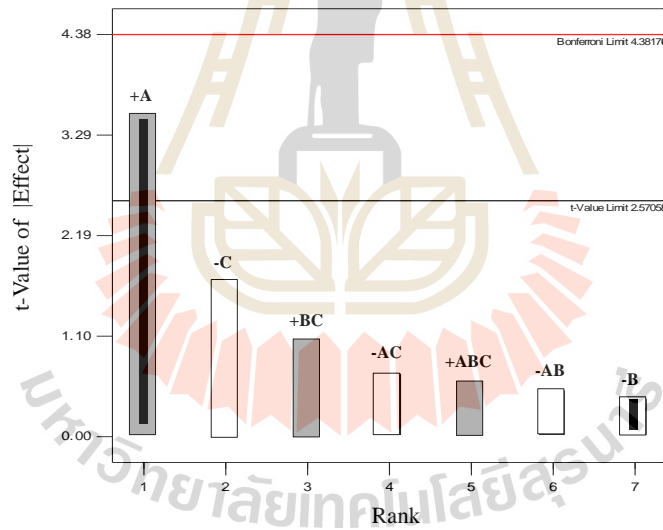


Figure 4.6 The pareto chart of the HDT (cured).

Table 4.6 ANOVA results obtained from the HDT (cured).

Source	Sum of squares	df	Mean square	<i>f</i> -value	<i>p</i> -value
Model	83.429	2	41.715	6.226	0.0439
A-Fiber	82.304	1	82.304	12.284	0.0172
B-Silane	1.125	1	1.125	0.168	0.6989
Residual	33.501	5	6.700		
Cor Total	116.931	7			

4.1.3 Impact strength of biocomposite

According to the test results summarized in Table 4.3 reveal that the composites with sauna treatment exhibit merely higher impact strength than the sample without the treatment for both notched and unnotched test modes. The silane/water crosslink would probably respond for the toughness enhancement of the composite.

The normal plot and pareto charts of the notched impact strength for the sample without sauna incubation are displayed in Figure 4.7 and 4.8, respectively. The statistical plot shows that the fiber (-A) and solid epoxy (-C) are out of the linear trend line. They are both negative (-) effect to the impact strength. In pareto chart, only *t*-value of factor A is higher the critical *t*-value. It is indicated that only fiber content is negatively and significantly effect on the notched impact strength of the biocomposite. ANOVA summarization shown in Table 4.5 confirms that the experimental model is significant as well as the fiber content as the calculated *p*-value at 0.0296 is obtained. The value is less than the assigned critical value at 0.05. It is

meant that the notched impact strength of the composite before sauna cured will be decreased with increasing the fiber content.

Similarly for the samples obtained from sauna treatment, the normal plot and also pareto chart are shown in Figure 4.9 and 4.10, respectively. There are two parameters that have possibility to be the significant effects to the impact strength. There are fiber content which is negative effect (-A) and the interaction between silane and epoxy which is positive effect (+BC). Because these two effects are excluded from the linear trend. Assisted by the pare to chart, it indicates that only t -value of the fiber content (A) is greater than the critical t -value. The result reveals that the level of fiber content has significant influence on the impact strength of the biocomposite. The ANOVA conclusion as presented in Table 4.8, reinforces that the parameters used in the designed models are significant because p -value of the model is 0.0025 that is lower the critical value at 0.05. Furthermore, the fiber content is also negatively and significantly (-A) effect on the impact strength of the sauna cure biocomposite. It can be implied that the impact strength of cured sample will decrease with increasing the fiber loading. This observation is similar to those original samples.

Taken the results both from original and cured sample, they are indicated that the fibers loading (-A) is negatively and significantly effect to the impact strength of the composite. It means that the impact strength of the composite will decrease when it is made from high EFB fiber content. It can be mechanically explained by the poor adhesion between the fiber and polymer matrix and hence the crack tips are quickly propagated through these weak regions.

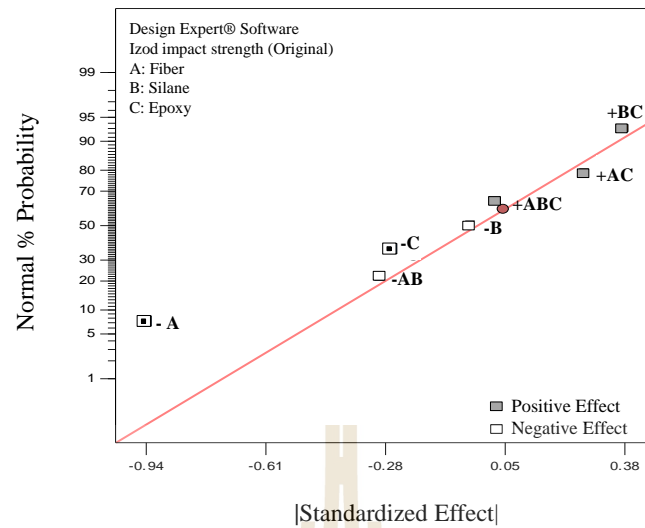


Figure 4.7 The normal plot of the standard effect obtained from the notched impact strength (original).

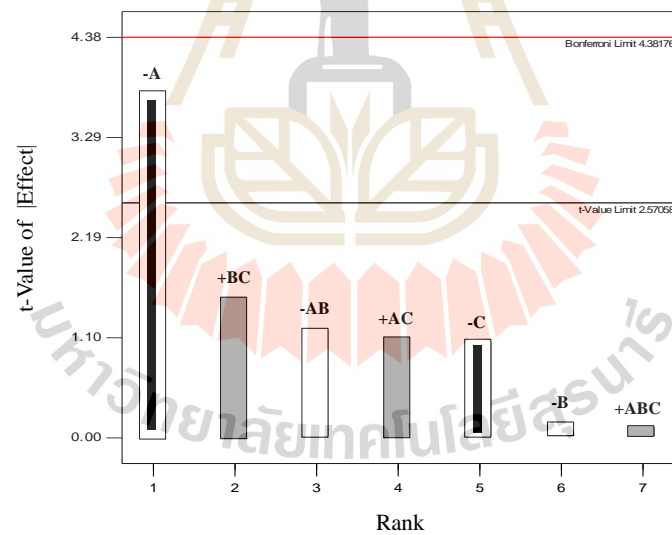
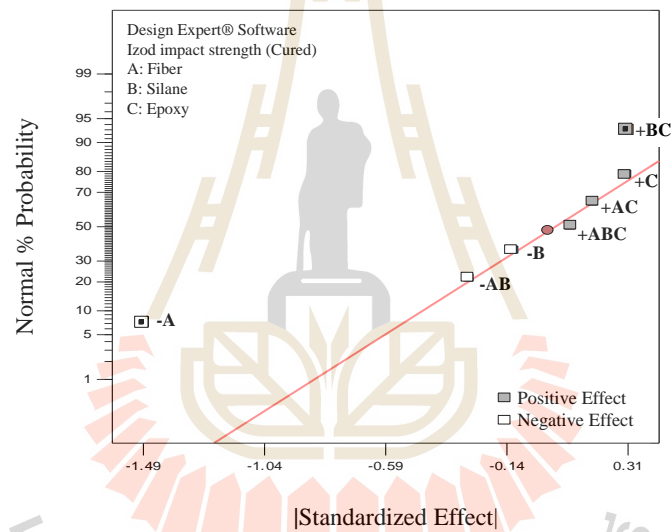


Figure 4.8 The pareto chart of the notched impact strength (original).

Table 4.7 ANOVA results obtained from the notched impact strength (original).

Source	Sum of squares	df	Mean square	<i>f</i> -value	<i>p</i> -value
Model	1.907	2	0.954	7.720	0.0296
A-Fiber	1.770	1	1.770	14.328	0.0128
C-Epoxy	0.137	1	0.137	1.112	0.3400
Residual	0.618	5	0.124		
Cor Total	2.525	7			

**Figure 4.9** The normal plot of the standard effect obtained from the notched impact strength (cured).

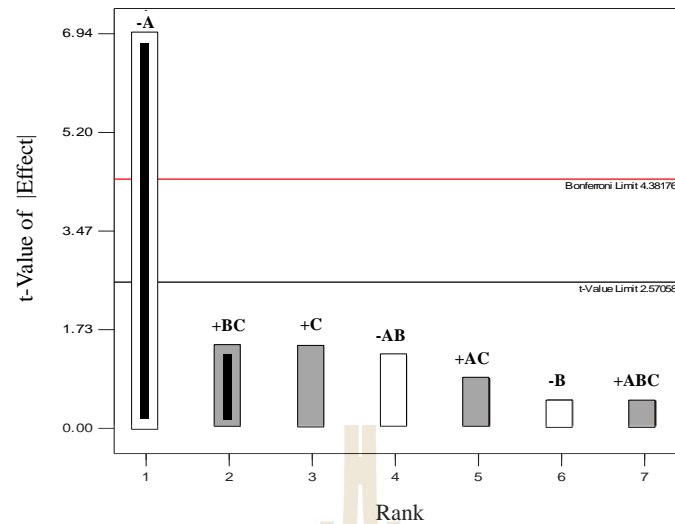


Figure 4.10 The pareto chart of the notched impact strength cured).

Table 4.8 ANOVA results obtained from the notched impact strength (cured).

Source	Sum of squares	df	Mean square	<i>f</i> -value	<i>p</i> -value
Model	4.626	2	2.313	25.140	0.0025
A-Fiber	4.429	1	4.429	48.137	0.0010
BC	0.197	1	0.197	2.142	0.2032
Residual	0.460	5	0.092		
Cor Total	5.086	7			

For the impact behavior without stress concentration tip, namely unnotched testing mode, Figure 4.11 and 4.12 are the normal plot and pareto chart of the unnotched impact response before sauna incubation, respectively. The plot reveals that most of the single and interacted parameters are well fitted with the linear trend except for the fiber content factor (-A) and interaction between fiber and silane contents (-AB) which are both negative effects to the unnotched impact strength. They are possibly indicated as significant parameters for the unnotched impact

property. Spontaneously observation with the pareto chart, it reveals that both -A and -AB have t -values higher than the critical one. It is strengthened that these two parameters are significant effect to the unnotched of the fiber composite. The ANOVA testing outcome as reported in Table 4.9 concludes that both the designed experiment models and also the parameters, fiber content (-A) and interaction between fiber and silane contents (-AB), are significant effect to the unnotched impact strength of the original composite samples as p -values of model and the parameters are lower than the critical value. Superior unnotched impact strength of the composites without surface improvement via the silane/moisture condensation reaction can be obtained by manufacturing the sample with low level of fibers content. The negative interaction between -AB, it suggests that if adding high fiber but low level of silane ((+A) \times (-B) = -AB) or vice versa without assisting of sauna cure, the unnotched toughness of the composite would become incompetency.

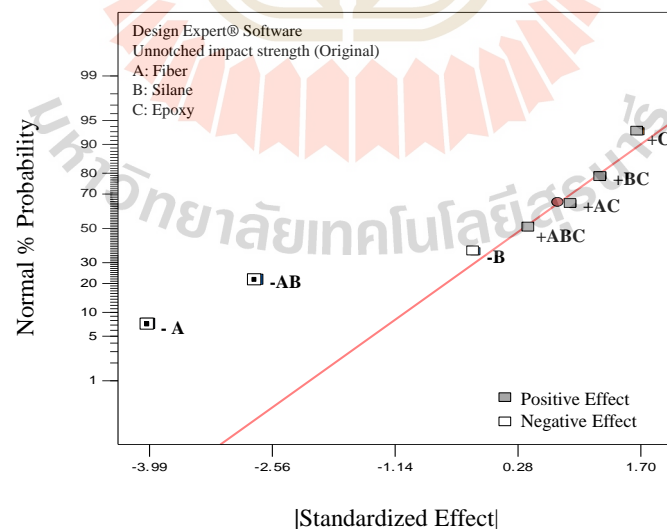


Figure 4.11 The normal plot of the standard effect obtained from the unnotched impact strength (original).

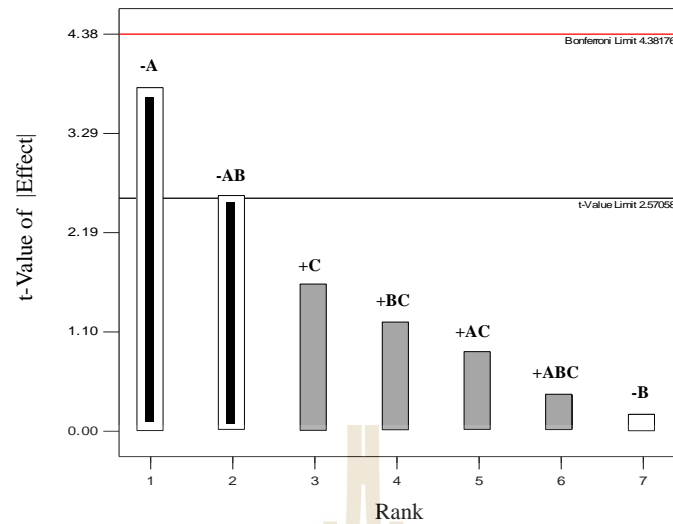


Figure 4.12 The pareto chart of the unnotched impact strength (original).

Table 4.9 ANOVA results obtained from the unnotched impact strength (original).

Source	Sum of squares	df	Mean square	<i>f</i> -value	<i>p</i> -value
Model	46.697	2	23.349	10.527	0.0161
A-Fiber	31.768	1	31.768	14.324	0.0128
AB	14.929	1	14.929	6.731	0.0486
Residual	11.089	5	2.218		
Cor Total	57.787	7			

On the other hand, the normal plot and pareto chart, for the case where the composite was cured, are presented in Figure 4.13 and 4.14, respectively. The plot shows that solid epoxy content (+C), and interaction between fiber and silane contents (-AB) slightly beyond the linear trend line. To verify either these two factors are significant effect on the unnotched impact strength or not, the chart of *t*-value against effect ranking is taken into account. The pareto reviews that both calculated *t*-values

of +C, and -AB are lower than the critical value. Consequently, these parameters are most likely to be non significant effect on the unnotched impact strength of sample after sauna treatment. Moreover, the ANOVA conclusion as given in Table 4.10 also confirms that the p -value of model ($p = 0.7587$) and also of those factors ($p = 0.6024$ and 0.6223) are above the critical value. Within the boundary of this experiment, the calculated figures conclude that the designed model, both parameters and their level of the composite constituent contents, has no significant on the unnotched impact strength of the composited obtained after sauna curing process.

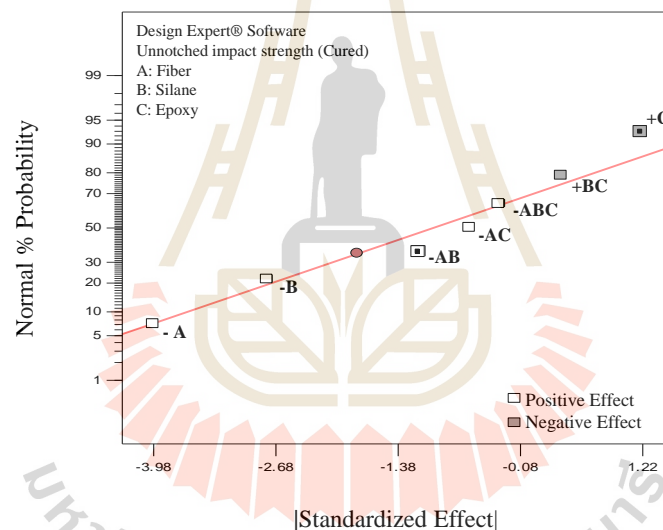


Figure 4.13 The normal plot of the standard effect obtained from the unnotched impact strength (cured).

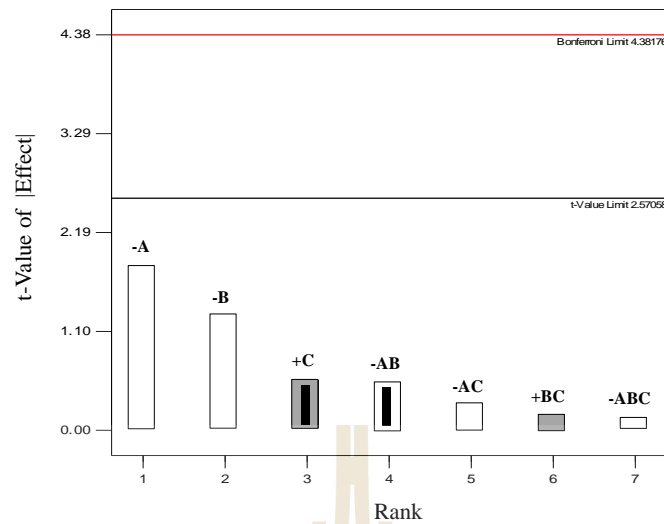


Figure 4.14 The pareto chart of the unnotched impact strength (cured).

Table 4.10 ANOVA results obtained from the unnotched impact strength (cured).

Source	Sum of squares	df	Mean square	<i>f</i> -value	<i>p</i> -value
Model	5.596	2	2.798	0.292	0.7587
C-Epoxy	2.959	1	2.959	0.309	0.6024
AB	2.637	1	2.637	0.275	0.6223
Residual	47.917	5	9.583		
Cor Total	53.513	7			

4.1.4 Flexural properties

General observation of the flexural properties of the samples in Table 4.3, it is noticed that most of the flexural strength obtained from sauna cured sample are slightly superior to the sample without curing. Vice versa, the flexural modulus is marginally lower. Again, this observation indicates that the reaction rise from the silane/moisture incubation procedure might improve somehow the interfacial

interaction between polymer matrix and the surface of fiber reinforcement. As it happen, rising in the bending toughness of the material would be evidenced.

Statistical evaluation by mean of the standard normal probability plot, pareto chart and ANOVA testing are presented in Figure 4.15, 4.16 and Table 4.11, respectively. From Figure 4.15, it is seen that only interacted factor between fiber and silane contents which is negative effect (-AB) on the flexural strength is obviously out of linear trend. As previous discussion, it is suspected to be the significant factor. However, confirmation of the pareto result, it reveals that its calculated t -value is not higher than critical number. So, it confident to say that this factor is most likely to be non significant parameter. Strengthen with the ANOVA conclusion, Table 4.11, it strongly reckons that the designed experiment is not significant. So that the suspected parameter.

In the contrary of the original sample, the statistical analysis of the sauna cured samples as given from Figure 4.17, 4.18 through Table 4.12, consecutively. The standard plot demonstrates that only fiber content (-A) is undoubtedly beyond the linear trend. It is also negative effect on the bending strength. It is no doubt to confirm that this factor is significant influence to the strength as the calculated t -value from the pareto chart, Figure 4.18, is much higher than the key figure. Moreover, the ANOVA conclusion as summarized in Table 4.12 points out that the calculated p -value ($= 0.0059$) of the design is visibly lower than 0.0500. From all of the statistical findings, it is no hesitation to conclude that fiber loading is negative and significantly effect on the flexural strength of the PLA/EFB palm oil biocomposite that undergone silane/moisture incubation at 60°C. So, adding to much palm oil fiber into the PLA matrix will inferior the flexural strength of the composite.

This is because the fact that, according to the rule of mixture, if volume fraction of fiber is increased but the fraction of matrix decreased and hence the strength of the composite will be decreased. Other hypothesis can be taken into account that loading natural fiber into the matrix at high level of content it would create more voids into the material. Consequently, highly brittle composite will be obtained.

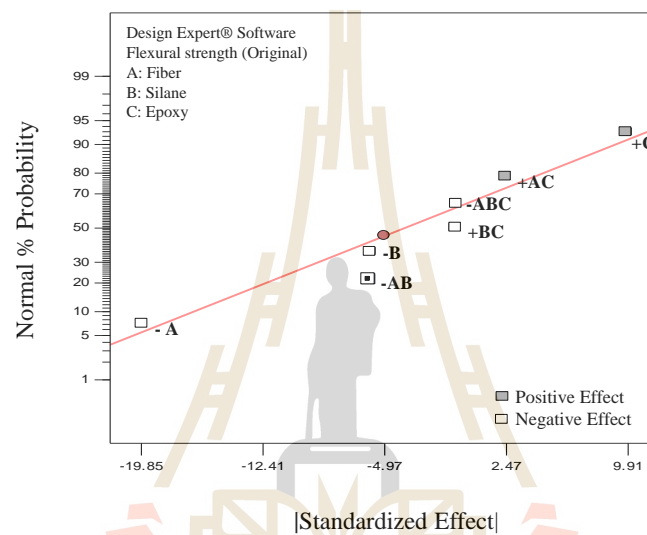


Figure 4.15 The normal plot of the standard effect obtained from the flexural strength (original).

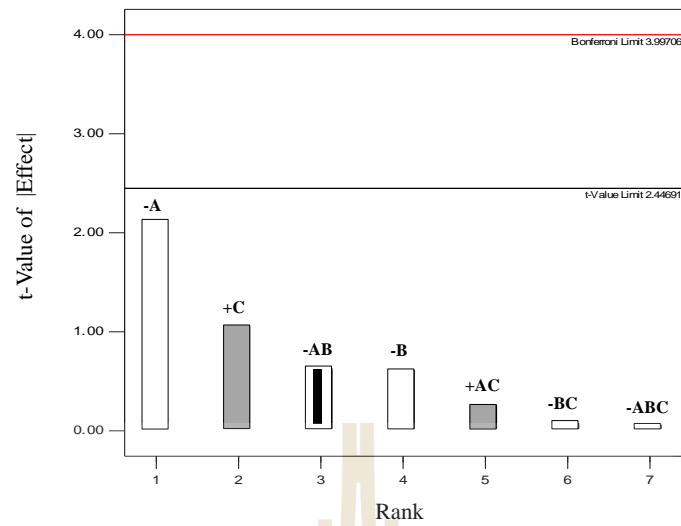


Figure 4.16 The pareto chart of the flexural strength (original).

Table 4.11 ANOVA results obtained from the flexural strength (original).

Source	Sum of squares	df	Mean square	<i>f</i> -value	<i>p</i> -value
Model	69.357	1	69.357	0.391	0.5548
AB	69.357	1	69.357	0.391	0.5548
Residual	1064.442	6	177.407		
Cor Total	1133.798	7			

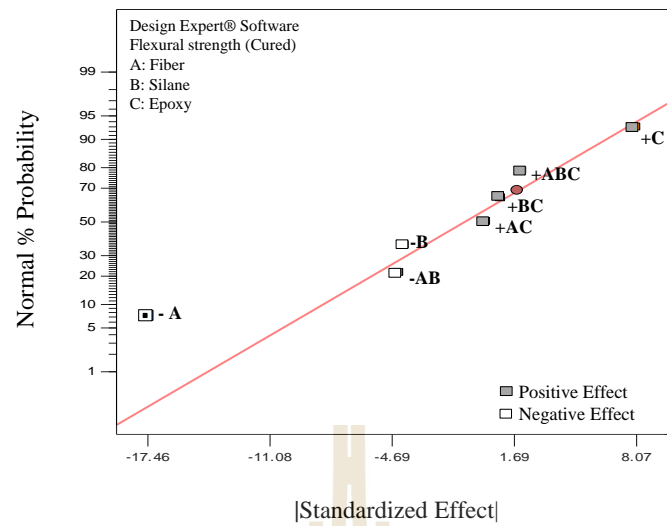


Figure 4.17 The normal plot of the standard effect obtained from the flexural strength (cured).

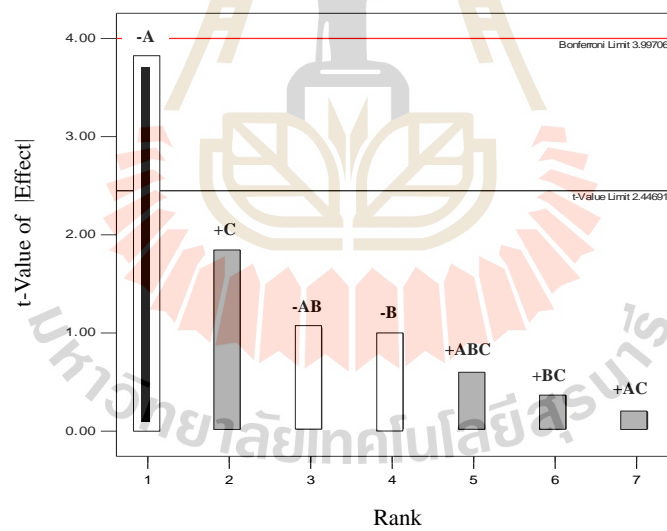


Figure 4.18 The pareto chart of the flexural strength (cured).

Table 4.12 ANOVA results obtained from the flexural strength (cured).

Source	Sum of squares	df	Mean square	<i>f</i> -value	<i>p</i> -value
Model	609.773	1	609.773	17.354	0.0059
A-Fiber	609.773	1	609.773	17.354	0.0059
Residual	210.8204	6	35.13674		
Cor Total	820.5935	7			

Statistical evaluations by mean of the converted normal probability plot and pareto chart are presented in Figure 4.19 and 4.20, respectively. The standard plot shows that all of the parameters can fit into the straight line except for the silane content (-B) is deviated from the line. It is suspected to be the significant effect to the flexural modulus of the original composite sample. However taken the pareto chart into consideration, the result manifests that its calculated *t*-value of this parameter is below the critical value. Therefore, the suspected argument is fault. Strengthen by the ANOVA testing conclusion as summarized in Table 4.13, it is seen that *p*-value of the designed model and also silane parameter are 0.1579. The values are higher than the critical value, 0.05. So that the parameters and levels used in this designed experiment are not significant effect to the flexural modulus of the biocomposites. Within the standard deviation, it can be stated that the flexural modulus of the biocomposite before sauna curing is not affected by the fiber, silane and epoxy contents used in this experiment.

Statistical analyzing of the sauna cured biocomposite in the identical manner as the above samples, Figure 4.21 and 4.22 are the normal plot and pareto chart results, respectively. The plot shows that fiber content (+A) is further out of the

linear trend line. It is probably positive and significant effect to the flexural modulus. The positive and significant effect of the fiber content is confirmed by the pareto analysis. It is obviously seen that the calculated t -value of factor A is above the critical t -value. The ANOVA testing as shown in Table 4.14 concludes that the designed model and also fiber content have the significant effect to the flexural modulus of the biocomposite as their p -value are lower than 0.050. Taking only the statistical results into consideration, it suggests that adding fiber at high level content, more than 40 phr, the flexural modulus of the moisture incubated composites will be elevated.

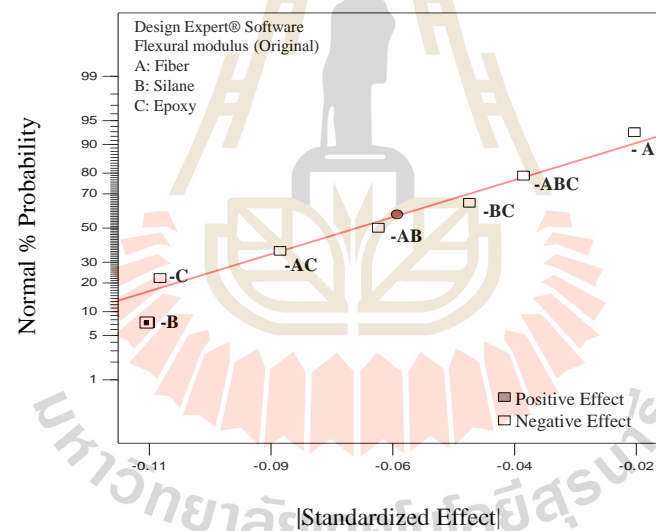


Figure 4.19 The normal plot of the standard effect obtained from the flexural modulus (original).

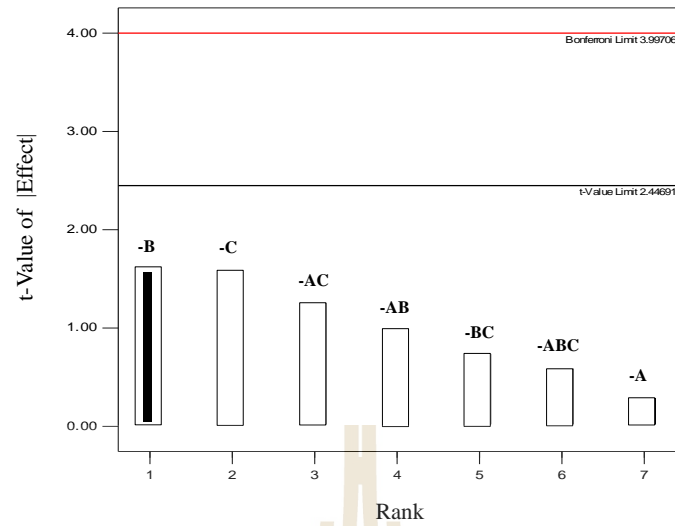


Figure 4.20 The pareto chart of the flexural modulus (original).

Table 4.13 ANOVA results obtained from the flexural modulus (original).

Source	Sum of squares	df	Mean square	<i>f</i> -value	<i>p</i> -value
Model	0.023	1	0.023	2.600	0.1579
B-Silane	0.023	1	0.023	2.600	0.1579
Residual	0.053	6	8.872E-0.03		
Cor Total	0.076	7			

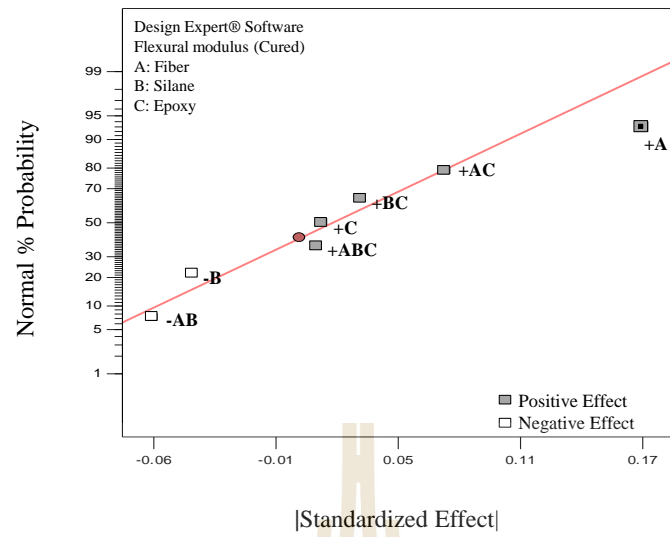


Figure 4.21 The normal plot of the standard effect obtained from the flexural modulus (cured).

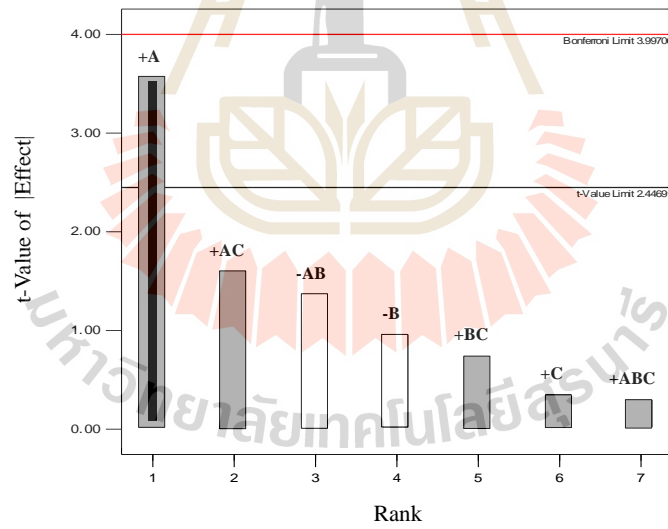


Figure 4.22 The pareto chart of the flexural modulus (cured).

Table 4.14 ANOVA results obtained from the flexural modulus response (cured).

Source	Sum of squares	df	Mean square	<i>f</i> -value	<i>p</i> -value
Model	0.058	1	0.058	12.620	0.0120
A-Fiber	0.058	1	0.058	12.620	0.0120
Residual	0.027	6	4.56E-0.03		
Cor Total	0.085	7			

Not only the effect values analysis were performed and discussed, the predicted equation, or regressed model, which is the function between the response properties and significant designed parameters can also be obtained from the DOE method. Table 4.15 summarizes the regressed models derived from the designed experiment. The given relationships can be carefully used to predict the composite properties that manufactured from the given parameters at the designed range of levels. For example, the equation for melt flow index is $46.83-14.21(A)+12.47(B)$. It is implied that maximized MFI of biocomposite can be achieved if it is compounded in twin screw mixing and injected at 190°C by using silane at high level (+B), more than 3.5 phr, and EFB fiber (-A) at low levels, less than 40 phr, respectively. The rest of the significant properties can be estimated as the identical approach. Within the boundary of this study, it is seen that EFB fiber, silane and epoxy do not have the significant effect on HDT, flexural strength, flexural modulus of original and unnotched impact strength of cured composite sample prepared.

Table 4.15 The predicted regression model of the biocomposite derived from DOE.

	Properties	Regressed models
Original	MFI	46.83-14.21(A)+12.47(B)
	HDT	No significant model
	Notched impact strength	4.70-0.47(A)
	Unnotched impact strength	11.55-1.99(A)-1.37(AB)
	Flexural strength	No significant model
	Flexural modulus	No significant model
Cured	HDT	57.63+3.21(A)
	Notched impact strength	5.47-0.74(A)
	Unnotched impact strength	No significant model
	Flexural strength	54.52-8.73(A)
	Flexural modulus	2.54+0.085(A)

4.1.5 Scanning electron microscopy (SEM)

From the previous statistical outcome, it notices that the toughness of the sample from both flexure and impacts testing are affected by the fiber and silane contents, especially on the sauna cured condition. Commonly, the surface adhesion between fiber and polymer matrix play the important role for this characteristic. It is worth to investigate the surface adhesion of the fractured surface of the composite samples by SEM technique. Figure 4.23 (a) - 4.23 (d) are the SEM photographs obtained from notched specimens of run#2 and run#5 for the original and sauna cured, respectively. The run#2 composite sample is derived from high fiber and silane but low epoxy contents. It shows the relatively lowest toughness. However run#5, at low

fiber but high silane and epoxy contents, manifests the highest test values, especially impact properties. Figure 4.23 (a) illustrates the trace of fiber pull-out, seen as large hole on the matrix surface. This is the evidence for the inferior in the interface bonding between polymer matrix and reinforcement that lead to lower the toughness of the sample. After sauna curing of the sample, as seen in Figure 4.23 (b), the improvement of the adhesion between fiber and matrix, via the silane/water condensation reaction, can be seen. It gives the marginally increase in the toughness. By decreasing the fiber content but increasing in the silane and epoxy contents, as in Figure 4.23 (c) to 4.23 (d) for run#5, there is an evidence for fiber debonding, better interfacial strength, and also higher in impact strengths for both original and cured samples, respectively. The SEM results suggest that increasing in the silane coupling/crosslink agent and epoxy compatibilizer could enhance the surface adhesion between fiber and matrix. But don't be over emphasis on the fiber/matrix adhesion. Because the higher toughness of the low fiber content sample might be due to the fact that the fracture toughness of polymer matrix, neat PLA, dominate the overall properties of this low fiber content biocomposite. The less of reinforcement added the fewer in contact void between fiber and matrix and hence better in the toughness especially unnotched impact and flexural property. However, by mean of statistical data, these two parameters do not guarantee that the toughness of the composite do increase in the same manner. It is because the fiber content plays the major and significant role in the mechanical properties of the biocomposite. The further investigation for fine tuning the parameters and also modifying the composite constituent are unavoidably.

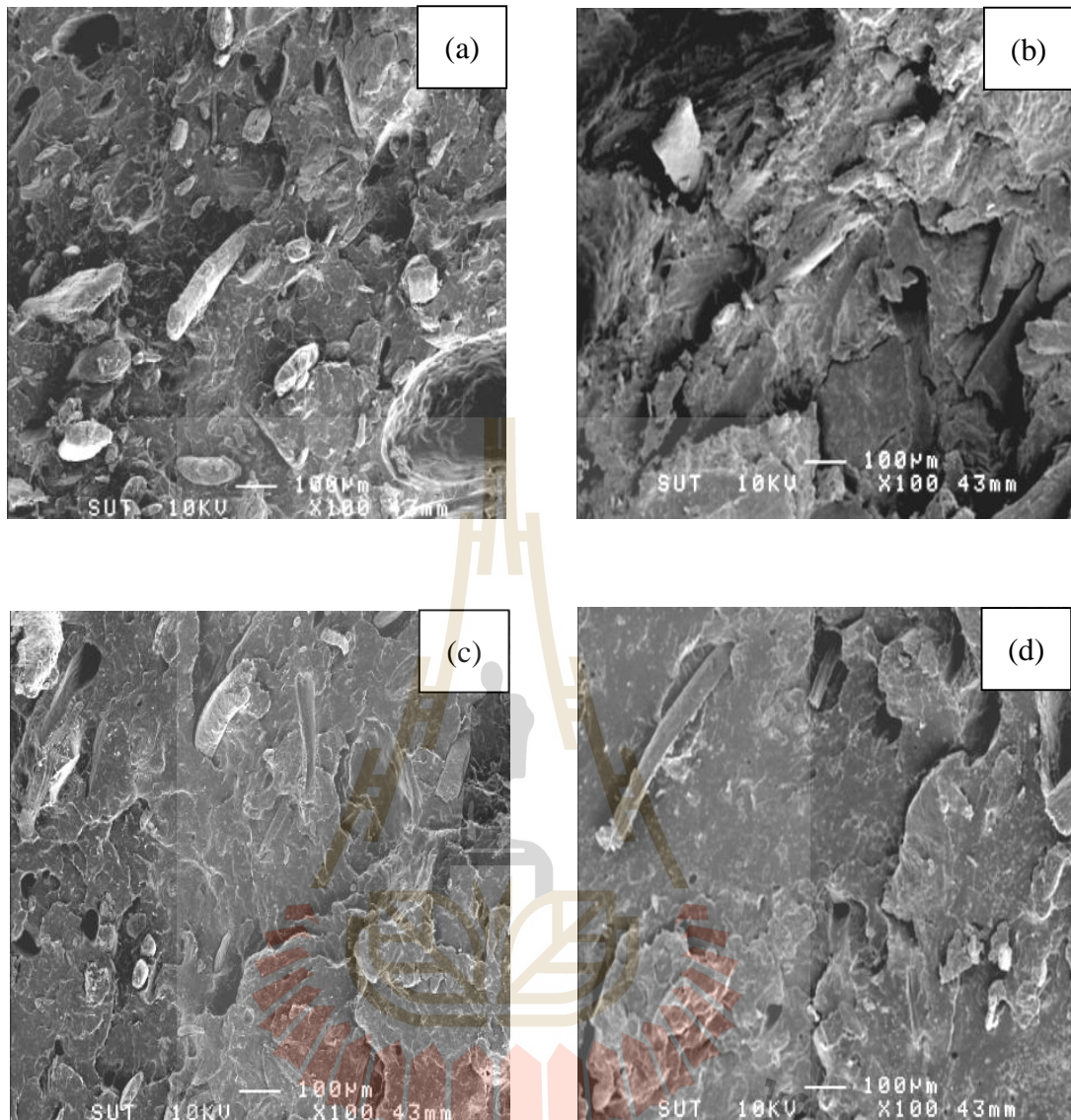


Figure 4.23 SEM micrograph of biocomposites; (a) run#2 (original),
(b) run#2 (cured), (c) run#5 (original) and (d) run#5 (cured).

Biocomposite from PLA and EFB palm fiber with adding silane as coupling agent and solid epoxy as compatibilizer was manufactured. It found that sauna cured via silane/water reaction does fractionally improve the thermal and mechanical properties of the composite via the enhancement of interfacial adhesion between PLA matrix and fiber. The statistical method by mean of DOE reviewed that

fiber content had importantly and significantly effect on the response properties. Adding too much fiber content would lower the toughness properties. However, the fibers at high levels of content will have the positively and significantly effect on HDT value of cured sample. Silane and epoxy does not clearly have great influence on the performance properties of the material. Further investigations will be discussed.

4.2 Effect of solid epoxy on biocomposite

From the previous experiment, the statistical and morphological results showed that composite derived from run#4 had maximum HDT value and modulate in others properties. It was compounded from high level of fiber, low level of silane and low level epoxy contents. Therefore, run#4 formula is interested in term of thermal property improvement of PLA/EFB composite especially HDT as the main objective of this research work. From DOE, it was found that the HDT property after sauna treatment of the biocomposite was highly promising and it had positive and significant effect with the fiber content. The solid epoxy added is acted as the reactive compatibilizer because its epoxy group can react with $-COOH$ or $-OH$ group in PLA and fiber, respectively. Therefore, it could enhance the surface adhesion between fiber and matrix. Even though from the DOE result, it was found that epoxy has no significant effect to the response properties of the tests but it showed the negative effect to the measured value especially the bending and impact toughness. The hypothesis could be mentioned at this point that the excess of this active compatibilizer might be cured and formed the highly brittle epoxy thermoset. On the other hand, another postulation can be taken into account is that unreacted or excess

epoxy groups sometimes can act as glycolysis agent for the PLA chain. This type of reagent would undergo the chain scission reaction. The acid terminated degraded chain can be reversely acted as acid curing agent for the excess epoxy groups. As the results, the biocomposite would effect to the polymer viscosity and lower the toughness at high level of solid epoxy content.

As mentioned above, in this experiment section the composites formula from run#4 with low level of solid epoxy contents varied from 0.1, 0.4, 0.8 and 1.2 phr, were assigned and explored. Table 4.16 summarizes the composite formulations for preparing composite. The test results obtained from the experiment are shown in Table 4.17. The discussions of the results are following.

Table 4.16 Composition of the composites.

Sample	Composition (phr)					
	Solid epoxy	PLA	EFB fiber	Silane (APS; A-1100)	ENR50	Stabilizer
1	0.1	100	65	3.5	20	2
2	0.4	100	65	3.5	20	2
3	0.8	100	65	3.5	20	2
4	1.2	100	65	3.5	20	2

Table 4.17 Material testing results.

Sample	Solid epoxy (phr)	MFI at 190/2.16 (g/10min)	HDT (°C)		Notched impact strength (kJ/m ²)		Unnotched impact strength (kJ/m ²)		Flexural strength (MPa)		Flexural modulus (GPa)	
			original	cured	original	cured	original	cured	original	cured	original	cured
1	0.1	10.542±1.034	54.9±0.8	55.3±0.9	5.93±0.22	6.07±0.28	11.25±0.87	13.74±0.51	47.55±1.92	47.83±3.48	2.32±0.15	2.52±0.15
2	0.4	14.231±0.912	55.4±0.1	56.4±0.5	5.88±0.17	5.98±0.45	10.30±1.55	12.14±1.07	46.70±0.64	52.88±4.08	2.51±0.05	2.52±0.25
3	0.8	18.302±1.270	55.6±0.3	55.7±0.6	5.76±0.10	5.79±0.20	10.08±1.27	11.53±1.13	46.69±2.07	47.94±3.33	2.45±0.10	2.47±0.11
4	1.2	14.090±0.893	55.1±0.4	55.6±0.4	5.55±0.22	5.67±0.10	10.20±1.01	11.63±0.10	44.73±1.84	44.69±2.77	2.43±0.08	2.53±0.09
5*	1.5	21.271±2.527	55.5±0.5	65.3±3.1	4.60±0.32	4.88±0.31	10.55±1.23	12.49±0.75	42.12±6.91	47.37±1.20	2.65±0.15	2.66±0.17

* Data from run#4 as shown in Table 4.3.



4.2.1 MFI of composite versus epoxy contents

The flow ability of the composite by mean of the melt flow index obtained at 190/2.16 in corresponding with epoxy contents as seen in Table 4.17 was plotted and shown in Figure 4.24. It is seen that the MFI are increased when increasing the epoxy content to 0.8 phr but the flow index was drop when further increased epoxy to 1.2 phr. The composite with epoxy loading at 0.8 phr manifests the highest MFI at 18.302 ± 1.270 g/10 min.

Taken only the MFI result, it indicates that at epoxy contents below 0.8 phr the glycolysis seems to become dominate but further increase loading the thermoset characteristic is found. However, this hypothesis will be supported by others tests properties which will be accordingly presented.

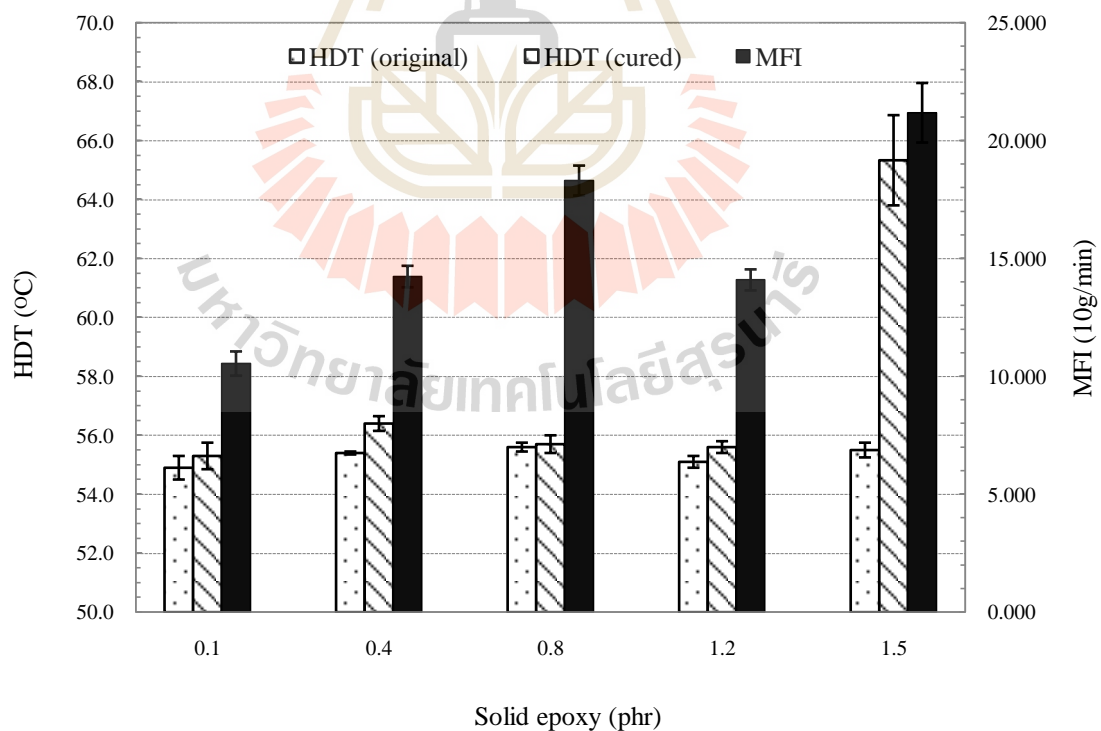


Figure 4.24 The plot of HDT and MFI with epoxy contents.

4.2.2 HDT and epoxy contents

Again, Figure 4.24 is the plot between HDT of composite with epoxy contents both before and after sauna treatment. As expected, within the accepted standard deviation, that HDT of the composite is similar to those found in virgin PLA for both original and cured. There is marginally increased in the thermal property of the sample after sauna curing at 60°C for 12 hours. It is in good agreement with the statistical result that epoxy is negative effect to the HDT of the composite. The test result seems to reduce with high epoxy loading. However, from the DOE experiment, the composite run#4, after sauna curing, with 1.5 phr of epoxy content have high HDT value at 65.3±3.1°C. It indicates that further increase in the epoxy contents and also combination with the positive influence of silane/moisture condensation reaction, the thermoset characteristic would be dominated. Normally, crosslinked epoxy show positive effect to the HDT of the polymer compound (Charoensuk, 2005).

4.2.3 Impact strength and epoxy contents

The notched and unnotched impact test results against epoxy contents summarized in Table 4.17 and graphically presented in Figure 4.25. Similar to those previously found, it is seen that the notched impact strength of the sauna cured composites is noticeably higher than the original sample. However, the difference is much wide in the unnotched mode of test. Closer observations, notched impact strength of both original and cured sample are decreased with increasing the epoxy content. This outcome strengthen that the reactive epoxy compatibilizer is somehow either degrade the PLA chain or forming short chain or network thermoset structure, respectively. Thus, the matrix phase becomes more brittle material.

The same trend is found for the unnotched impact strength. It is slowly decreased with increasing the epoxy addition. However, with the compensation of silane/moisture reaction during sauna cure, the strength of the sample is significantly higher than the original sample but still gradually lower with the epoxy content. Improving in the interfacial adhesion between fiber and matrix during the sauna cure process, can be used to explain the superior impact strength of the cured composite. The composite with 0.1 phr of epoxy displays the highest impact strength value both before and after sauna treatment. However, the impact strengths of the composite samples, both original and cured, relatively constant when the epoxy content is increased beyond 0.4 phr. Again, degradation of PLA chain and possible network structure of epoxy would be explained for the lowering of the impact strengths.

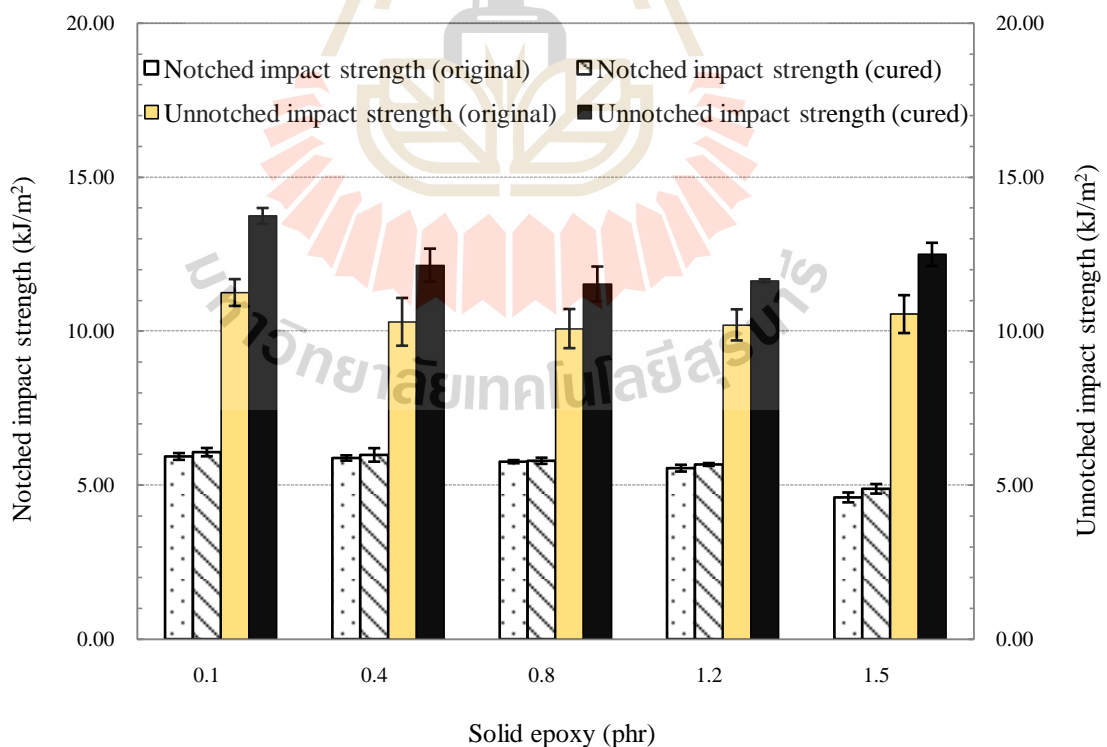


Figure 4.25 The plot of impact properties with epoxy contents.

4.2.4 Flexural properties and epoxy contents

The flexural strength and flexural modulus with the epoxy contents are plotted in Figure 4.26. Within the statistical error, it is found that flexural strength of the original sample is slightly decreased with increasing the epoxy content. But, the flexural strength of cured composite maximum, 52.88 ± 4.08 MPa, at 0.4 phr of epoxy but strengths are decreased when further increases epoxy loading.

The identical trend is observed for flexural modulus of the composites with epoxy content for both before and after sauna curing. Higher in flexural strength and also higher in the modulus mean that the of material is superior. Vice versa, lower in the strength but higher in the modulus, the more brittle material is obtained. Taken both impact and flexural properties, it is reviewed that the toughness of the composite becomes lower when adding more of reactive solid epoxy compatibilizer into the PLA matrix. Even though the compensation of interfacial adhesion between matrix and fiber through the silane/moisture reaction is taken into account.

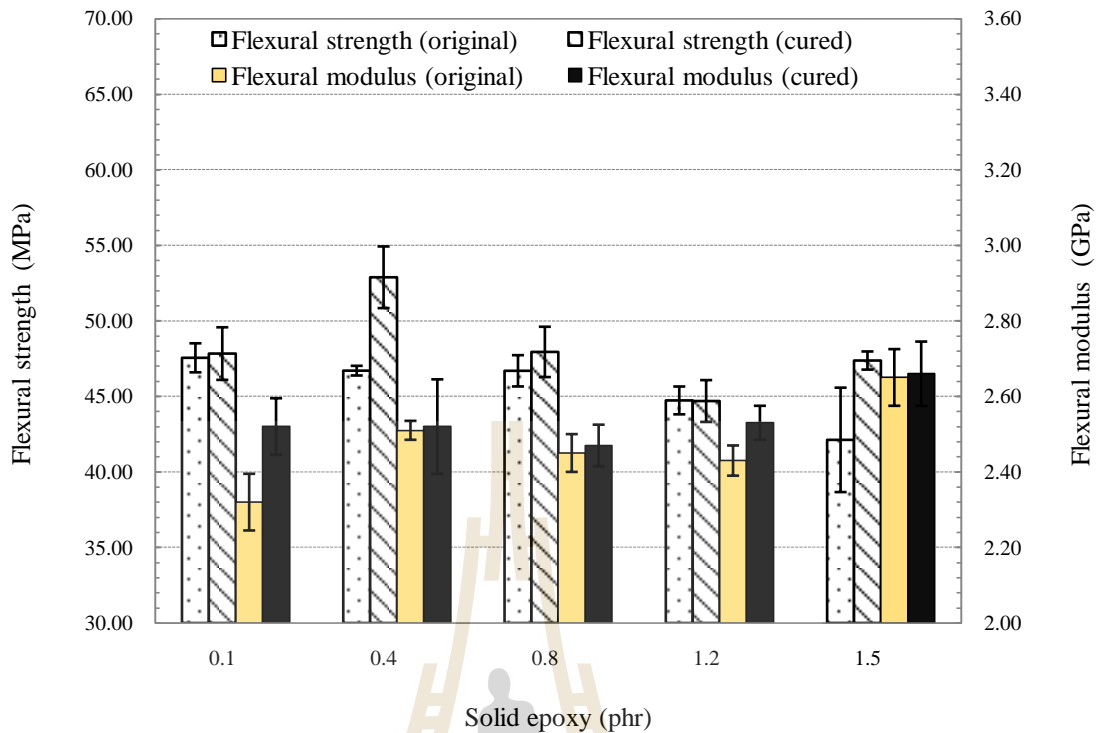


Figure 4.26 The plot of flexural properties with epoxy contents.

4.2.5 Scanning electron microscopy (SEM)

Figure 4.27 (a) - 4.27 (d) are the fractured surface SEM photographs obtained from notched specimens of composites with epoxy contents 0.4 and 1.2 for the original and sauna cured, respectively. It was found from the previous section that the impact strength of the composite were slowly decreased with increasing the epoxy contents. From the SEM results, it is observed that smoother surface is found at the lower epoxy content. However, sauna treatment does not much improve the adhesion between fiber and matrix. The evidence of the fiber pull out is remained on the sauna cured specimen. Taken these SEM observations, it could state that the more epoxy addition into the matrix phase, it become more brittle. Additional sauna treatment that perhaps generate the brittle crosslink structure. Taken this two folds negative effect on

the toughness of matrix phase and moreover the diminish improvement of surface adhesion derived from the silane/moisture reaction, hence, the lower in toughness of material is resulted.

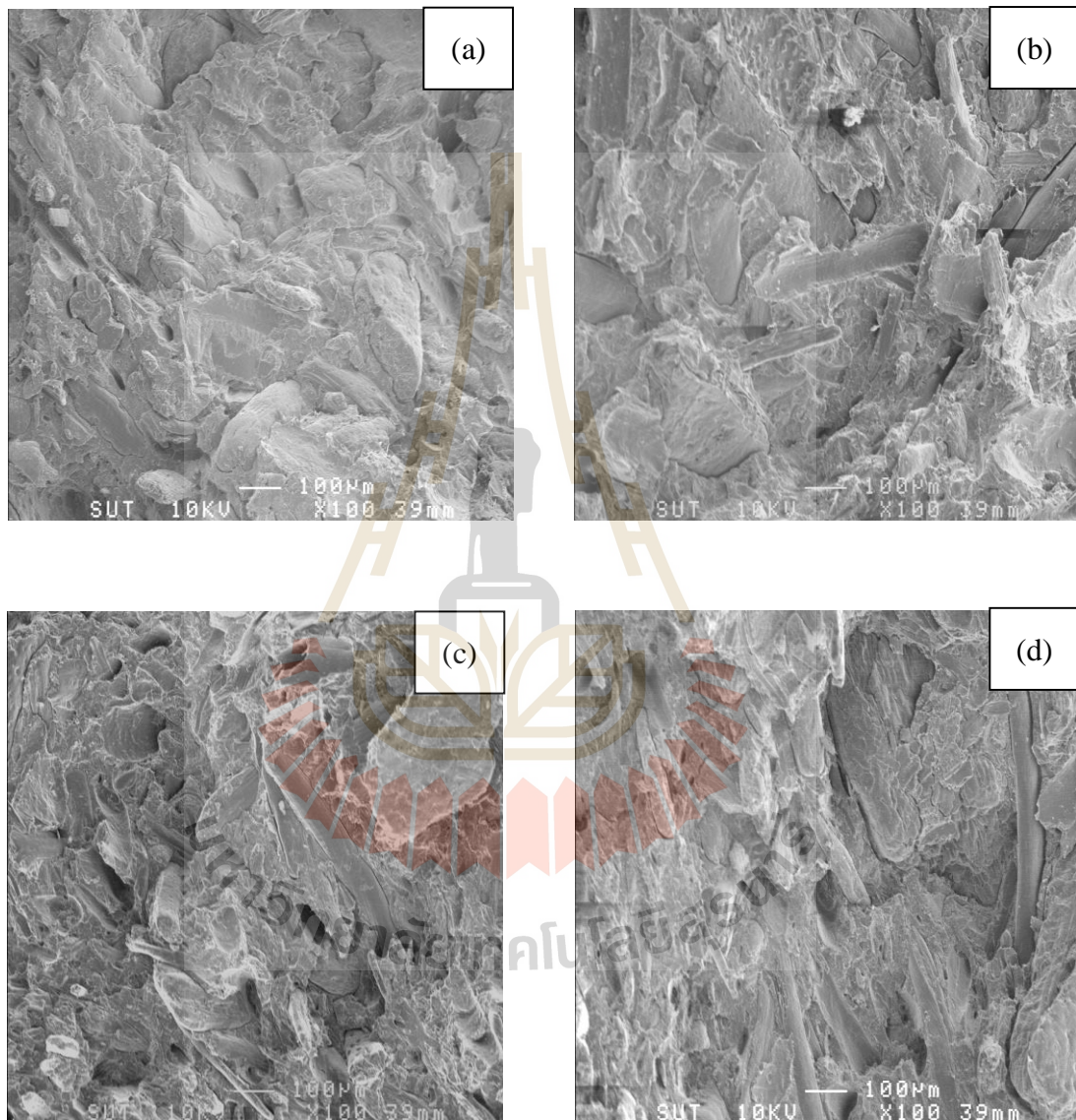


Figure 4.27 SEM of the biocomposite with; (a) 0.4 phr (original), (b) 0.4 phr (cured), (c) 1.2 phr (original) and (d) 1.2 phr (cured) of epoxy contents.

From the results discussed, adding solid epoxy at 0.1 - 1.2 phr into the composite matrix had more or less negative effect to the mechanical properties of the biocomposite. The properties are slightly lowered at higher epoxy content. It was also found that the HDT did not change with the amount of the solid epoxy added. More brittle matrix was also observed. Curing by silane/moisture incubation at 60°C had marginally increased the properties.

4.3 Effect of cotton fiber

From the previous experiment found that the solid epoxy at high content, more than 0.8 phr, deplete the mechanical properties especially toughness of the biomaterial. The service temperature by mean of HDT does not also superior. Therefore, in this section, further improvement of the composite is needed. In this section, the hybrid reinforcement system; cotton and EFB fibers, was explored. Cotton fiber is natural fiber that consist of 80 - 90% cellulose and it is well known that cotton is high strength. So that the biocomposite reinforced with cotton would become higher in the strength. In the experiment not only 3-aminopropyltriethoxysilane (APS; A-1100) was added but the epoxide type silane, *gamma*-glycidoxypropyltrimethoxysilane (GPS; A-187) was also used. The mixture of the two silanes at 1:1 by weight was prepared and used. Epoxy group on the silane could react with -OH group of fiber, and -COOH or -OH end group of PLA chain. This phenomenon could improve the interfacial adhesion between fiber and matrix and hence superior in mechanical/thermal properties of the composite material. Moreover, polyester polyols was employed as reactive plasticizer in this experiment.

Table 4.18 shows the experimental composite formulations for twin screw mixing. Also, the standard test results obtained from the injected specimen are summarized in Table 4.19. In this experiment, the vacuum drying, at 80°C for 2 hours, on the sauna cured samples of HDT specimen were also preliminary observed to see the influence of moisture residual in the test property.

Table 4.18 The hybrid composite formula.

Sample	EFB:Cotton weight ratio	Composition (phr)							
		EFB fiber	Cotton fiber	PLA	Silane (A-1100+A-187 at 1:1 by wt.)	Solid epoxy	Polyols	ENR50	Stabilizer
1	100:0	65.00	0.00	100	3.5	0.4	4	20	2
2	75:25	48.75	16.25	100	3.5	0.4	4	20	2
3	50:50	32.5	32.50	100	3.5	0.4	4	20	2
4	25:75	16.25	48.75	100	3.5	0.4	4	20	2
5	0:100	0.00	65.00	100	3.5	0.4	4	20	2

Table 4.19 Material testing results.

Sample	EFB:Cotton ratio (wt/wt)	MFI at 190/10.0 (g/10min)	HDT (°C)			Notched impact strength (kJ/m ²)		Unnotched impact strength (kJ/m ²)		Flexural strength (MPa)		Flexural modulus (GPa)	
			original	cured	cured&dried	original	cured	original	cured	original	cured	original	cured
1	100:0	56.050±1.923	50.5±0.5	95.0±1.0	103.0±1.0	4.46±0.68	5.34±0.77	10.02±2.21	10.91±2.24	38.07±6.68	36.65±3.03	2.64±0.22	2.65±0.24
2	75:25	17.020±0.840	52.1±0.2	115.3±3.2	125.0±1.3	5.77±0.37	6.04±0.35	23.33±2.24	20.95±1.58	63.02±1.87	66.69±2.75	2.82±0.09	3.10±0.10
3	50:50	7.209±0.452	53.8±0.3	64.5±1.2	130.7±1.2	6.13±0.20	6.22±0.81	26.42±1.28	27.90±3.88	74.85±2.03	74.03±7.74	3.11±0.22	3.37±0.10
4	25:75	2.210±0.142	54.0±1.0	65.0±4.3	129.3±1.5	6.63±0.16	6.95±0.22	34.78±7.23	32.86±5.04	77.35±4.34	76.10±3.24	3.20±0.34	3.21±0.33
5	0:100	1.331±0.099	54.6±0.5	67.3±2.3	130.7±0.9	6.81±0.15	6.99±0.33	28.92±5.56	34.74±7.15	81.89±1.44	79.24±3.71	3.16±0.14	3.15±0.28



4.3.1 MFI of composite versus cotton fraction

The flow ability of the composite by mean of the melt flow index obtained at 190/10.0 in corresponding with proportion between EFB and cotton ratio as concluded in Table 4.19 was plotted and presented in Figure 4.28. It is seen that the MFI is obviously and significantly decreased with increasing the cotton ratio. The decreasing in flow ability, increasing in viscosity, of the material is probably due to higher in L/D ratio of cotton fiber in comparison with the EFB palm oil fiber. The superior in toughness of the cotton that resist the flow of the composite could be also used to explain this observation.

4.3.2 HDT of composites versus cotton fraction

In this experiment, there was a hypothesis about whether the residual moisture contained in the specimen during the sauna curing process had any effect of the test properties or not. To resolve this technical issue, the cured sample was vacuum dried at 80°C for at least 2 hours to completely removed the trace residual moisture in the specimen. This piece is called cured/dried sample. The test was conducted and compared to the original and cured ones. Figure 4.28 also shows the plot of HDT versus the ratio between EFB and cotton fibers of three type of samples. First observation found that the original samples show more or less unchanged in HDT at approximately 54°C with respect to the cotton ratio. Secondly, HDT of sauna cured specimen have the tendency to increase with increasing the cotton fraction but the ambiguous figures are still unexplained for example at the ratio of 75:25. The test value is as high as 115°C compare to those ratio at 100:0 or 50:50 which had the HDT at approx. 95°C and 65°C, respectively. Finally, the cured/dried samples are found that HDT values are dramatically increased to more than 110°C and it is seemingly

increased with increasing the cotton fraction. From the phenomena, perhaps, it can be explained that silane/moisture condensation reaction and combination from addition of high strength cotton fiber improve the ability of the composite material to resist the thermal stress that come from the surrounding. Moreover, the further complete elimination of moisture residual from the samples by vacuum drying can also enhance the thermal resistance.

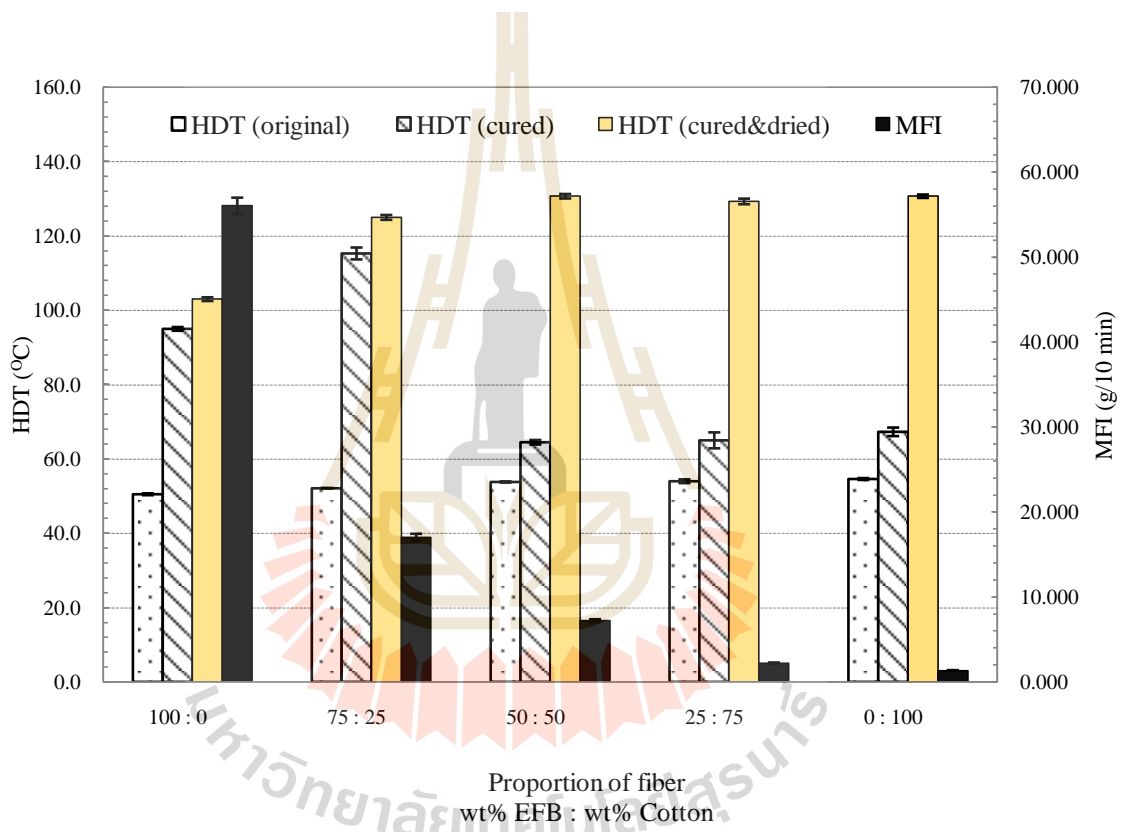


Figure 4.28 Plot of HDT and MFI of the hybrid biocomposite as a function of EFB and cotton fiber ratios.

4.3.3 Impact properties and cotton fraction

The notched and unnotched impact strengths of the biocomposite are presented as function of ratio between EFB and cotton fiber loading in Figure 4.29. The results show that the impact strengths of both original and sauna cured sample are generally increased with increasing the cotton ratio. For the notched mode of testing, cured sample reviews higher in test value than the original one. Vice versa in the unnotched mode of testing, it seems that the test results obtained from cured specimen are fractionally lower than the original at the given fibers ratio. The higher in the impact strengths with increasing the cotton loading might be come from the fact that the fiber has outstanding in toughness and high in L/d ratio. According to the two folds affects, higher in fraction loading would superior in the impact properties. For the unnotched impact mode of the sauna cured samples, the excess moisture residual remained in the sample and also the hydrophilic in nature of EFB oil palm fiber would be respond for the reduction of the test values. If the incubated moisture penetrate into EFB fiber or in between fiber/matrix interface, the fiber bonding or interfacial bonding would become weaker. Consequently, the unnotched impact strength would be also inferior with respect to the increase in EFB fraction as the above observed. The fracture vision by SEM of the cured/dried sample; complete removal of residual moisture, will be presented and further discussed in the next experiment.

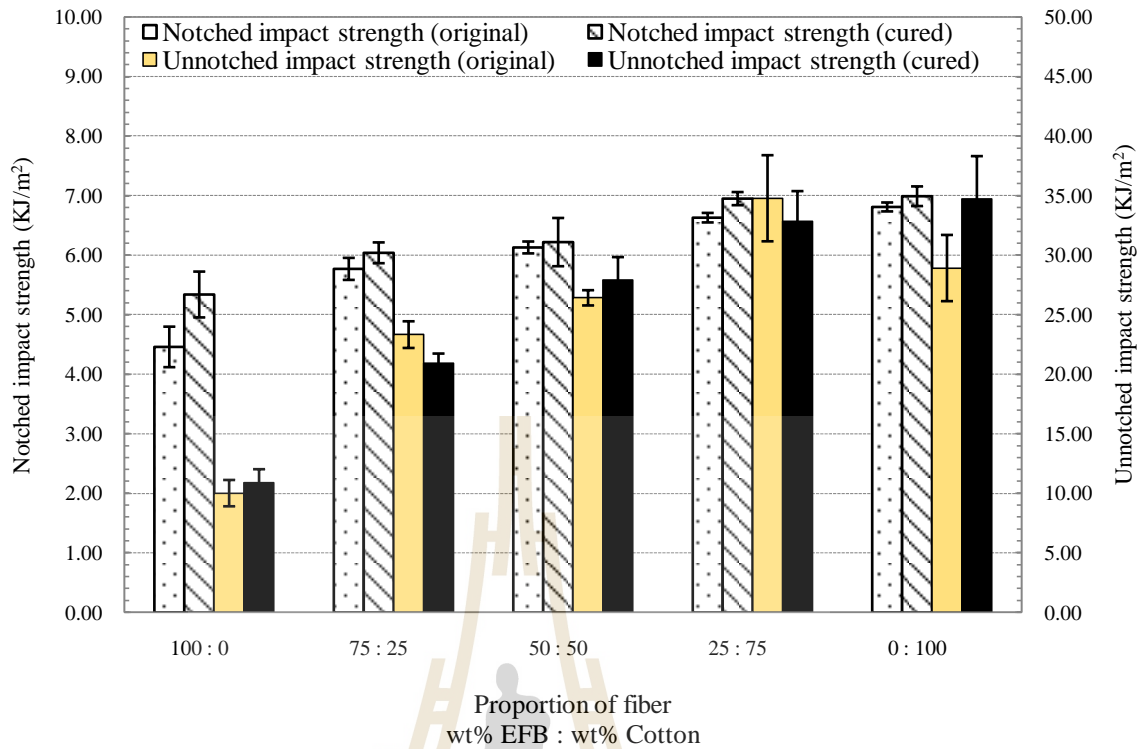


Figure 4.29 Plot of impact properties of the hybrid biocomposite as a function of EFB and cotton fiber ratios.

4.3.4 Flexural properties versus cotton fraction

Flexural properties; strength and modulus, of the composite are graphically represented in respect to the cotton fraction in Figure 4.30. As expected, it is seen that the flexural strength of both original and sauna cured samples are increased with increasing the cotton ratio. Also, the bending strength is marginally diminished for the sample after sauna curing. This found out is strengthen the previous statement that the residual moisture during the high humid incubation process and hydrophilic characteristic of EFB have the negative effect on the toughness of the material. Taken the flexural modulus into account, the test values are also increased with increasing the cotton loading. But the sauna cured slightly

increases the modulus of the biocomposite. Normally, increasing in the modulus with constant strength or lower, it is meant that the toughness of material become incompetence. So that, moisture contamination would introduce the inferior in the toughness of this biocomposite.

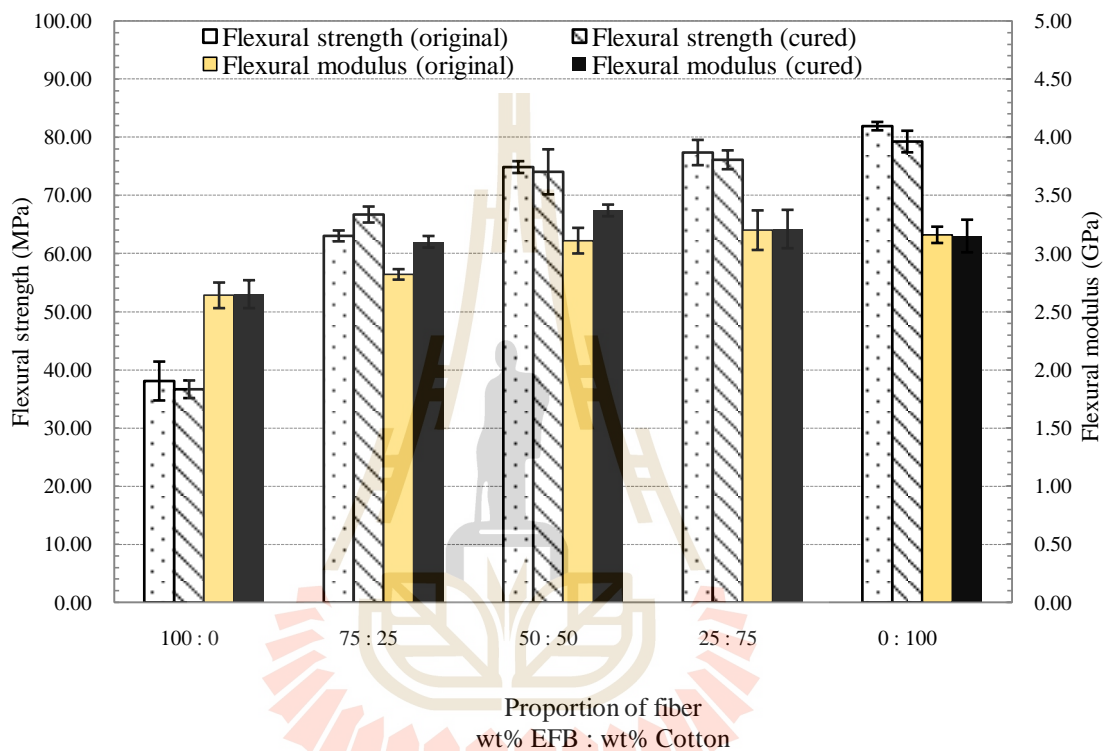


Figure 4.30 Plot of flexural properties of the hybrid biocomposite as a function of EFB and cotton fiber ratios.

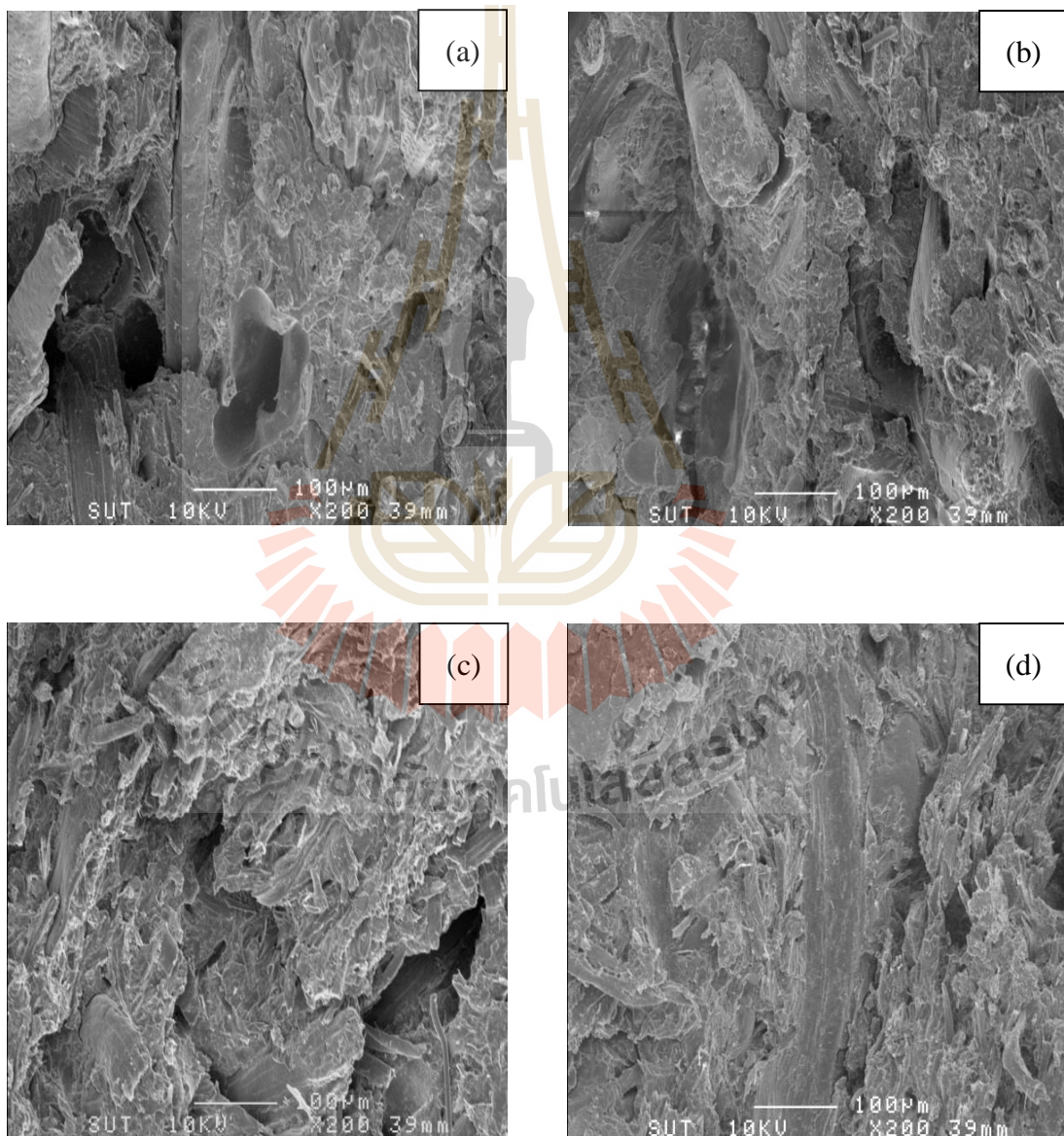
From the physical properties of the EFB:cotton hybrid reinforced biocomposite system found in this experiment, it can be concluded that addition of high stiffness and L/d ratio cotton fiber into the composite can improve the thermal and mechanical properties of the material but at high fraction of this fiber the flow ability of the compound become insufficient. So that, the processability especially by injection molding would become restriction. Balancing between the mechanical

properties and flow ability and within the boundary of this research study, the hybrid fiber between EFB and cotton fiber at the weight ration of 25:75 is selected and will be further explored through this study.

4.3.5 Scanning electron microscopy (SEM)

From the previous results, they were seen that the properties of the composite were superior with increasing the cotton ratio. Not only the higher in L/d ratio of cotton fiber was superiorly responded for those positive outcome but also the interfacial adhesion between fiber and matrix could be taken into consideration. To verify the effect, SEM investigation is needed. Figures 4.31 (a) - 4.31 (f) conclude the SEM micrograph obtained from notched impact fracture surface specimen of the composites. Figure 4.31 (a) and 4.31 (b) are the fractured surface of original and cured samples of the composite contained 100% of EFB. It is obviously evidenced that the presence of fiber pull out and also weak interfacial adhesion between fiber and polymer matrix. Especially, the inter phase bonding is inferior after the sauna curing process. Increasing in the space of fiber/matrix interface is apparently noticed. Therefore, lower in the toughness is found. By increasing the cotton content in the composite samples as shown in Figure 4.31 (c) to 4.31 (f), 50:50 and 100:0 cotton ratio, respectively. It is certainly seen, at the same magnifying, from the picture that the diameter of cotton fiber is much smaller than the EFB fiber. The L/d ratio is also much larger. This is the initial clue that explain the better reinforcing characteristic of the fiber. In the same hand, when comparing between original and sauna cured samples, it is also visible that the adhesion between cotton fiber and PLA matrix is retained as it was confirmed by the above mechanical testing results. However, the adhesion is not stronger than the strength of cotton fiber. Because the traces of cotton

pull out from the matrix phase are mainly observed at the fractured surface for both original and cured specimen. This SEM investigation confirms that the composites with adding cotton fibers had better reinforcing characteristic and also interfacial adhesion when compare with EFB only. The observations describe the results of increasing in the impact and flexural tests with increasing the cotton loading ratio.



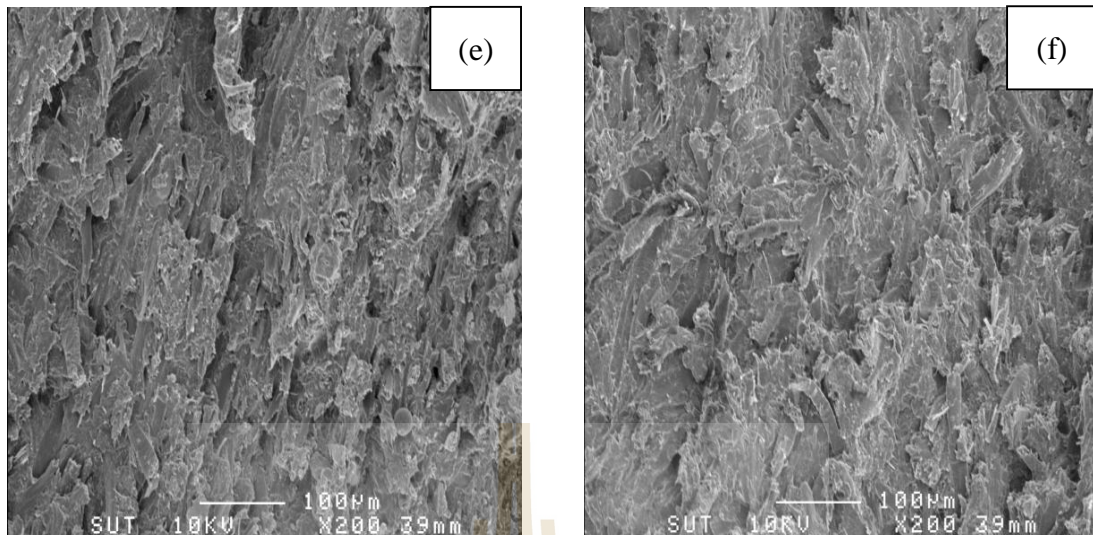


Figure 4.31 SEM micrograph of the biocomposites reinforced with;
 (a) 100:0 (original), (b) 100:0 (cured), (c) 50:50 (original),
 (d) 50:50 (cured), (e) 0:100 (original) and (f) 0:100 (cured) of
 EFB/cotton ratios.

4.3.6 Biodegradability testing

One of the main purposes of this study is obtaining biocomposite which has good mechanical properties and also it can be biodegraded under the landfill condition. Therefore biodegradability testing is necessarily and it was tested by using simulated landfill chamber as previously described in the experimental at 60°C under aerobic atmosphere. Figure 4.32 shows the plot between sample weight lost against buried times of the composite and pure PLA specimen. The result indicates that PLA sample is slightly degraded in the period of four weeks buried time. After that the rate of biodegradation is dramatically increased. Within eight weeks of the composting time, PLA sample were disintegrated into small pieces where weight loss measurement cannot be performed. Similarly, the biocomposite

obtained at 50% cotton content both original and cured manifest that the degradation process is initially observed after four weeks of burying. After that, it is sharply increased in weight loss and again the specimen were completely fall apart within fourteen weeks. However, the degradability of cured sample is slightly slower than the original one. The difficulty to break the network bonding arisen from silane/moisture crosslink could be taken into the explanation.

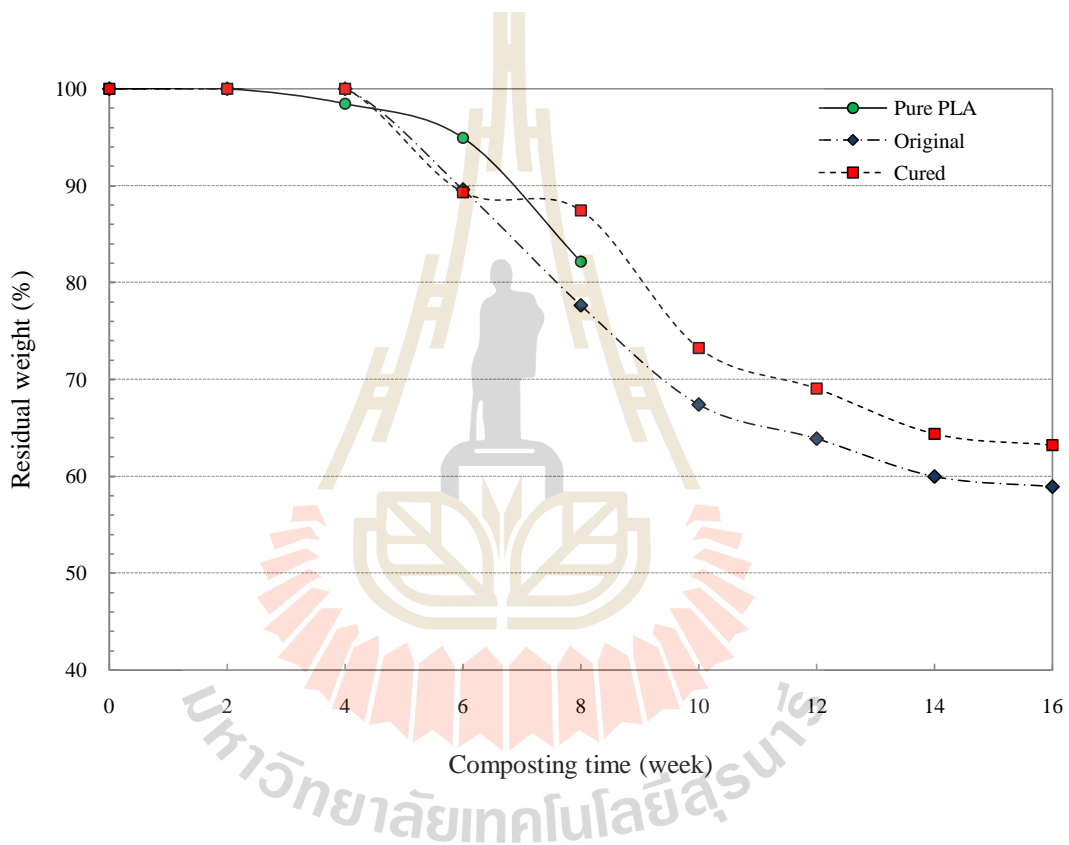


Figure 4.32 Relationship between weight loss and the composting time of hybrid composite at 50:50 EFB/cotton and neat PLA.

From the results discussed, adding cotton into the composite provides the improvement on the thermal and mechanical properties of the biocomposite. Silane/moisture incubation can also enhance the HDT of composite. Also, removing the residual moisture by vacuum drying at 80°C for 2 hours further increase the HDT

the EFB:cotton reinforced composite. The mechanical properties were enhanced by increasing cotton ratio. SEM strengthen that the composites with adding cotton fibers had better reinforcing characteristic and also interfacial adhesion when compare with EFB only. Finally, the composite manufactured from PLA reinforced with EFB:cotton hybrid can be degraded in the similar manner with PLA degradation.

4.4 Effect of talc

From the recent experiment, the hybrid composite derived from the hybrid fibers; EFB and cotton, at the ratio of 25:75 offered the promising properties. However, it was seen that the hybrid fibers composites with high cotton content had low flow ability. This obstruction would retard the feasibility of production the composite product by injection molding process. Also, it was found that the HDT of the composite material was ambiguously lower than 100°C which also limit the possibility to broader the application of material into other high heat resistance products. In this research section, the talc added hybrid fibers composite to improve processability especially injection process and perhaps thermal property will be discussed. The incorporation of talc as a filler in thermoplastic is a common practices in the plastic industry with the purpose of reducing the production cost of mold product, but also improve the stiffness and strength. Moreover, talc can act as lubricating material in composites so the flow ability of the compound is normally increased. In this experiment, the hybrid composites were establish by varying the fibers contents from 20 - 65 phr and talc contents from 0 - 50 phr. Moreover, the extra vacuum drying, at 80°C for 2 hours, on the sauna cured samples of specimen, as called cured/dried samples, before conducting the test were also performed in order to

investigate the influence of excess moisture residual in the composite sample on the thermal and mechanical properties.

Table 4.20 summarizes the composite formulations for preparing the talc filled composited in twin screw mixer. The standard test results obtained from the injected specimen are also concluded in Table 4.21.

Table 4.20 Formulation of the talc filled hybrid composite.

Sample	Talc:Fiber (phr)	Composition (phr)								
		Talc	EFB fiber	Cotton fiber	PLA	Silane (A-1100+A-187 at 1:1 by wt.)	Solid epoxy	Polyols	ENR50	Stabilizer
1	0:65	0	16.25	48.75	100	3.5	0.4	4	20	2
2	20:50	20	12.50	37.50	100	3.5	0.4	4	20	2
3	30:40	30	10.00	30.00	100	3.5	0.4	4	20	2
4	40:30	40	7.50	22.50	100	3.5	0.4	4	20	2
5	50:20	50	5.00	15.00	100	3.5	0.4	4	20	2

Table 4.21 Test results of the talc filled hybrid composite.

Sample	Talc (phr)	Fiber (phr)	MFI at 190/10.0 (g/10min)	HDT (°C)			Notched impact strength (kJ/m ²)			Unnotched impact strength (kJ/m ²)			Flexural strength (MPa)			Flexural modulus (GPa)		
				original	cured	cured&dried	original	cured	cured&dried	original	cured	cured&dried	original	cured	cured&dried	original	cured	cured&dried
1	0	65	4.788±0.171	55.5±1.3	133.4±1.2	131.2±1.3	6.30±0.06	6.32±0.18	6.30±0.22	23.59±4.19	25.46±4.32	24.86±5.69	71.46±4.29	72.87±3.62	68.72±2.66	3.37±0.17	3.42±0.10	3.25±0.22
2	20	50	8.443±0.507	54.2±0.6	124.0±1.1	122.1±2.7	5.60±0.16	5.76±0.18	5.69±0.04	23.81±3.71	24.36±2.45	22.12±4.39	73.90±2.43	74.44±2.07	76.39±6.71	2.88±0.14	3.00±0.27	2.78±0.35
3	30	40	10.413±1.053	53.8±0.3	120.6±1.7	121.6±3.1	5.58±0.43	5.74±0.20	5.60±0.46	21.96±2.68	20.51±1.52	22.04±4.48	62.94±1.22	68.34±1.43	67.80±2.05	2.40±0.19	2.41±0.19	2.53±0.15
4	40	30	10.608±1.042	53.7±0.3	118.5±1.8	120.7±2.6	5.41±0.21	5.47±0.28	5.58±0.12	23.90±4.53	23.77±5.09	23.46±4.59	63.12±2.64	65.60±0.42	71.44±5.72	2.45±0.09	2.56±0.11	2.59±0.21
5	50	20	12.316±1.342	53.0±0.0	107.3±3.3	105.8±5.2	5.10±0.21	5.23±0.15	5.13±0.33	22.83±3.91	23.66±8.83	23.24±2.84	57.35±0.91	61.78±0.85	63.66±9.07	2.42±0.06	2.37±0.15	2.48±0.20



4.4.1 Flow ability of hybrid composite

The flow ability of the composite measured by the melt flow index at 190/10.0 in corresponding with talc and fiber ratio as concluded in Table 4.21 was plotted and presented in Figure 4.33. At 65 phr of fibers without talc, it shows the lowest MFI. When decreasing fiber but increasing talc content, it is found that flow ability of hybrid composites is increased. This result reinforce the previous statement that talc could be act as the compound lubricant. But the MFI is almost constant at fiber:talc ratio reach 40:30. From the result found, it could suggest that for a better flow ability with retaining the properties of the composite the composite can be prepared from 50 phr of the EFB:cotton hybrids fiber and 20 phr of talc.

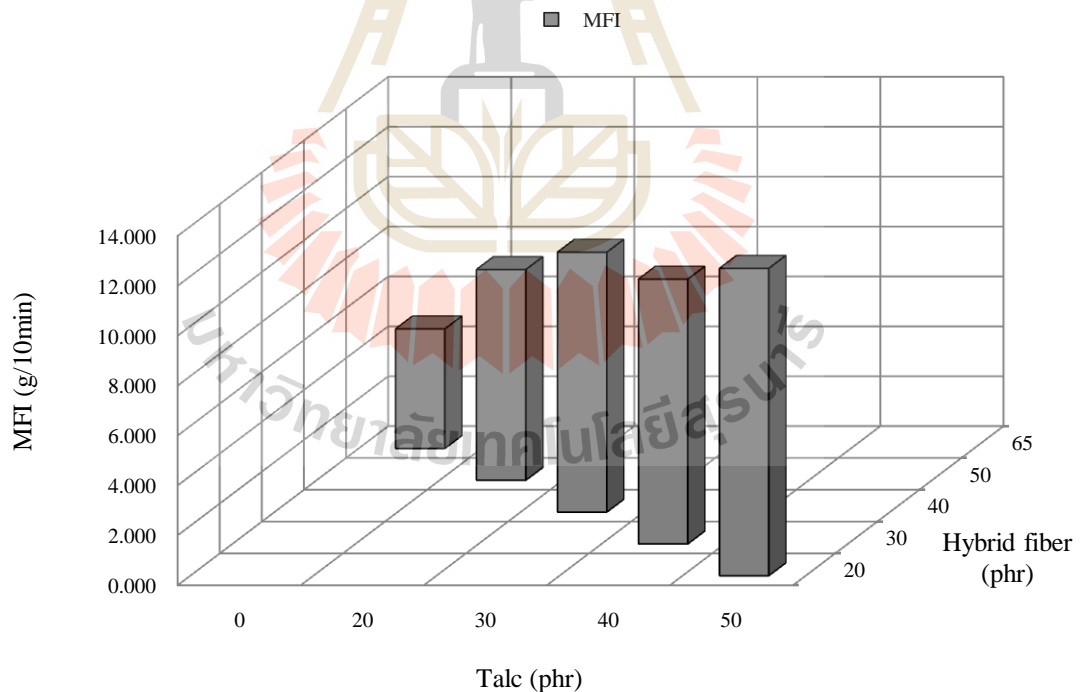


Figure 4.33 MFI of biocomposite as a function of talc and the hybrid fiber contents.

4.4.2 HDT of the talc filled hybrid composite

The HDT of the talc filled biocomposite is plotted and presented as function of fiber and talc ratio in Figure 4.34. General observation, it is witness that all the HDT obtained are above 100°C after sauna curing. For the original sample, HDTs are roughly 54°C and they are independent of the fibers and talc ratio and contents. However, after sauna curing process and also sauna cured/dried samples they are found that the heat resistance, HDT, is dramatically increased to over 100°C and there is very small deviation of the HDT value between cured and cured/dried, respectively. It is also observed that the HDT is decreased when increasing talc ratio. This outcome reinforces that fiber is positive effect on the HDT of the biocomposite as previously concluded. The suspect for examining the cured/dried specimen is that moisture residual during the sauna incubation might has the significant on the properties of the hydrophilic biocomposite. Completely removing of the moisture would enhance the test result. But for the HDT characteristic, there is no different between those two samples. From this result, perhaps, it can be suggested that silane/moisture condensation reaction can be used to significantly improve the ability of the composite material to resist the high temperature thermal stress.

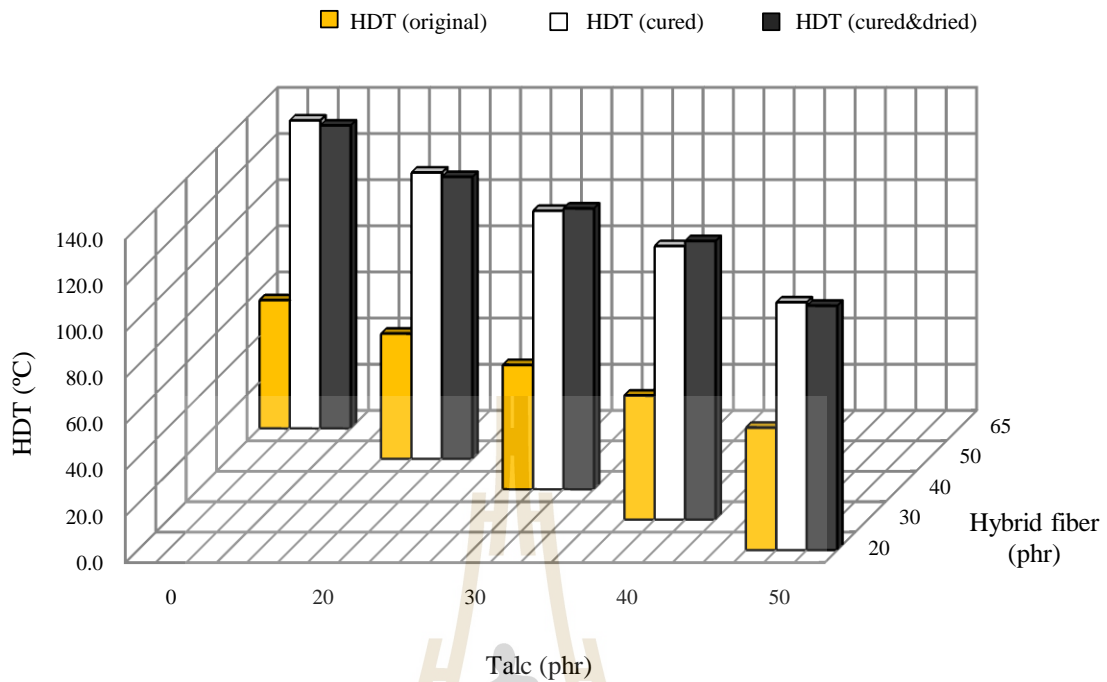


Figure 4.34 HDT of biocomposite as a function of talc and the hybrid fiber contents.

4.4.3 Impact properties of the talc filled hybrid composite

In Table 4.21 and the plotted graphs illustrated in Figure 4.35 - 4.36 reveal the impact strengths of the talc filled biocomposite obtained using 25:75 EFB and cotton hybrid fibers. For the notched testing mode, Figure 4.35, it is seen that the strength of the hybrid composite is slowly decreased with increasing the talc ratio for all samples. Sauna incubation is slightly enhanced the impact value. But after get rid of the residual moisture in the specimen by vacuum drying, the value is gone down to the original sample. With decent matrix to fiber adhesion, it is very common to see that the higher fiber content the better impact strengths. Vice versa, higher solid filler loading would lower the notched strength. It is from the fact that rigid particulate filler normally provide the negative effect to toughness of polymer compound. The

touch of softness by residual moisture in the material would attribute of the fracture toughness.

The exact trend is found for unnotched impact strength testing, Figure 4.36. The hybrid composites without talc indicates the highest impact value for all samples. Increasing the talc ratio with lowering the fiber fraction, the unnotched impact strength is gradually decreased. Moisture residual during the sauna curing procedure provide marginally superior in the test value but after removing the residual most of the strength somehow is reduced to the original value. The identical explanation stated on the above discussion would be supported this research outcome.

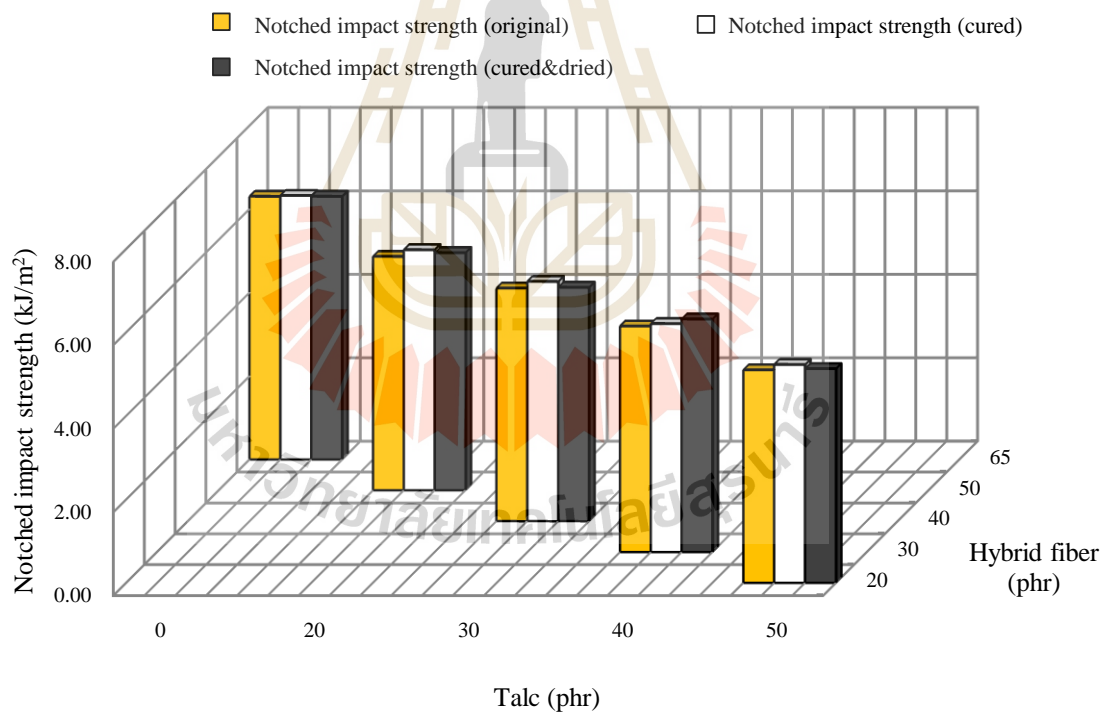


Figure 4.35 Notched impact strength of biocomposite as a function of talc and the hybrid fiber contents.

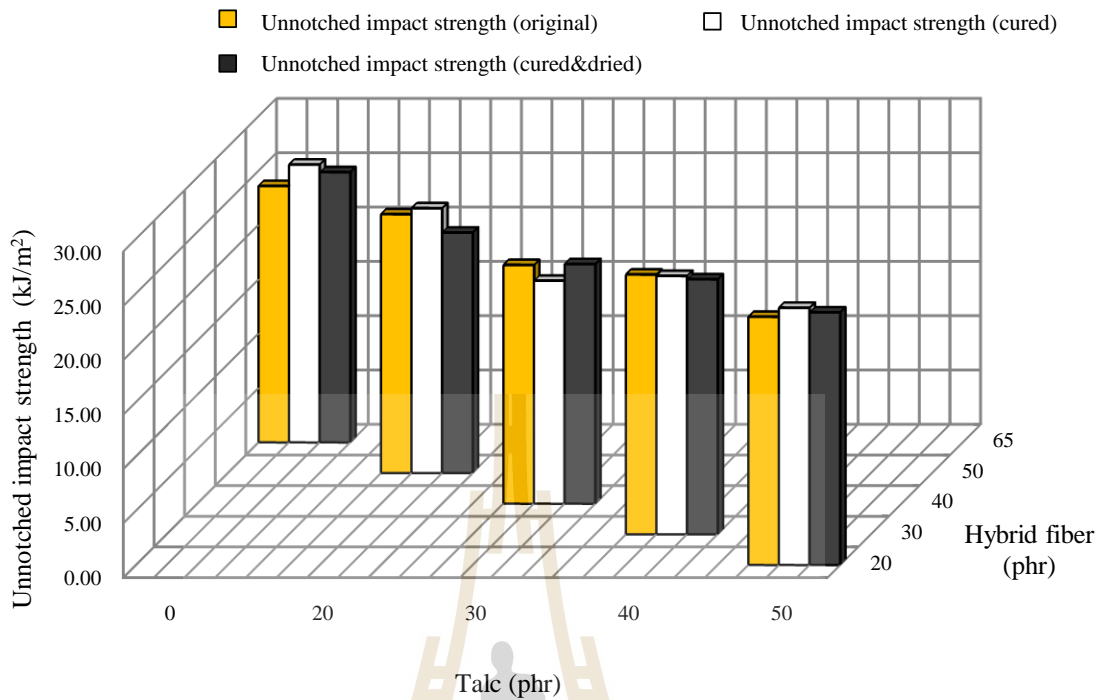


Figure 4.36 Unnotched impact strength of biocomposite as a function of talc and the hybrid fiber contents.

4.4.4 Flexural properties of the talc filled hybrid composite

The flexural strength and modulus of the composite are graphically presented in respect to the talc and fiber contents in Figure 4.37 and 4.38, respectively. Figure 4.37 shows that the strength of composite is gradually decreased when increasing talc content from 20 phr to 50 phr. Vice versa, the strength is increased with increasing the fiber content. However, when compare with the original, sauna cured and cured/dried samples, it is seen that the cured and dried sample is normally superior than the others. The identical trend are observed for flexural modulus of the hybrid composites with talc and fiber content as given in Figure 4.38. As expected, adding the talc filler into composites would deteriorate the bending

ductility the material. On the other word, the material would become brittle. But, reinforcement addition with good surface adhesion between fiber and matrix, the higher fiber content the more tougher material would be. According to this flexural results, it would say that compulsory addition of talc as filler into the hybrid composite the flexural properties of the material become inferior. The increase in matrix, talc filled PLA, viscosity and then lower the surface wettability between matrix and fiber would be taken to explain the observation.

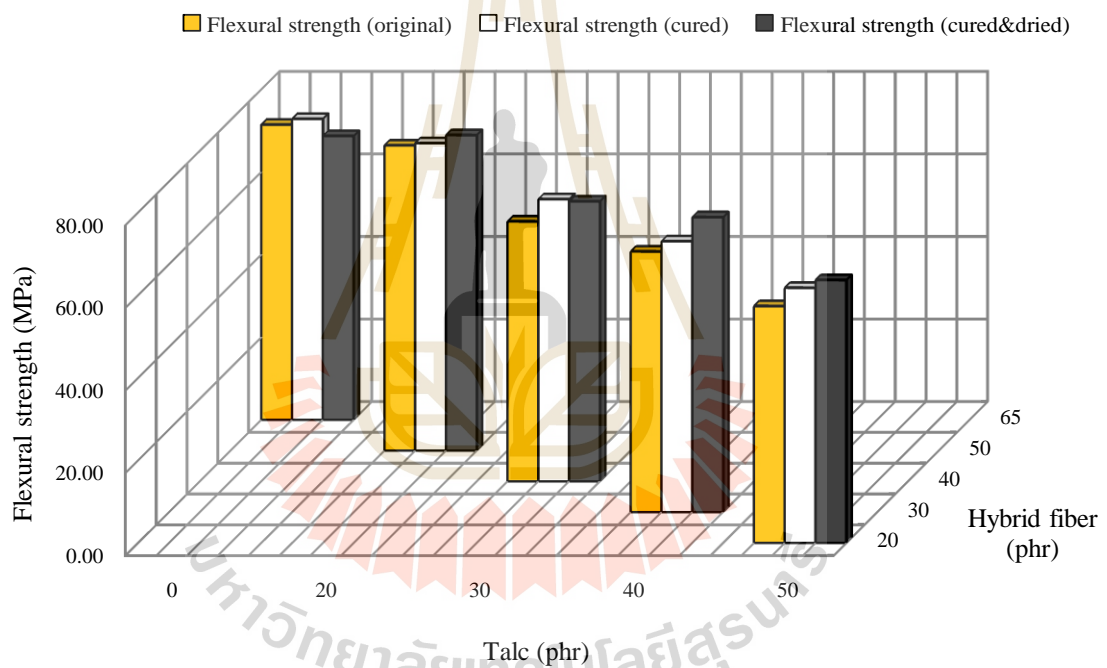


Figure 4.37 Flexural strength of biocomposite as a function of talc and the hybrid fiber contents.

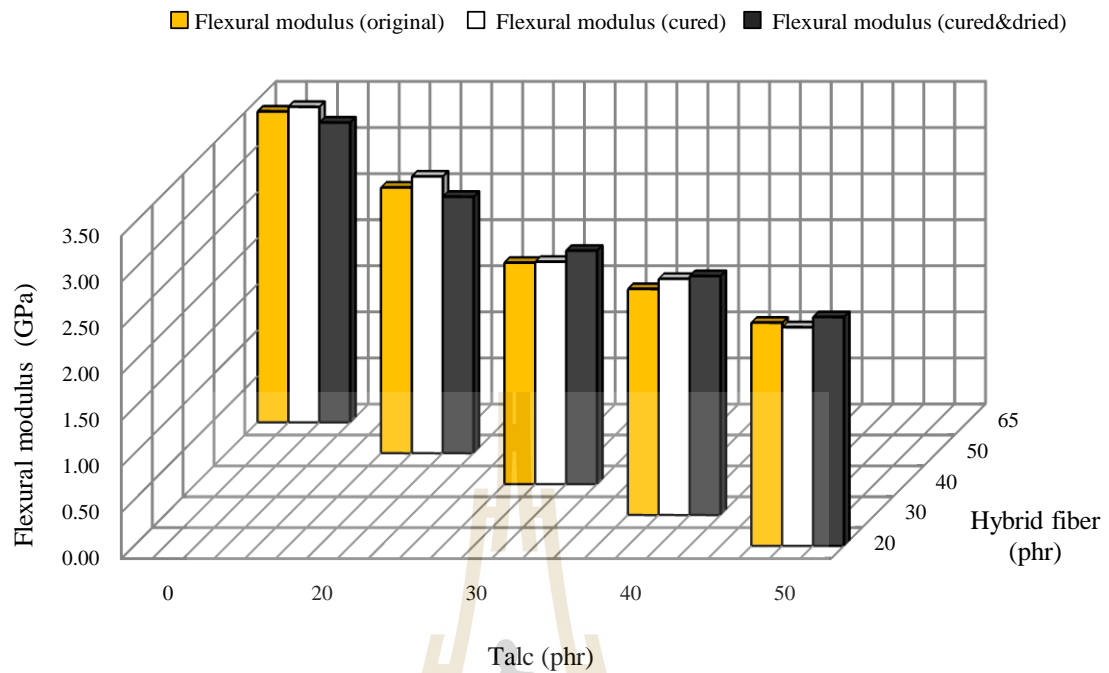


Figure 4.38 Flexural modulus of biocomposite as a function of talc and the hybrid fiber contents.

4.4.5 Scanning electron microscopy (SEM)

Figures 4.39 (a) - 4.39 (f) exhibit the SEM micrograph of the fractured surface obtained from the composites having only fiber and 50 phr of talc and 20 phr of fiber, respectively. Figure 4.39 (a) to 4.39 (c) are the fractured surface of the original, cured and cured/dried samples, respectively, of the composite contained 65 phr of fiber and 0 phr of talc. From the previous discussion, the impact and flexural strengths of those samples are marginally different. They show the highest in tests value. Figures also show the trace of mainly fiber pull out mode from the matrix with tiny evidence of fiber debonding phenomenon. Vice versa, Figure 4.39 (d) - 4.39 (f) are the original, sauna cured and cured/dried sample, respectively, of the composition with 50 phr of talc and 20 phr of fiber. Closer look on the photographs, it is observed

that all the fibers are mostly pulled out during the impact fracturing. This observation indicates that the fiber/matrix surface adhesion of the composite is poor. The statement go along very well with the mechanical testing values that they are declined after increasing talc but decreasing fiber contents.

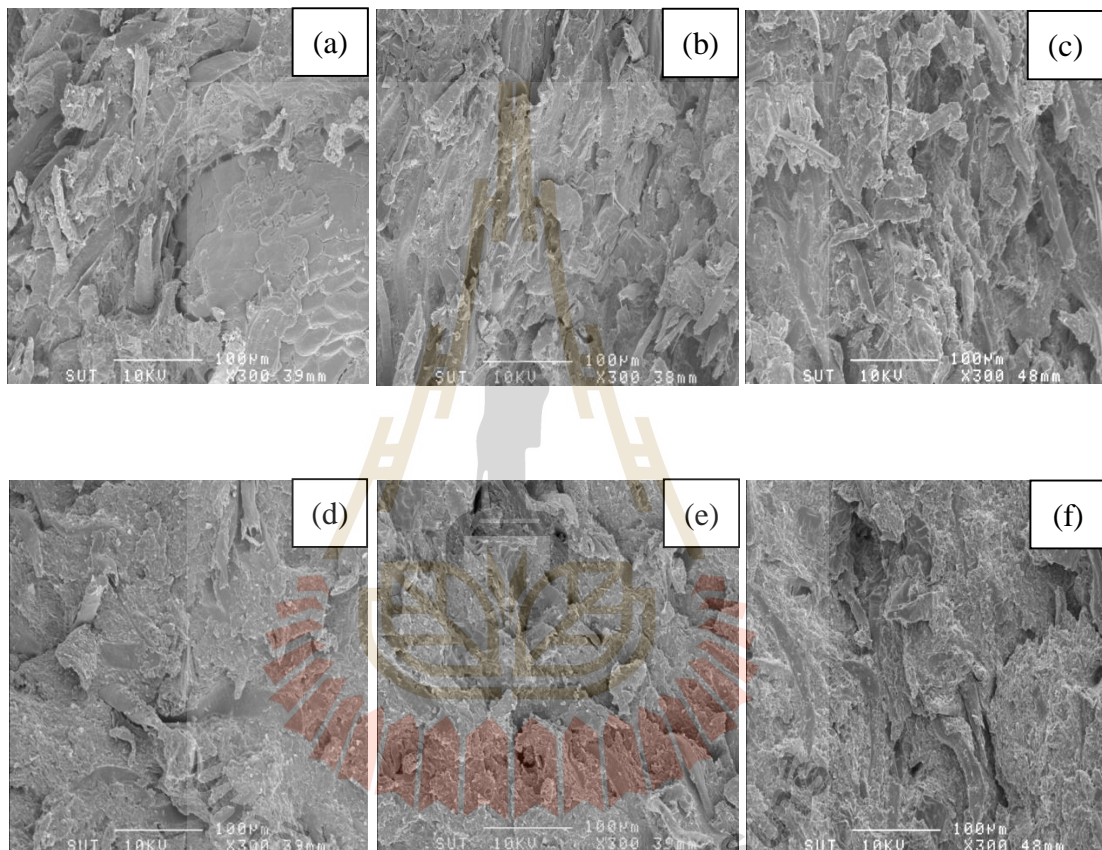


Figure 4.39 SEM micrograph of the hybrid biocomposite with; (a) 0:65 (original), (b) 0:65 (cured), (c) 0:65 (cured/dried), (d) 50:20 (original), (e) 50:20 (cured) and (f) 50:20 (cured/dried) of talc and hybrid fiber ratios.

From the results discussed, adding talc into the composite provides the improvement on the MFI properties of the hybrid biocomposite. Decreasing fiber but increasing talc content, the flow ability of composites is increased. Silane/moisture incubation can also enhance the HDT of composite. For the cured/dried sample, to get rid of moisture residual, HDT of sample show no difference from cured sample. Moreover, the rest of the tests also indicate that there is no dramatically different between these two type of samples. Composite with higher talc and low fiber contents has shown the inferior in the mechanical properties. Increasing in the matrix viscosity and hence lower in surface wettability, surface adhesion, would be responsible for the weakness.

4.5 Design of experiment#2: Hybrid biocomposite from crosslinked PLA using peroxide/silane system

So far, the biocomposite manufactured from PLA matrix, ENR, talc filler, epoxy/polyester polyols compatibilizer, EFB/cotton hybrid fibers and amino and epoxy types silane coupling agents demonstrated excellent in thermal and modulate in mechanical properties. The outstanding in the service temperature, HDT, of the composite material is partly contributed from the bonding of silane linkage via the condensation reaction. They are several research works published that combination of vinyl type silane can be initiated by free radical from the peroxide decomposition. The crosslinked PLA could be obtained by the silane addition/condensation reaction system. The crosslinked chain led to the improved the toughness of the composite. Vinyl trimethoxysilane (VTMS; A-171) is normally grafted onto the polymer backbone by reactive extrusion melt mixer. The grafting reaction is usually initiated

by free radicals using small amounts of peroxide. The reactive sites are formed. Further moisture induced condensation through the reactive site to form the intermolecular bonding bridges is typically involved. In this section, using the VTMS/dicumyl peroxide (DCP) to attempt the matrix crosslinking is experimented and discussed. The improvement of both mechanical and thermal properties are expected.

The optimization of the compound constituents was statistically performed by means of 2^k factorial design of experiment (DOE). As usual, thermal, rheological and mechanical, including flexural and impacts, properties were measured and used for the statistical response analysis. The amount of DCP and VTMS was statistically assigned as parameter A and B, respectively. The levels of the parameters are shown in Table 4.22. According to the rule of design, $2^2 = 4$, four combinations of the designed formula are constructed and they are summarized in Table 4.23. The test samples obtained from the designed compound were prepared and measured. The test values are reported in Table 4.24.

General observation, only the HDT of the biocomposite is vastly increased after the sauna treatment. Because the test value transforms from a two digit value, $\sim 54^\circ\text{C}$, to a three digit value, $\sim 130^\circ\text{C}$. Whereas the mechanical properties do not dramatically change through the sauna process. Moreover, the removing of moisture residual on the sauna cured sample, or cured/dried sample, does not have a huge effect on the test values. The small differences in the values are probably statistical error in nature. However, closer investigation by means of statistical verification is needed and being analyzed as follows.

Table 4.22 The parameters and level for DOE.

Parameters	Low level (-1)		High level (+1)	
	Peroxide (phr)	0.3	0.5	0.7
Silane (phr)	3.0	5.0	8.0	10.0

Table 4.23 The 2² factorial design matrix.

Condition	Factor			Composition (phr)									
	A	B	AB	(A) Peroxide (DCP)	(B) Silane (VTMS;A-171)	PLA	Talc	Cotton fiber	EFB fiber	Solid epoxy	Polyols	ENR50	Stabi- lizer
Run#1	+	+	+	(+)0.7	(+)10.0	100	20	37.5	12.5	0.4	5	20	2
Run#2	+	-	-	(+)1.0	(-)3.0	100	20	37.5	12.5	0.4	5	20	2
Run#3	-	+	-	(-)0.5	(+)8.0	100	20	37.5	12.5	0.4	5	20	2
Run#4	-	-	+	(-)0.3	(-)5.0	100	20	37.5	12.5	0.4	5	20	2

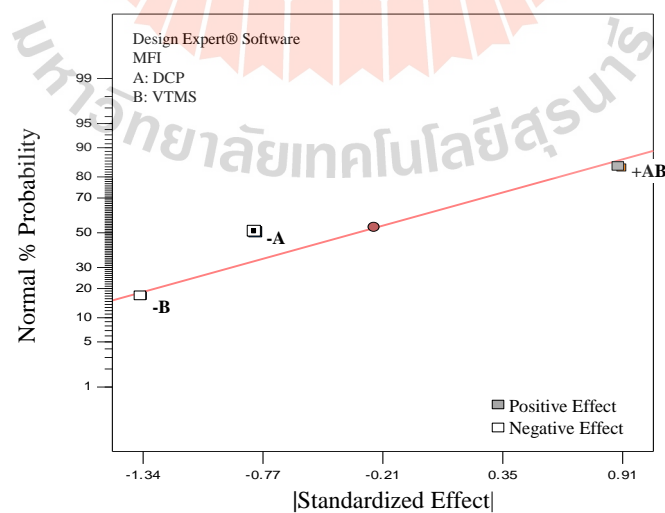
Table 4.24 Results of the designed responses.

Sample	Composition (phr)		MFI at 190/10.0 (g/10min)	HDT (°C)			Notched impact strength (kJ/m ²)			Unnotched impact strength (kJ/m ²)			Flexural strength (MPa)			Flexural modulus (GPa)		
	(A) DCP	(B) VTMS		original	cured	cured&dried	original	cured	cured&dried	original	cured	cured&dried	original	cured	cured&dried	original	cured	cured&dried
Run#1	(+)0.7	(+)10.0	4.594±0.101	53.8±0.3	130.1±1.5	132.2±1.7	6.66±0.22	6.81±0.24	6.79±0.26	30.26±3.77	26.77±3.46	26.74±1.79	80.16±2.52	82.90±2.93	82.10±2.41	2.98±0.04	3.03±0.19	2.97±0.16
Run#2	(+)1.0	(-)3.0	5.022±0.312	53.6±0.3	129.1±1.6	129.5±1.3	6.33±0.16	6.72±0.30	6.90±0.31	28.40±0.70	26.58±2.82	26.90±3.02	80.74±1.28	84.41±1.44	85.17±1.53	3.06±0.15	3.22±0.16	3.20±0.13
Run#3	(-)0.5	(+)8.0	4.490±0.457	54.0±0.5	127.8±1.7	130.6±1.7	6.72±0.07	6.63±0.34	6.80±0.25	30.14±2.31	28.59±4.03	29.42±3.12	84.82±2.50	82.06±0.85	83.71±3.35	3.23±0.40	3.11±0.13	3.12±0.13
Run#4	(-)0.3	(-)5.0	6.735±0.303	54.1±0.7	125.5±2.5	127.2±1.4	6.66±0.16	6.93±0.09	6.93±0.12	30.39±2.44	31.44±3.84	30.27±2.38	82.90±2.20	83.04±2.18	85.55±1.41	3.16±0.26	3.03±0.20	2.93±0.19



4.5.1 Flow ability of hybrid biocomposite

Rheological properties by mean of the melt flow index obtained at 190/10.0 are illustrated in Table 4.24. The standard effects of the parameter(s) were calculated and plotted with the normal probability is shown in Figure 4.40 (a). Taken both highest effect values as the beginning and end of linear line, therefore the middle effect will be verify either its is included or excluded from the linear trend line. If it is excluded that mean it is the significant effect to the statistical response. From the MFI response plot, it is seen that DCP (-A) content is excluded from the linear trend line and it is the negative effect. Verifying this parameter by both pareto chart shown in Figure 4.40 (b) and ANOVA conclusion given in Table 4.25, it confirms that the DCP content does not have the significant effect to the MFI. Because the calculated t -values and p -value are lower and higher than the critical values, respectively. The analysis result concludes that the designed model, parameters and the levels used, does not have the significant to the flow ability of the material.



(a)

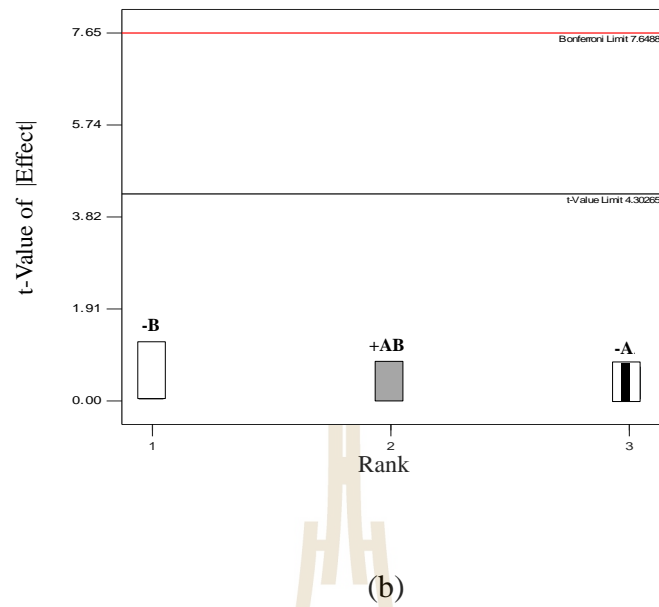


Figure 4.40 (a) normal plot and (b) pareto chart of the MFI.

Table 4.25 ANOVA results obtained from the MFI.

Source	Sum of squares	df	Mean square	<i>f</i> -value	<i>p</i> -value
Model	0.648	1	0.648	0.498	0.5534
A-Peroxide	0.648	1	0.648	0.498	0.5534
Residual	2.601	2	1.301		
Cor Total	3.249	3			

4.5.2 HDT of hybrid biocomposite

The plot of standardized effect and normal probability of the HDT response of the original sample given in Table 4.24 is presented in Figure 4.41 (a). Silane content is suspected as the significant effect of the HDT. Again, combining of pareto plot and ANOVA testing that shown in Figure 4.41 (b) and Table 4.26,

respectively, it concludes that silane does not has an effect to the HDT of the biocomposite before sauna curing.

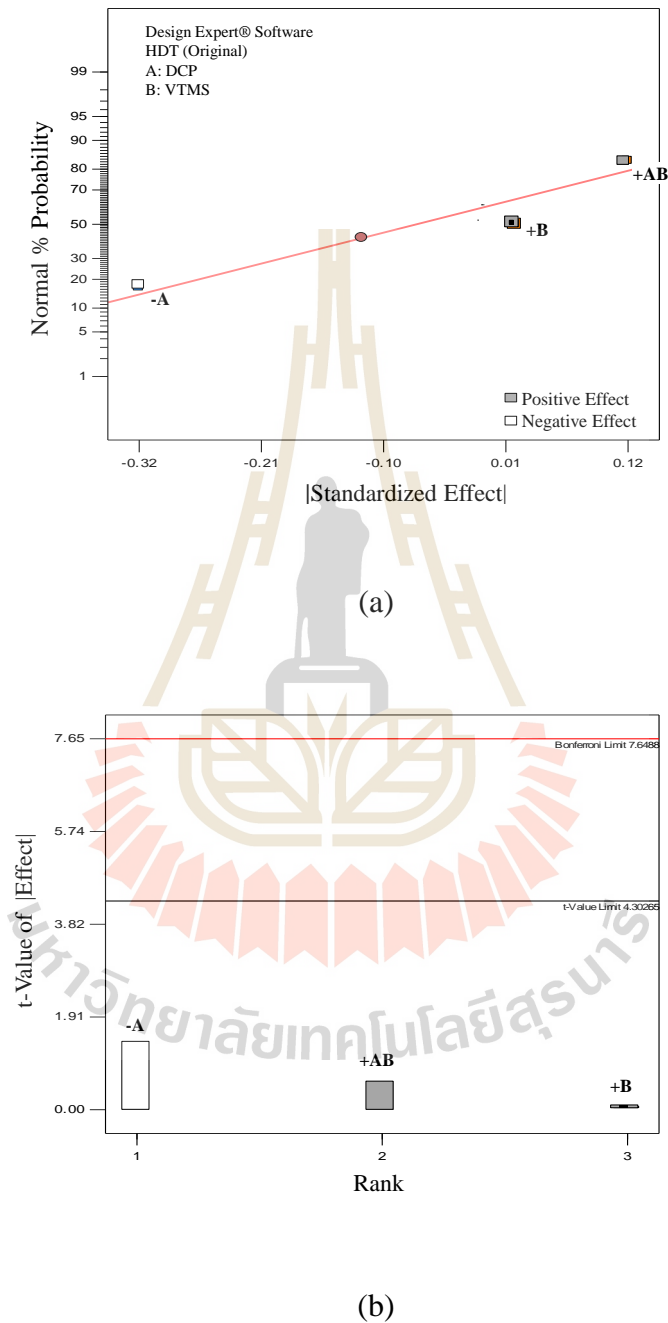
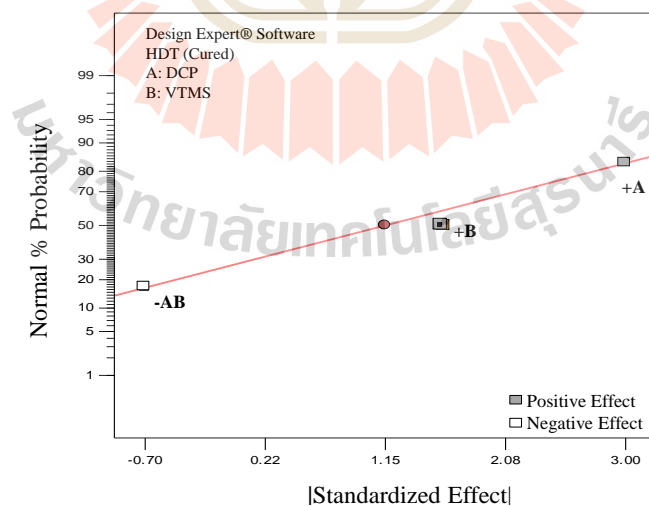


Figure 4.41 (a) normal plot and (b) pareto chart of the HDT (original).

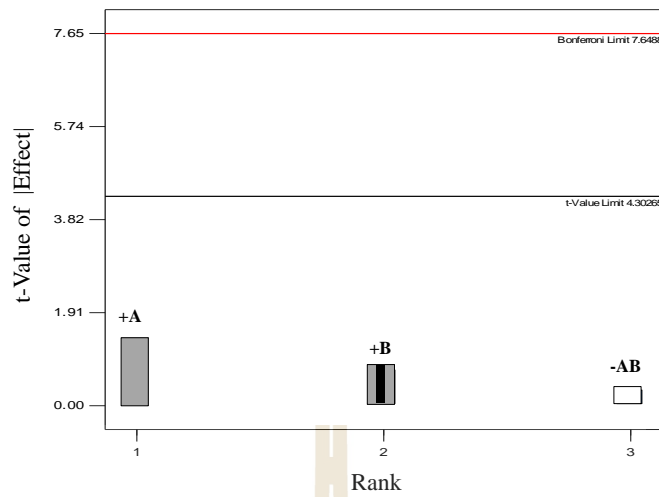
Table 4.26 ANOVA results obtained from the HDT (original).

Source	Sum of squares	df	Mean square	<i>f</i> -value	<i>p</i> -value
Model	2.778E-04	1	2.778E-04	4.878E-03	0.9507
B-Silane	2.778E-04	1	2.778E-04	4.878E-03	0.9507
Residual	0.114	2	0.057		
Cor Total	0.114	3			

For the HDT analysis of the sauna incubated sample, the normal plot, pareto chart and ANOVA conclusion are shown in Figure 4.42 (a), 4.42 (b) and Table 4.27, respectively. It is seen that all the calculated effects are perfectly fitted onto the linear line. Also, by enhancing from the pareto and ANOVA, it is confident to say that DCP and silane contents with in this experiment do not have the effect on the HDT of the sauna cured biocomposite.



(a)



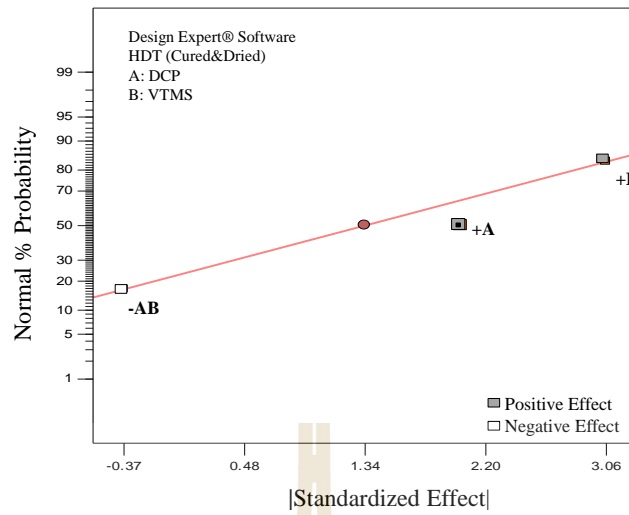
(b)

Figure 4.42 (a) normal plot and (b) pareto chart of the HDT (cured).

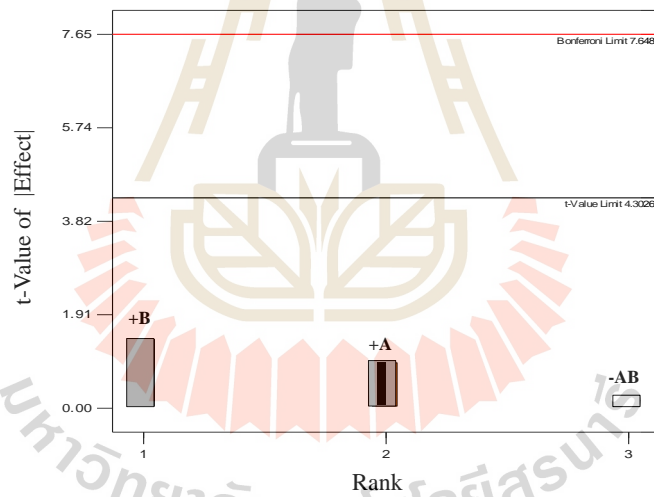
Table 4.27 ANOVA results obtained from the HDT (cured).

Source	Sum of squares	df	Mean square	<i>f</i> -value	<i>p</i> -value
Model	2.560	1	2.560	0.540	0.5391
B-Silane	2.560	1	2.560	0.540	0.5391
Residual	9.490	2	4.745		
Cor Total	12.050	3			

The exact analysis manner were applied for the HDT of cured/dried samples. The statistical results are given in Figure 4.43 (a), 4.43 (b) and Table 4.28, respectively. There is no significant parameter that has truly affect to the HDT of the completely cured and dried sample.



(a)



(b)

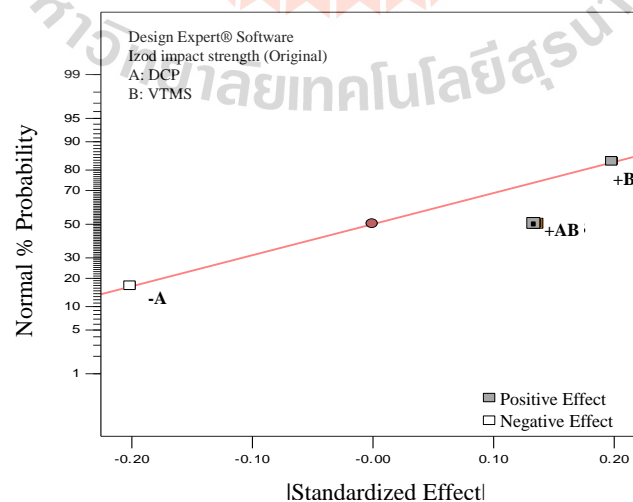
Figure 4.43 (a) normal plot and (b) pareto chart of the HDT (cured/dried).

Table 4.28 ANOVA results obtained from the HDT (cured/dried).

Source	Sum of squares	df	Mean square	<i>f</i> -value	<i>p</i> -value
Model	4.101	1	4.101	0.864	0.4508
A-Peroxide	4.101	1	4.101	0.864	0.4508
Residual	9.494	2	4.747		
Cor Total	13.595	3			

4.5.3 Impact Strengths of Hybrid Biocomposite

The notched impact strength response of the original specimen of the hybrid biocomposite was statistically analyzed and its result is illustrated in Figure 4.44 (a), 4.44 (b) and Table 4.29, consequently. The analysis of the notched impact strength of sauna cured and cured/dried are also performed and their results are given from Figure 4.45 (a), 4.45 (b) to 4.46 (a), 4.46 (b) and Table 4.29 to 4.30, respectively. They conclude that the notched impact strengths of both cured and cured/dried samples are not affected by the given parameters.



(a)

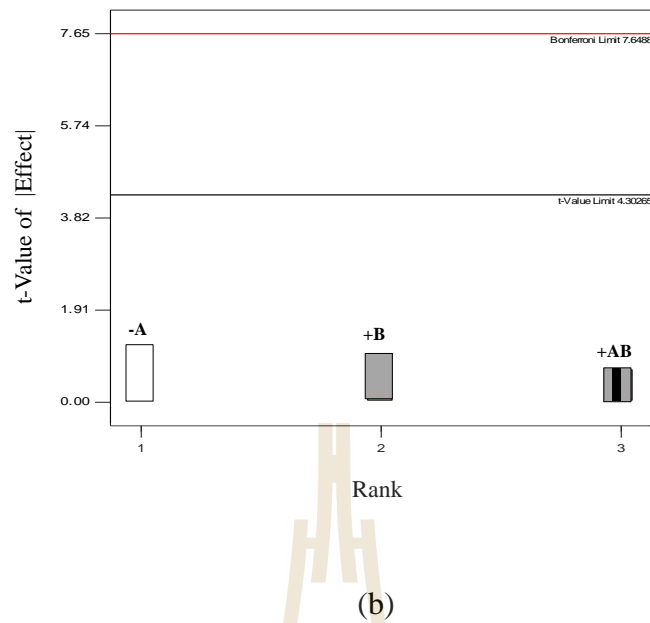


Figure 4.44 (a) normal plot and (b) pareto chart of the notched impact strength (original).

Table 4.29 ANOVA results obtained from the notched impact strength (original).

Source	Sum of squares	df	Mean square	<i>f</i> -value	<i>p</i> -value
Model	0.018	1	0.018	0.452	0.5707
AB	0.018	1	0.018	0.452	0.5707
Residual	0.079	2	0.039		
Cor Total	0.096	3			

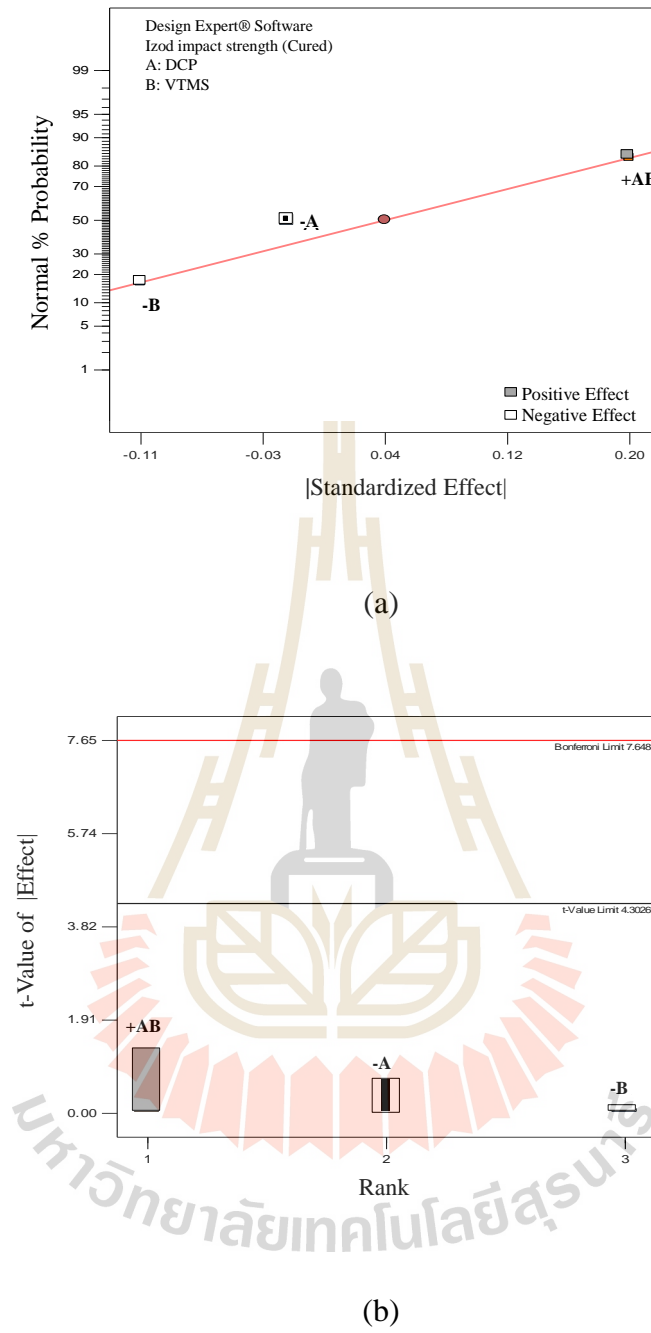
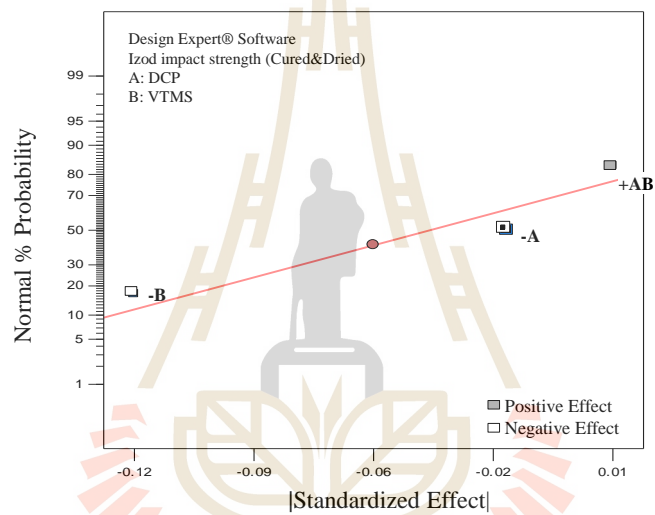


Figure 4.45 (a) normal plot and (b) Pareto chart of the notched impact strength (cured).

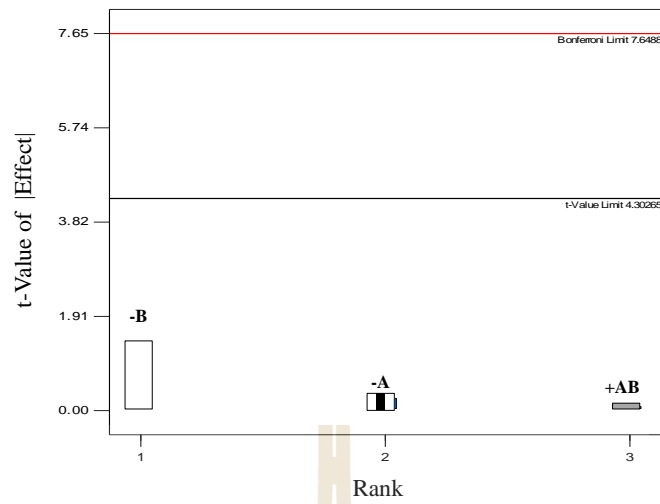
Table 4.30 ANOVA results obtained from the notched impact strength (cured).

Source	Sum of squares	df	Mean square	<i>f</i> -value	<i>p</i> -value
Model	2.250E-04	1	2.250E-04	9.174E-03	0.9324
A-Peroxide	2.250E-04	1	2.250E-04	9.174E-03	0.9324
Residual	0.049	2	0.025		
Cor Total	0.049	3			



(a)

มหาวิทยาลัยเทคโนโลยีสุรนารี



(b)

Figure 4.46 (a) normal plot and (b) pareto chart of the notched impact strength (cured/dried).

Table 4.31 ANOVA results obtained from the notched impact strength (cured/dried).

Source	Sum of squares	df	Mean square	<i>f</i> -value	<i>p</i> -value
Model	4.431E-04	1	4.431E-04	0.062	0.8271
A-Peroxide	4.431E-04	1	4.431E-04	0.062	0.8271
Residual	0.014	2	7.190E-03		
Cor Total	0.015	3			

The exactly conclusion is also found for the unnotched impact strengths of all conditioned sample of the biocomposite as they are seen from Figure 4.47 to 4.49 and Table 4.32 to 4.34, respectively.

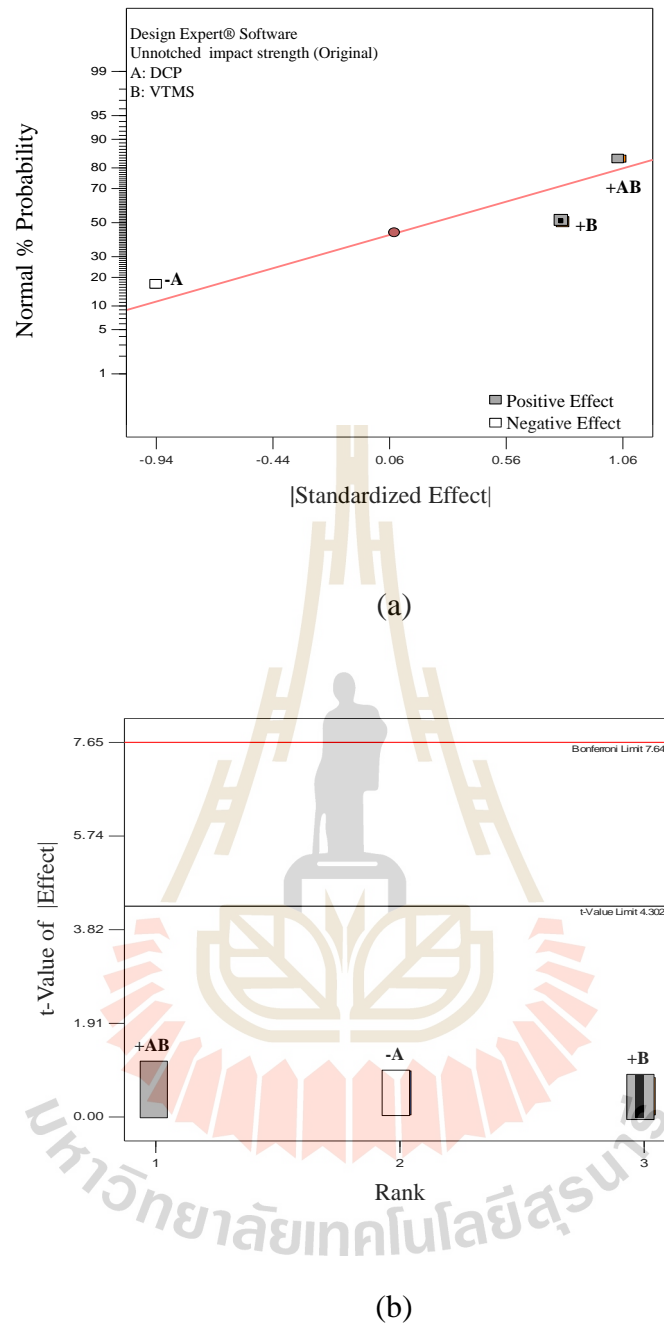
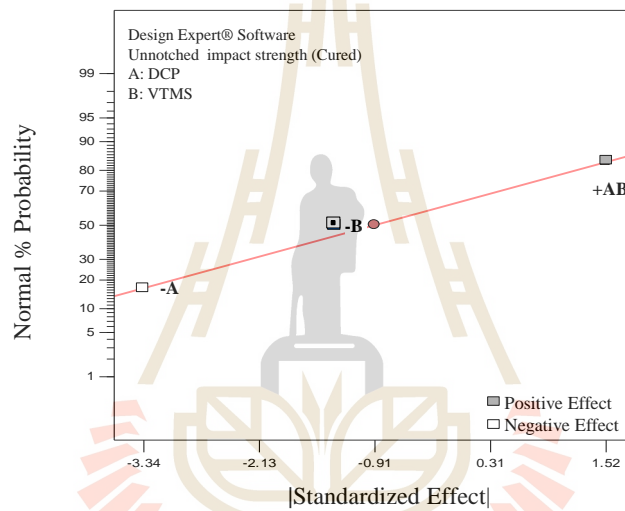


Figure 4.47 (a) normal plot and (b) pareto chart of the unnotched impact strength (original).

Table 4.32 ANOVA results obtained from the unnotched impact strength (original).

Source	Sum of squares	df	Mean square	<i>f</i> -value	<i>p</i> -value
Model	0.646	1	0.646	0.648	0.5052
B-Silane	0.646	1	0.646	0.648	0.5052
Residual	1.994	2	0.997		
Cor Total	2.641	3			



(a)

มหาวิทยาลัยเทคโนโลยีสุรนารี

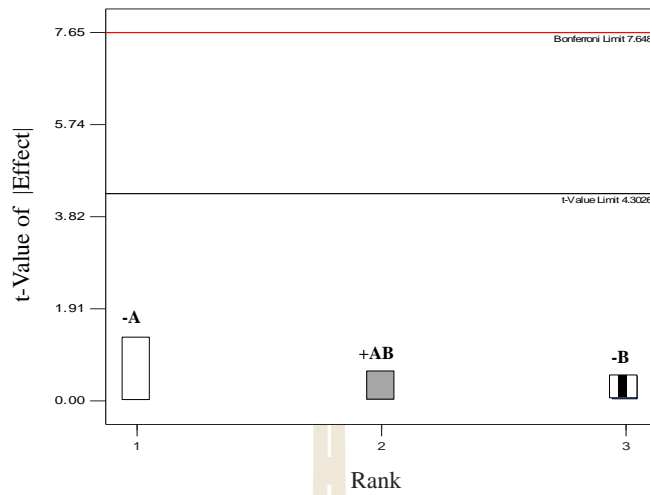
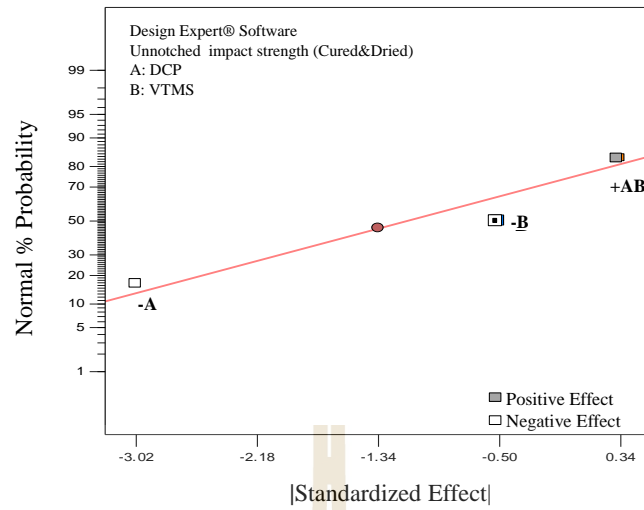


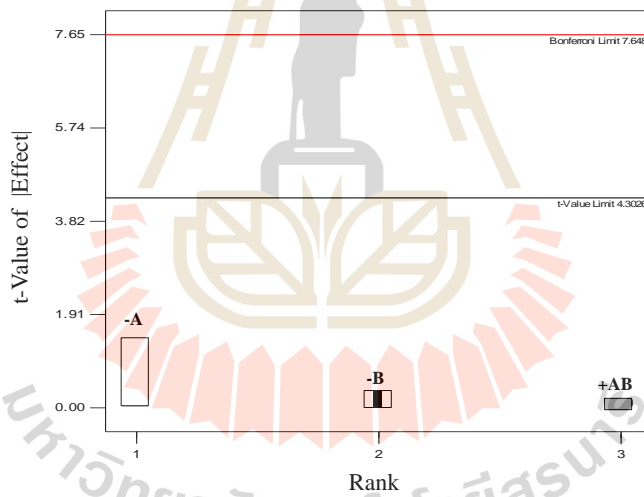
Figure 4.48 (a) normal plot and (b) pareto chart of the unnotched impact strength (cured).

Table 4.33 ANOVA results obtained from the unnotched impact strength (cured).

Source	Sum of squares	df	Mean square	<i>f</i> -value	<i>p</i> -value
Model	1.769	1	1.769	0.263	0.6593
B-Silane	1.769	1	1.769	0.263	0.6593
Residual	13.466	2	6.733		
Cor Total	15.235	3			



(a)



(b)

Figure 4.49 (a) normal plot and (b) pareto chart of the unnotched impact strength (cured/dried).

Table 4.34 ANOVA results obtained from the unnotched impact strength (cured/dried).

Source	Sum of squares	df	Mean square	<i>f</i> -value	<i>p</i> -value
Model	0.257	1	0.257	0.056	0.8357
B-Silane	0.257	1	0.257	0.056	0.8357
Residual	9.257	2	4.629		
Cor Total	9.514	3			

4.5.4 Flexural Properties of Hybrid Biocomposite

Flexural properties by mean of the strength and modulus of the composite affected by the peroxide and silane used from the design of experiment as given in Table 4.24, were analyzed. It is also found that the levels amount of peroxide and silane assigned in the designed experiment do not have the significant influence on both flexural strength and modulus of the composite with no respect to any mean of sample treatment conditions. The statement is confirmed by the statistical result presented from Figure 4.51 to 4.55 and ANOVA Table 4.36 to 4.40, respectively.

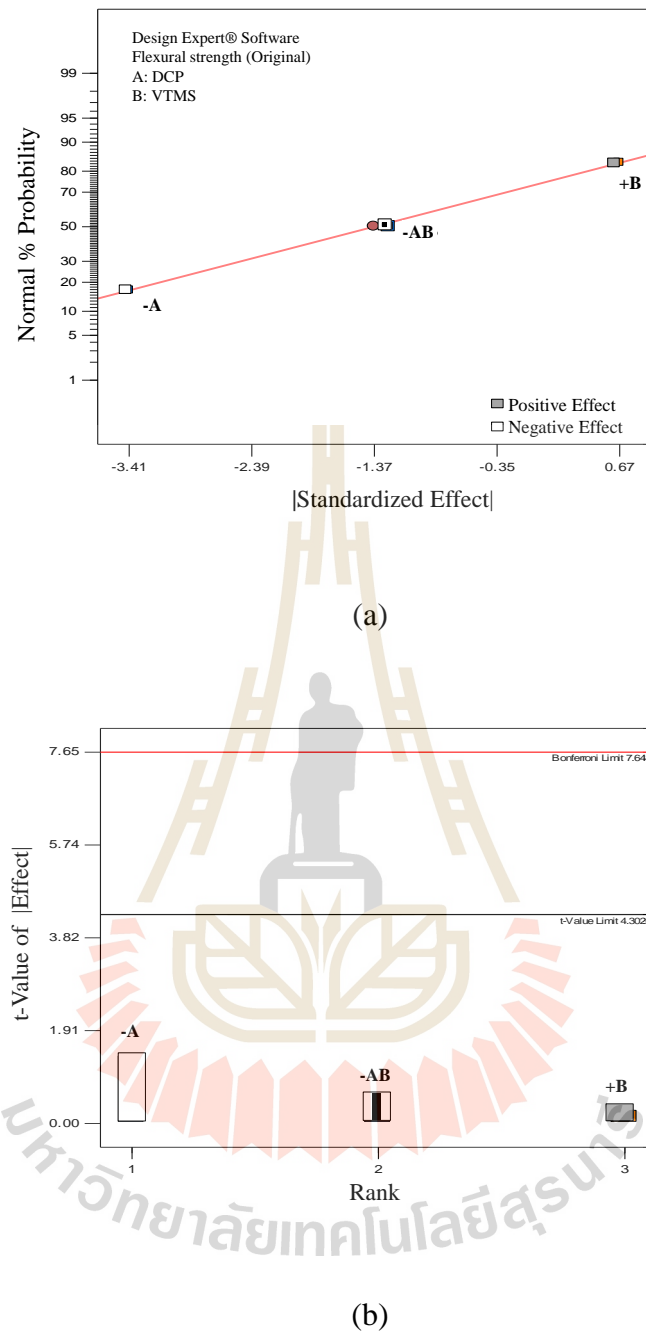
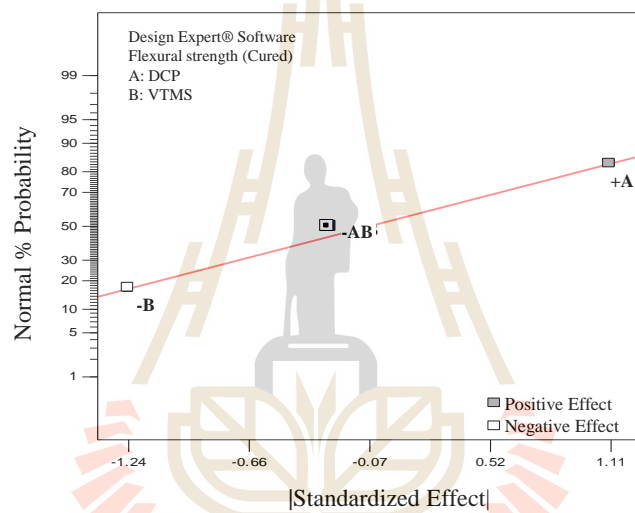


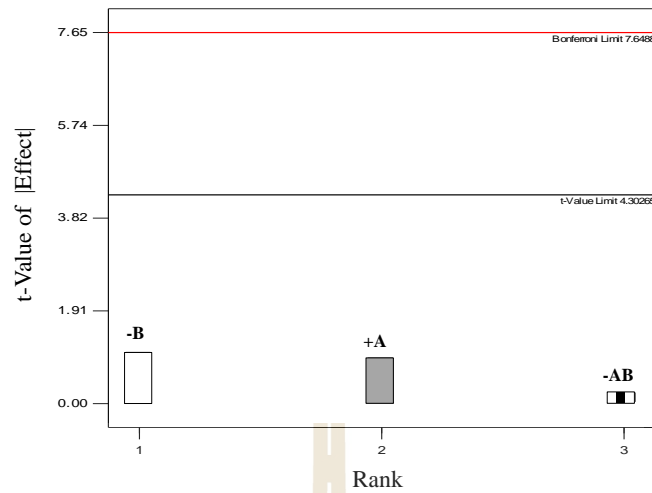
Figure 4.50 (a) normal plot and (b) pareto chart of the flexural strength (original).

Table 4.35 ANOVA results obtained from the flexural strength (original).

Source	Sum of squares	df	Mean square	<i>f</i> -value	<i>p</i> -value
Model	1.565	1	1.565	0.259	0.6615
AB	1.565	1	1.565	0.259	0.6615
Residual	12.093	2	6.047		
Cor Total	13.658	3			



(a)



(b)

Figure 4.51 (a) normal plot and (b) pareto chart of the flexural strength (cured).

Table 4.36 ANOVA results obtained from the flexural strength (cured).

Source	Sum of squares	df	Mean square	<i>f</i> -value	<i>p</i> -value
Model	0.069	1	0.069	0.050	0.8437
AB	0.069	1	0.069	0.050	0.8437
Residual	2.766	2	1.383		
Cor Total	2.835	3			

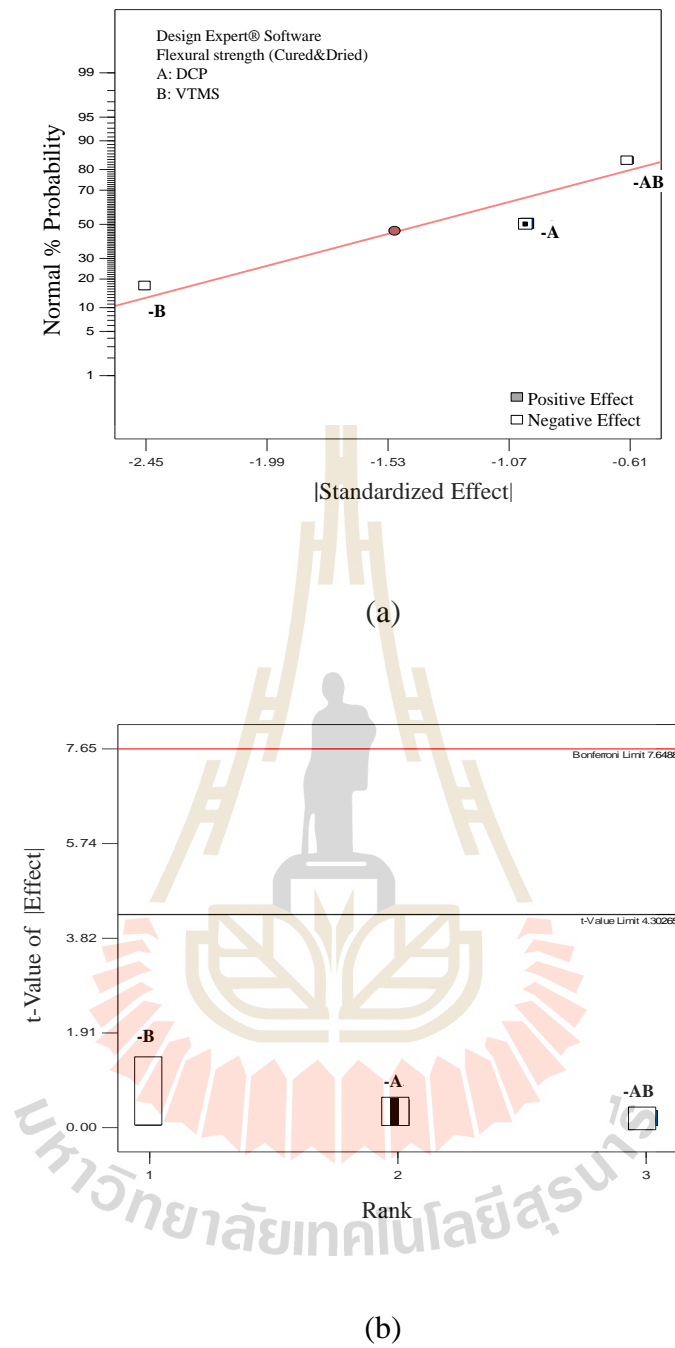
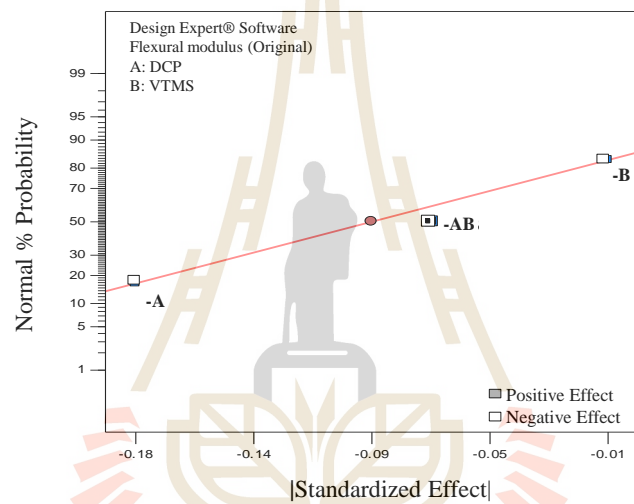


Figure 4.52 (a) normal plot and (b) pareto chart of the flexural strength (cured/dried).

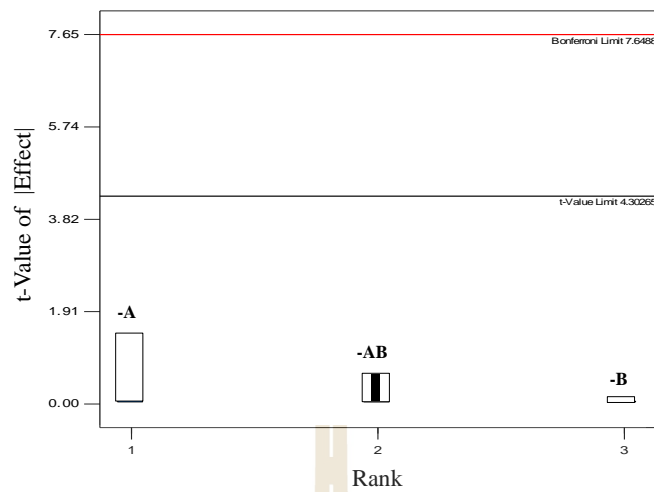
Table 4.37 ANOVA results obtained from flexural strength (cured/dried).

Source	Sum of squares	df	Mean square	<i>f</i> -value	<i>p</i> -value
Model	0.998	1	0.998	0.312	0.6325
A-Peroxide	0.998	1	0.998	0.312	0.6325
Residual	6.393	2	3.196		
Cor Total	7.391	3			



(a)

มหาวิทยาลัยเทคโนโลยีสุรนารี



(b)

Figure 4.53 (a) normal plot and (b) pareto chart of the flexural modulus (original).

Table 4.38 ANOVA results obtained from the flexural modulus (original).

Source	Sum of squares	df	Mean square	<i>f</i> -value	<i>p</i> -value
Model	5.041E-03	1	5.041E-03	3.142E-01	0.6315
AB	5.041E-03	1	5.041E-03	3.142E-01	0.6315
Residual	0.032	2	0.016		
Cor Total	0.037	3			

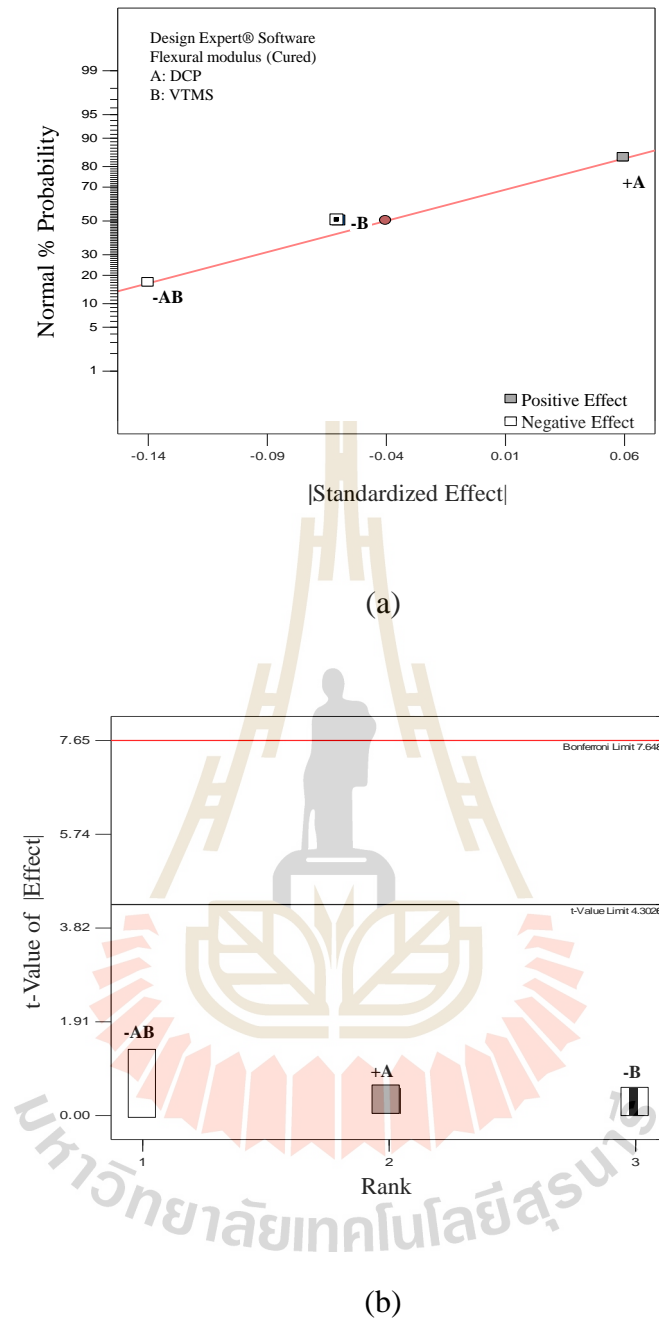
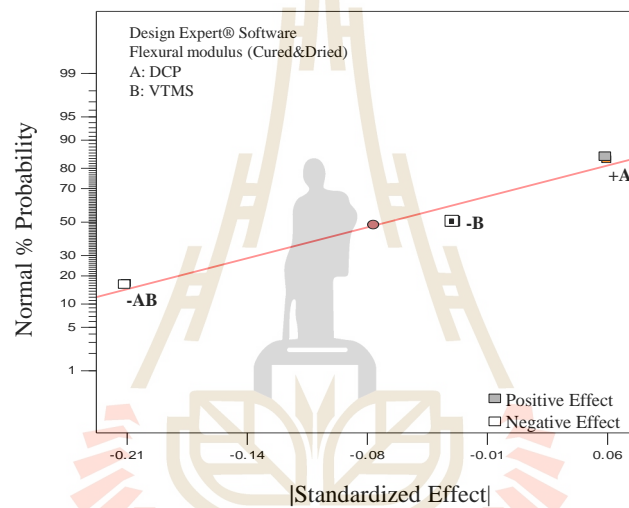


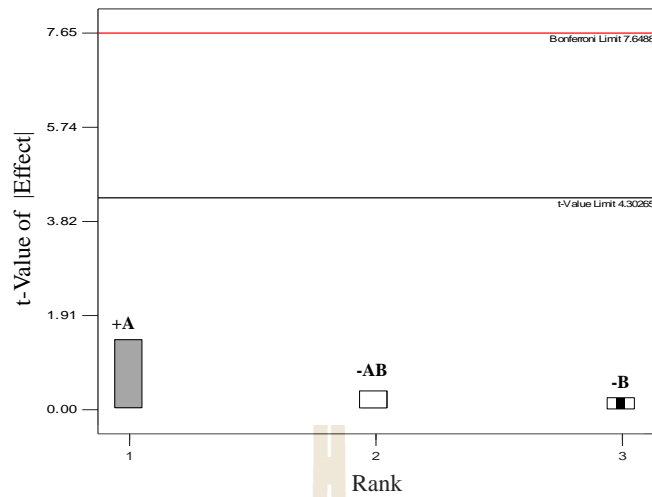
Figure 4.54 (a) normal plot and (b) pareto chart of the flexural modulus (cured).

Table 4.39 ANOVA results obtained from the flexural modulus (cured).

Source	Sum of squares	df	Mean square	<i>f</i> -value	<i>p</i> -value
Model	3.364E-03	1	3.364E-03	3.078E-01	0.6348
B-Silane	3.364E-03	1	3.364E-03	3.078E-01	0.6348
Residual	0.022	2	0.011		
Cor Total	0.025	3			



(a)



(b)

Figure 4.55 (a) normal plot and (b) pareto chart of the flexural modulus (cured/dried).

Table 4.40 ANOVA results obtained from the flexural modulus (cured/dried).

Source	Sum of squares	df	Mean square	<i>f</i> -value	<i>p</i> -value
Model	7.290E-04	1	7.290E-04	0.030	0.8777
B-Silane	7.290E-04	1	7.290E-04	0.030	0.8777
Residual	0.048	2	0.024		
Cor Total	0.049	3			

Table 4.41 DOE conclusions.

	Responses	Effect			Significant factor(s)
		A (Peroxide)	B (Silane)	AB	
Original	MFI	-	-	+	None
	HDT	-	+	+	None
	Notched impact strength	-	+	-	None
	Unnotched impact strength	-	+	+	None
	Flexural strength	-	+	-	None
	Flexural modulus	-	-	-	None
Cured	HDT	+	+	-	None
	Notched impact strength	-	-	+	None
	Unnotched impact strength	-	-	+	None
	Flexural strength	+	-	-	None
	Flexural modulus	+	-	-	None
Cured&dried	HDT	+	+	-	None
	Notched impact strength	-	-	+	None
	Unnotched impact strength	-	-	+	None
	Flexural strength	-	-	-	None
	Flexural modulus	+	-	-	None

From the entire DOE analysis, it can be conclude that DCP and silane at the given level of contents used in the present design of experiment do not the effect to the interested response. The variation of the value of the responses might be come from the parameter. But within the statistical error and assigned degree of confidential to validate the results it can conclude that the test results are no significant

differences. However, for the future exploration but not yet in this research work, the positive and negative direction of the parameters and the test responses are summarized in Table 4.41. This conclusion would be the guideline for the further investigation in term of setting the level of the parameters into higher or lower than the present work.

4.6 Comparison of peroxide/silane ratios and mixing procedures

The whole previous experiments, peroxide and silane was incorporated with other ingredient by preblending or coating on the solid ingredient before feeding into melt mixing twin screw extruder. The free radical initiation chemicals would normally and equally disperse onto surface of the solid mixture. When the crosslink is occurred with the assumption of well dispersed mixing, it would be linked throughout the dispersed phase. This mixing procedure is schematically summarized in Figure 4.56 and it is called method#I and the sample obtained is assigned as sample#I. It would be interesting to compare the incorporating procedure of peroxide/silane in the difference way.

In this experimental section, the DCP and VTMS addition were performed on the ENR rubber using two roll mill kneading process. Then, the kneaded rubber was incubated at 60°C for at least 12 hours. By doing so, the vinyl group on silane molecule and/or some non epoxidized vinyl segment of the ENR chain would be initiated by the thermal decomposed free radical from DCP to form silane grafted rubber. Finally, the fibers was brought to mix with the runner. The rest of the mixing method was identical to the method#I. This mixing procedure is named as method#II and shown in schematic Figure 4.57 and the injected sample obtained from this

mixing procedure is also named as sample#II. The composite formula for both mixing methods were identical and summarized in Table 4.42. DCP content is kept constant at 0.5 phr but VTMS is varied from 0.0 to 5.0 phr, respectively. The standard test results obtained from the injected specimen are concluded in Table 4.43 and 4.44.

Table 4.42 Experimental formulation for manufacturing the hybrid composite with increasing VTMS content.

Formula	Composition (phr)									
	Silane (VTMS; A-171)	Peroxide (DCP)	PLA	Talc	Cotton fiber	EFB fiber	Solid epoxy	Polyols	ENR50	Stabilizer
VTMS#0	0.0	0.5	100	20	37.5	12.5	0.4	5	20	2
VTMS#2	2.0	0.5	100	20	37.5	12.5	0.4	5	20	2
VTMS#3	3.0	0.5	100	20	37.5	12.5	0.4	5	20	2
VTMS#4	4.0	0.5	100	20	37.5	12.5	0.4	5	20	2
VTMS#5	5.0	0.5	100	20	37.5	12.5	0.4	5	20	2

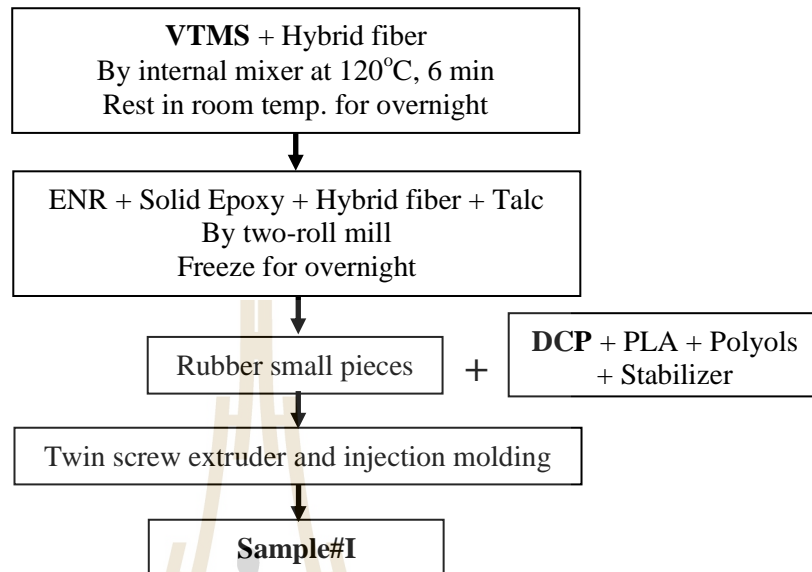
Method#I

Figure 4.56 Flow chart of compounding process of method#I.

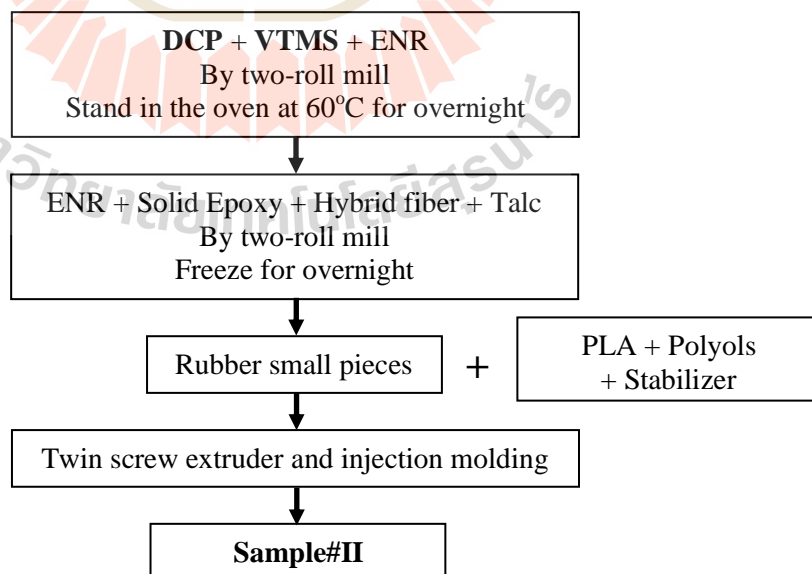
Method#II

Figure 4.57 Flow chart of compounding process of method#II.

Table 4.43 The MFI and HDT result of sample#Is and sample#IIs.

Formula	VTMS (phr)	MFI at 190/10.0 (g/10min)		HDT (°C)			
				original		cured	
		sample#I	sample#II	sample#I	sample#II	sample#I	sample#II
VTMS#0	0	3.827±0.276	3.270±0.240	53.8±0.3	54.3±0.3	119.9±4.2	126.5±2.3
VTMS#2	2	3.527±0.143	3.378±0.223	53.4±0.4	54.2±0.3	120.5±1.3	128.3±2.9
VTMS#3	3	3.258±0.316	3.411±0.211	52.2±0.8	53.8±0.8	124.1±4.2	129.2±2.8
VTMS#4	4	4.978±0.227	3.280±0.205	52.7±0.6	54.3±0.3	128.9±1.4	128.3±2.1
VTMS#5	5	4.330±0.202	4.324±0.283	52.7±0.3	53.7±0.6	129.6±2.0	127.9±3.1

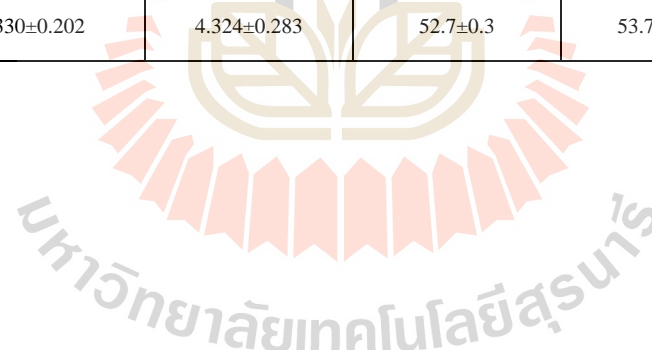


Table 4.44 The mechanical properties of sample#Is and sample#IIs.

Formula	Notched impact strength (kJ/m ²)				Unnotched impact strength (kJ/m ²)				Flexural strength (MPa)				Flexural modulus (GPa)			
	original		cured		original		cured		original		cured		original		cured	
	sample#I	sample#II	sample#I	sample#II	sample#I	sample#II	sample#I	sample#II	sample#I	sample#II	sample#I	sample#II	sample#I	sample#II	sample#I	sample#II
VTMS#0	6.58±0.51	7.53±0.11	6.45±0.24	7.53±0.13	27.78±2.46	28.46±1.41	27.42±0.59	29.38±4.06	84.98±1.92	82.25±3.09	84.43±3.21	83.84±1.84	3.27±0.24	2.86±0.18	3.32±0.10	2.88±0.12
VTMS#2	6.97±0.36	7.77±0.16	6.76±0.08	7.93±0.33	32.59±3.36	32.88±2.52	28.73±1.10	29.81±4.89	81.61±2.01	80.41±3.12	81.60±2.83	83.34±2.97	3.24±0.07	2.99±0.25	3.12±0.08	2.78±0.11
VTMS#3	6.70±0.13	7.60±0.30	6.73±0.41	8.09±0.50	33.41±2.26	31.76±1.39	30.08±4.03	32.39±3.47	78.36±1.63	78.26±3.15	80.38±0.79	81.19±0.64	2.95±0.28	2.83±0.22	3.02±0.11	2.77±0.08
VTMS#4	6.98±0.33	7.91±0.26	6.75±0.16	8.16±0.25	33.99±3.21	33.58±5.47	30.67±0.89	32.54±1.14	77.11±2.40	78.33±1.46	80.40±1.60	81.77±0.92	3.03±0.07	3.00±0.14	2.82±0.08	2.72±0.08
VTMS#5	6.53±0.25	7.98±0.18	6.84±0.34	8.43±0.31	30.45±2.46	32.20±4.42	30.58±4.61	29.34±1.27	76.63±2.23	77.69±1.76	77.60±2.09	79.24±1.38	2.94±0.17	2.98±0.05	2.83±0.08	2.64±0.06



4.6.1 Flow ability of hybrid biocomposite versus VTMS contents

The flow ability of the PLA based biocomposite by mean of the melt flow index obtained by standard at 190/10.00 is illustrated in Figure 4.58 for both compounding methods, respectively. It is seen that the flow ability of the sample#I, VTMS and DCP separately added, are slightly decreased when increasing VTMS from 0.0 to 3.0 phr but the flow index are higher when further increased silane from 4.0 to 5.0 phr. However, the sample#II, VTMS and DCP used as solution mixture, the MFI do not obviously change with the silane addition from 0.0 to 4.0 phr. The common observation found for both compounding methods is that the flow index of the composite material is noticeably high at 5.0 phr of silane. One of the main reasons to explain the MFI increasing of the composite could be due to the crosslinking or branching of the polymers chain via the silane/water intermolecular condensation. In this experiment, amount of peroxide used was limited, at 0.5 phr. Therefore, the generated free radical to react with the excess vinyl group of silane could be limited and it is the crosslink density controller of the system. Taken only the MFI result, it might be concluded that increasing the vinyl silane had increased the molar mass of chain via crosslinking or grafting reaction. Further increase the vinyl silane above the stoichiometric ratio between vinyl group and free radical, the excess of vinyl silane may degrade the PLA backbone introducing the chain scission reaction and hence decreasing the melt viscosity, higher in MFI. Whenever, the chain scission occurred in the compounding process, it will lead to low mechanical properties of hybrid composite. The inferior in mechanical properties observation will be discussed later on. When compare the effect of mixing method, method#I and method#II, the MFI of

the composite material at the given silane content are not so much difference except at the 4.0 phr of silane where the different in the flow index of the material is evidenced. It could be explained by the excess vinyl silane in the treated fiber portion would rather likely to react with polymer chain than the decomposed free radical. Consequently, the degradation would be taken place before the chain crosslinking or branching. As the result, the flow index of the compound would be increased. According to this experimental research, it would say that mixing the composite by using pre mixing DCP and silane solution is better procedure by means of the controlling the chain degradation via excess silane reaction.

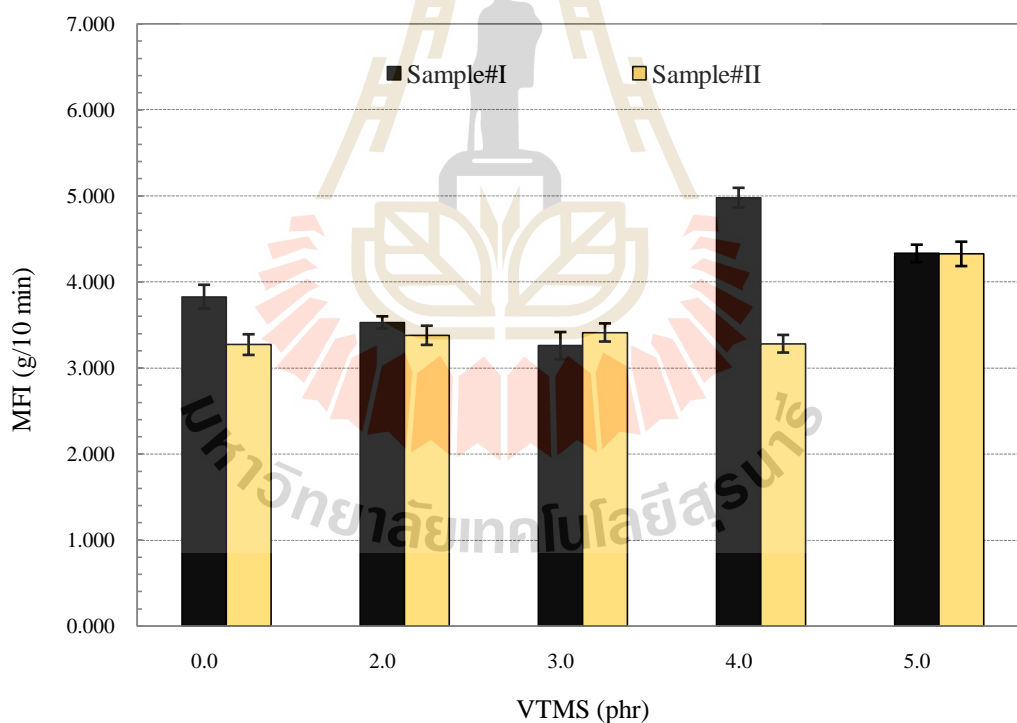


Figure 4.58 MFI of the hybrid composite with VTMS contents.

4.6.2 HDT of hybrid biocomposite versus VTMS contents and mixing procedures

Figure 4.59 shows the HDT of the composites with increasing the silane contents and comparing the mixing procedures. From the result it is evidenced that the heat distortion temperature of the composites are more or less independence on either the silane content and mixing methods for both samples with and without sauna treatment. From the plot the test values are almost unchanged. However, with the closer investigation especially for the sauna cured samples, there is the small tendency that the HDT is increased at 0 phr of silane added to 4.0 phr. Further adding silane beyond this boundary, the HDT seem to be decreased. This observation may be attributed to the silane/moisture induced chain crosslinking or branching as stated in the previous MFI discussion. The rising in the chain molecular mass could improve the HDT of the polymer. Other contribution hypothesis for the improvement of HDT of the fiber reinforce composite with increasing the silane incorporation is the enhancement of the interfacial bonding between polymer matrix and the reinforcement.

Again when compare between the HDT of the composite material obtained from mixing method#I and method#II, it is noticed that the method#II offer the superior HDT than the method#I for both original and cured samples. So, the ability of the excess silane in both methods to degrade the polymer chain as explained earlier could be the main responsibility for the observation.

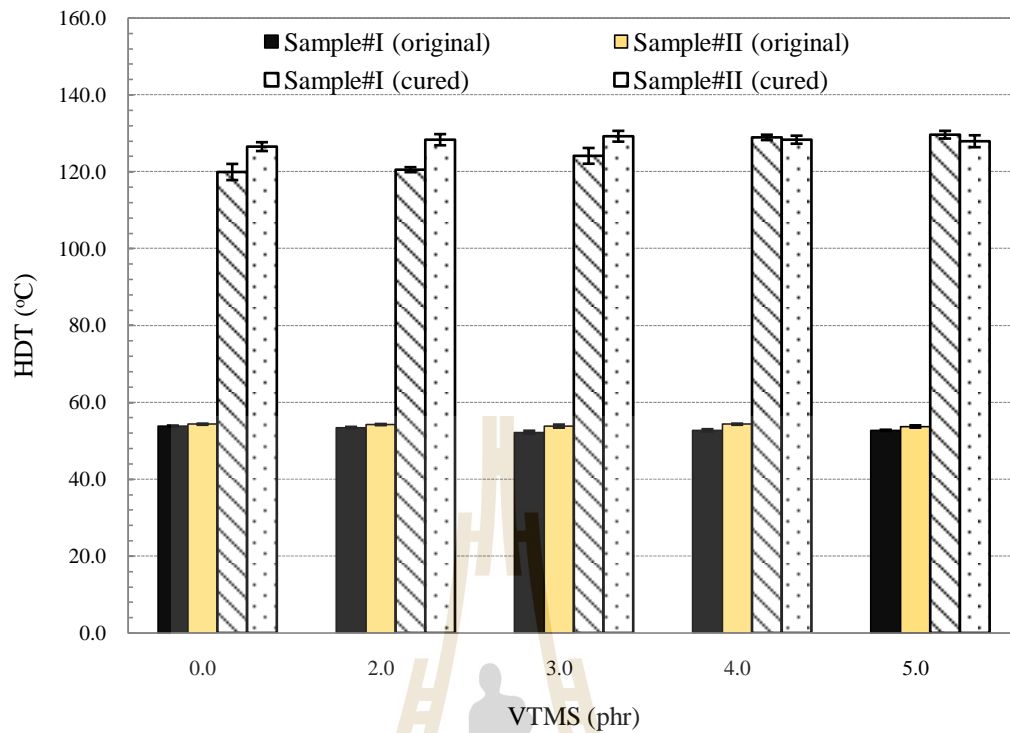


Figure 4.59 HDT of the hybrid composite with VTMS contents.

4.6.3 Impact properties of hybrid biocomposite versus VTMS contents and mixing procedures

Figure 4.60 reveals the tendency of notched impact strengths of the biocomposite sample versus the VTMS contents and also the compounding methods. The figure shows that the impact of the original sample does not depend on the silane addition. However, for the sample underwent sauna incubation, it indicates that it is slightly increased while increasing the silane content. The similar trend is also found for the sample prepared by compounding method#II.

In addition, by comparison between the notched impact strength of the hybrid composite obtained from mixing method#I and method#II, it is observed that the impact value of cured sample, at identical silane content, obtained from method#II

is fractionally higher than the mixing method#I sample. The better in fracture toughness of sample#II can be explained by the direct grafting reaction of the peroxide and silane solution onto ENR chain. The crosslink chemicals solution could react with the vinyl group on epoxidized ENR backbone forming silane grafted rubber. Crosslink reaction would, then, occur during the sauna treatment procedure. In contrast with the mixing method#I, the crossing structure would rather be presented on PLA chain because the crosslink reagents were incorporated in the PLA pellet. As the result, the crosslinked PLA would be more rigid than the crosslinked ENR. Hence, the notched impact value of sample#II were enhanced.

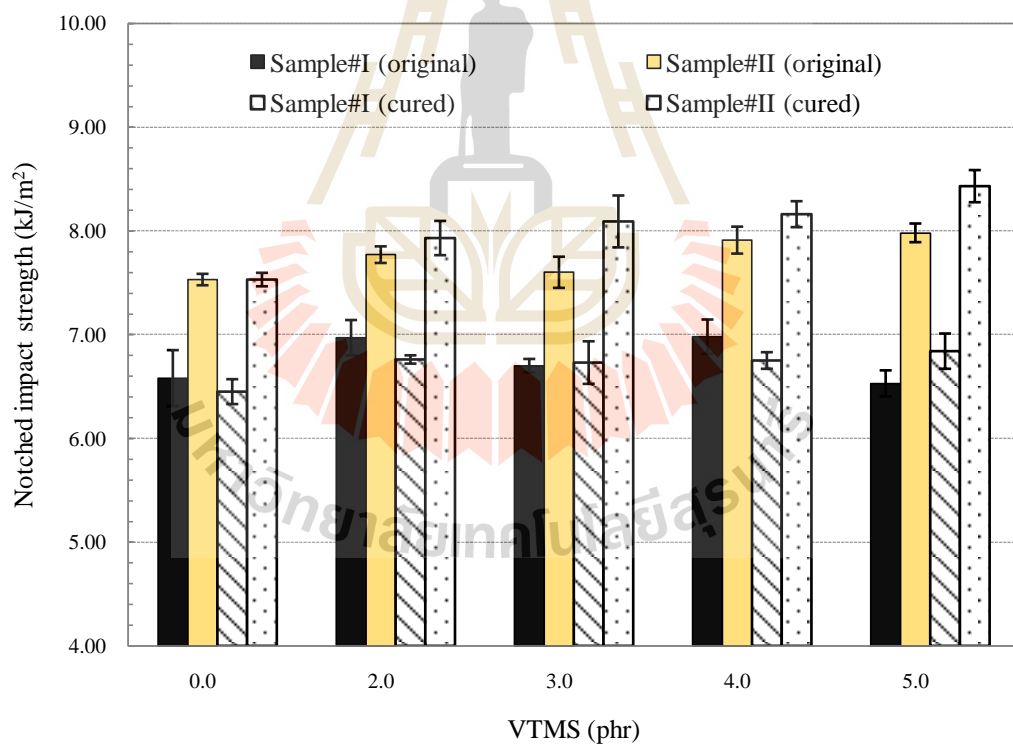


Figure 4.60 Notched impact strength of the hybrid composite with VTMS contents.

For the unnotched impact strength as seen in Figure 4.61, the hybrid composite without silane coupling agent indicates that lowest impact value. Adding silane from 2.0 to 4.0 phr shows the improvement of the unnotched impact value for both sample conditioned and mixing methods. The strength is vastly lowered when further increasing in silane content to 5.0 phr. There is no consensus in term of the improvement of the unnotched impact strength by the sauna incubation and regardless to the silane contents.

When compare those two mixing methods, it is quite ambiguous to verify between the two. Because there is no consensus by using the unnotched impact strength. Nonetheless, by judging the majority, it seems that the unnotched impact strength of the sample mixed from method#II is better than the sample compounded by method#I, especially for the cured sample, at the given silane content.

From the results, it could be hypothesized that the excess of silane, at 5.0 phr, in ENR could further react with PLA chain during melt mixing. As occurred, the thermosetting characteristic could be dominated in the polymer matrix phase. Hence, the unnotched strength would be reduced. Similar explanation would conclude for the difference in mixing procedures.

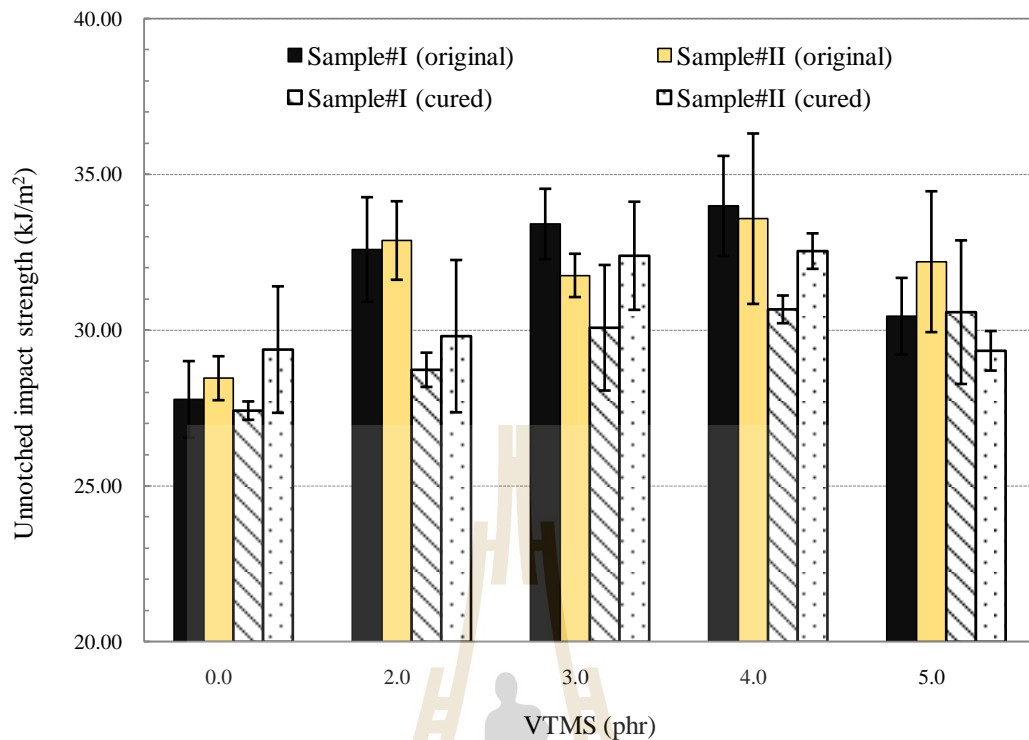


Figure 4.61 Unnotched impact strength of the hybrid composite with VTMS contents.

4.6.4 Flexural properties of hybrid biocomposite versus VTMS contents and mixing procedures

Flexural strength and modulus of hybrid composite are plotted with respect to the silane usage in Figure 4.62 and 4.63, respectively. Figure 4.62 indicates that the flexural strength is decreased by adding silane into matrix phase. However, the flexural strength of silane added composite is increased by the sauna curing. The magnitude of increasing in test value is also direct proportion to the silane content. The elevated in the strength of silane added composite is not enough to complete with the sample without silane addition. It indicates that the more silane in the matrix the

more network structure formed. Hence, the brittle like thermoset polymer would be observed.

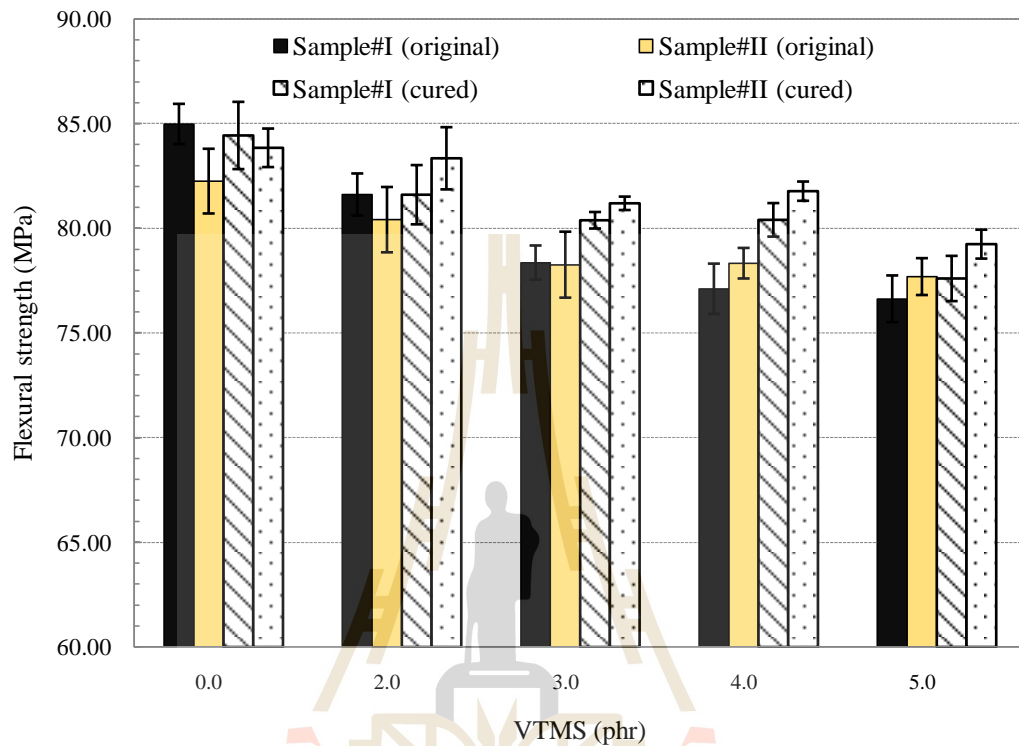


Figure 4.62 Flexural strength of the hybrid composite with VTMS contents.

Similarly, the flexural modulus are likely to decrease by adding silane into matrix phase of the composite, regardless to sample conditioning and mixing procedures. Closer observation, it is seen that the modulus of the original sample is almost constant at the silane content from 3.0 to 5.0 phr.

The flexural strength of the composite prepared by mixing method#II shows the superiority than mixing method#I. But, the contradict trend is found for the modulus. As previously purposed, the hybrid composite having the ENR directly compounded with silane and peroxide solution, method#II, there would be higher in

crosslink density in rubber phase. Vice versa, method#I, network structure is dominated in the polymer matrix. Hence, the higher flexural strength would be observed in the high crosslinked rubber matrix phase than in the network polymer.

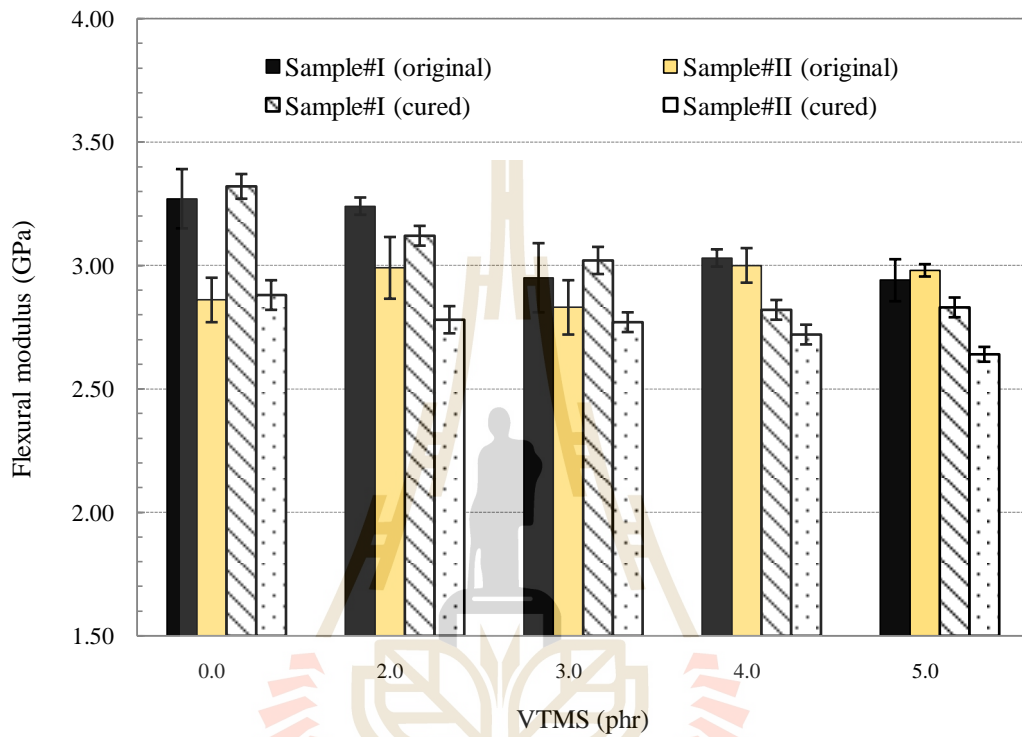


Figure 4.63 Flexural modulus of the hybrid composite with VTMS contents.

4.6.5 Scanning Electron Microscopy (SEM)

Figure 4.64 (a) - 4.64 (d) illustrate the SEM micrograph of the fractured surface obtained from the composites having VTMS content at 5.0 phr and compounded by method#I and method#II, respectively. In case of mixing method#I, Figure 4.64 (a) and 4.64 (c), the fractured surface of the original and cured samples are, what so ever, identical. The SEM traces reflect the toughness properties, both impact and flexural, which were not changed by the sauna treatment. Similar SEM evidences are also found for the samples mixed by method#II. Closer observation between the specimen from mixing method#I and method#II both original and sauna treated ones, there is a few different on the broken surface of the continuous phase. Adding crosslink agent directly onto the ENR50 rubber, method#II, the evidence of tougher material, rougher surface, is observed both original and cured samples, respectively. The observation would explain the higher notched impact result found for the mixing method#II. This SEM investigation would support the statement announced in the previous section that the rubber crosslink induced by mixing method#II enhances the fracture strength of the biocomposite. Vice versa, the thermosetting characteristic derived from PLA chain crosslink via silane/peroxide reaction, mixing method#I, would drawback the ductility of the material. However, in term of the interfacial adhesion between continuous phase and reinforcement, it is hardly seen the marvelous improvement between two those mixing methods. The common phenomenon is that there is lesser fiber pull out on the sample underwent sauna treatment than the one without the incubation process.

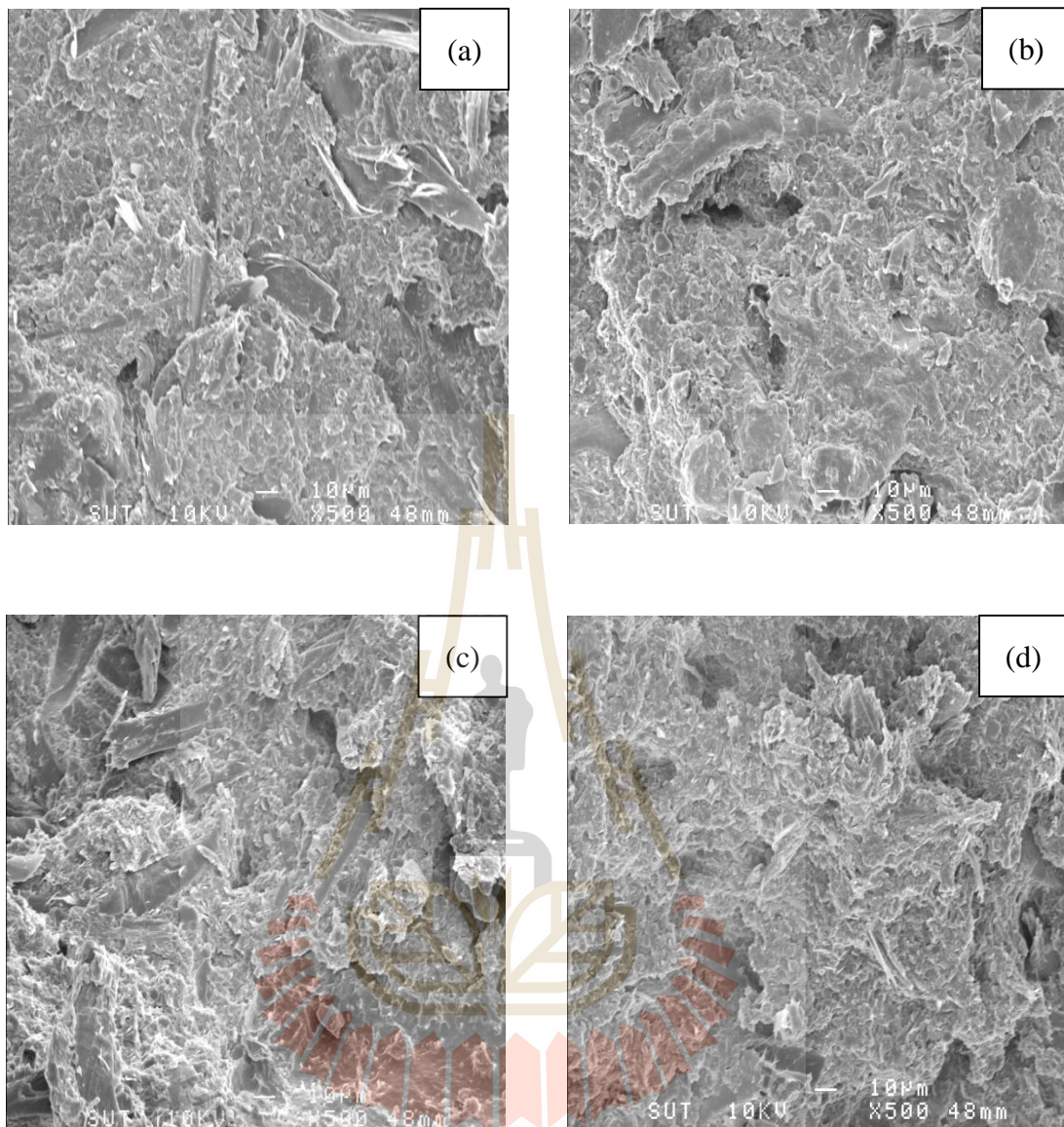


Figure 4.64 SEM micrograph of the hybrid biocomposite having 5.0 phr of VTMS

(a) sample#I (original), (b) sample#II (original),

(c) sample#I (cured) and (d) sample#II (cured).

Taking all the results from the standard testing methods and SEM investigation shown above, some of the statement could be drawn that the melt flow ability of the composite was increased with increasing the VTMS. It could not be differentiated between the HDT of original sample with the silane used but when incubated in sauna oven the HDT was enhanced with respect to the VTMS content. The impact and flexure of the composite obtained is likely to decrease with increasing the silane addition. It was marginally improved by sauna treatment of the sample but not enough to overcome the test value of the sample without silane. The crosslink density of the matrix phase via the radical induced grafted of silane onto the polymer chain was owed as the prime hypothesized to explain the testing outcome.

Mixing the composite by difference routes showed that direct incorporating the crosslink reagents, peroxide/silane onto ENR rubber, method#II, generally give rise to the better properties, especially the toughness. The high crosslink density of the rubber phase by direct mixing, method#II, with peroxide/silane comparing with high network density of polymer phase by direct polymer/peroxide/silane incorporation is the prime suspect for the superiority found.

CHAPTER V

CONCLUSIONS

By employing the statistical approach namely 2^k factorial design of experiment (DOE) to study the effect of EFB fiber, solid epoxy and 3-aminopropyl triethoxysilane content on the properties of the PLA/EFB biocomposite, it is found that fiber content (A) was negative and significantly effect on the MFI and impact strengths of the sample without sauna curing. It was also found that the similar influence on the notched impact strength and flexural strength of the sauna cured composite. But it was the positive effect on the HDT and flexural modulus. Further investigation by varying the amount of solid epoxy in the matrix phase, it was found that adding solid epoxy into the composite matrix had more or less lowered the mechanical properties of the biocomposite. It was also seen that the HDT did not change with the amount of the solid epoxy added. Manufacturing the cotton and EFB hybrid reinforced system; fibers, were explored. The thermal and mechanical properties of the material were improved by increasing the fraction of cotton fiber. However, the flow ability of the compound became insufficient and hence the processability especially by injection molding would become restriction. High stiffness and high L/d ratio of cotton fiber were taken into explanation. Preliminary investigation found that the composite manufactured from PLA reinforced with EFB:cotton hybrid was biologically degraded in the similar manner to the neat PLA. Within the boundary of this research study, the hybrid fiber between EFB and cotton fiber at the weight ratio of 25:75 was selected and was further explored.

Adding talc into the composite provided the improvement on the MFI of the hybrid biocomposite. Decreasing fibers but increasing talc contents, the flow ability of composites was increased. For the effect of moisture residual existed in the sample via the prolong sauna incubation, the test result concluded that there was no dramatically differentiate between the normal and vacuum dried sauna cured samples. Composite with higher talc and low fiber contents has shown the inferior in the mechanical properties. Increasing in the matrix viscosity and hence lower in surface wettability, surface adhesion, would be responsible for the weakness.

The crosslink system; silane/peroxide, using vinyl type silane (VTMS) and DCP was introduced into the PLA matrix of the hybrid reinforced biocomposite. The DOE findings concluded that DCP and silane had no significant effect on the given response properties. In the refinement of VTMS used, it was found that the melt flow ability of the composite was increased with increasing the VTMS. The HDT of sauna cured sample was enhanced by adding more VTMS. The toughness, both impact and flexure, of the composite obtained was likely to decrease with increasing the silane addition. Investigation of the procedures of adding silane/peroxide crosslink system into the composite ingredient during compounding, it was seen that direct incorporating the reagents into the ENR50 was generally given rise to the better properties, especially the toughness, than adding into PLA pellet. The high crosslink density of the rubber phase through the direct polymer/peroxide/silane incorporation compare with high network density of polymer chain was the prime suspect for properties improvement.

In conclusion, there were two main EFB/cotton hybrid reinforced biocomposite formula derived from this research study as summarized in Table 5.1.

Those recipes were resolved from the statistic and direct experimental design approaches. These hybrid composites offered the desired both thermal and mechanical properties.

Table 5.1 Hybrid composite formulations.

Formula ingredient		Weight (g)	
		Hybrid I	Hybrid II
PLA		100	100
Talc		20	20
Cotton fiber		37.5	37.5
EFB fiber		12.5	12.5
ENR50		20	20
Stabilizer		2	2
Solid epoxy		0.4	0.4
Polyester polyols		4	5
Dicumyl peroxide (DCP)		-	0.5
Silane typs	APS (A-1100)	1.75	-
	GPS (A-187)	1.75	-
	VTMS (A-171)	-	2.0

REFERENCES

- Badri, K. H., Othman, Z. B., and Razali, I. M. (2005). Mechanical properties of polyurethane composites from oil palm resources. **Iranian Polymer Journal (English Edition)**. 14: 441-448.
- Beltran, M., and Mijangos, C. (2000). Silane grafting and moisture crosslinking of polypropylene. **Polymer Engineering and Science**. 40: 1534-1541.
- Bax, B., and Mëssig, J. (2008). Impact and tensile properties of PLA/cordenka and PLA/flax composites. **Composites Science and Technology**. 68: 1601-1607.
- Bengtsson, M., and Oksman, K. (2006). Silane crosslinked wood plastic composites: Processing and properties. **Composites Science and Technology**. 66: 2177-2186.
- Bhat, G., Kamath, M. G., Mueller, D., Parikh, D. V., and McLean, M. (2004). **Cotton-based composites for automotive applications**. Paper presented at the Global Plastics Environmental Conference 2004 - Plastics: Helping Grow a Greener Environment.
- Charoensuk, O. (2005). **Evaluation of compounding techniques for short fibers reinforced polycarbonate**. M.Eng. thesis, Suranaree University of Technology, Thailand.
- Cheng, S., Lau, K.-T., Liu, T., Zhao, Y., Lam, P.-M., and Yin, Y. (2009). Mechanical and thermal properties of chicken feather fiber/PLA green composites. **Composites Part B: Engineering**. 40: 650-654.

- Chuayjuljit, S., Soatthiyanon, N., and Potiyaraj, P. (2006). Polymer blends of epoxy resin and epoxidized natural rubber. **Journal of Applied Polymer Science**. 102: 452-459.
- Djidjelli, H., Boukerrou, A., Founas, R., Rabouhi, A., Kaci, M., Farenc, J., et al. (2007). Preparation and characterization of poly(vinyl chloride)/ virgin and treated sisal fiber composites. **Journal of Applied Polymer Science**. 103: 3630-3636.
- Fávaro, S. L., Ganzerli, T. A., de Carvalho Neto, A. G. V., da Silva, O. R. R. F., and Radovanovic, E. (2010). Chemical, morphological and mechanical analysis of sisal fiber-reinforced recycled high-density polyethylene composites. **Express Polymer Letters**. 4: 465-473.
- Graupner, N. (2008). Application of lignin as natural adhesion promoter in cotton fibre-reinforced poly(lactic acid) (PLA) composites. **Journal of Materials Science**. 43: 5222-5229.
- Grubbström, G., and Oksman, K. (2009). Influence of wood flour moisture content on the degree of silane-crosslinking and its relationship to structure-property relations of wood-thermoplastic composites. **Composites Science and Technology**. 69: 1045-1050.
- Hakkou, M., Pétrissans, M., Zoulalian, A., and Gérardin, P. (2005). Investigation of wood wettability changes during heat treatment on the basis of chemical analysis. **Polymer Degradation and Stability**. 89: 1-5.
- Han, C., Bian, J., Liu, H., Han, L., Wang, S., Dong, L., et al. (2009). An investigation of the effect of silane water-crosslinking on the properties of poly(L-lactide). **Polymer International**. 59: 695-703.

- Hegde, R.R., Dahiya, A., and Kamath M. G. (2004). **Cotton fibers** [On-line]. Available: [http://www.engr.utk.edu/mse/pages/Textiles/Cotton fibers.htm](http://www.engr.utk.edu/mse/pages/Textiles/Cotton%20fibers.htm).
- Hornsby, P., Hinrichsen, E., and Tarverdi, K. (1997). Preparation and properties of polypropylene composites reinforced with wheat and flax straw fibres: Part II Analysis of composite microstructure and mechanical properties. **Journal of Materials Science**. 32: 1009-1015.
- Huda, M. S., Drzal, L. T., Mohanty, A. K., and Misra, M. (2006). Chopped glass and recycled newspaper as reinforcement fibers in injection molded poly(lactic acid) (PLA) composites: A comparative study. **Composites Science and Technology**. 66: 1813-1824.
- Huda, M. S., Drzal, L. T., Mohanty, A. K., and Misra, M. (2008). Effect of fiber surface-treatments on the properties of laminated biocomposites from poly(lactic acid) (PLA) and kenaf fibers. **Composites Science and Technology**. 68: 424-432.
- Ismail, H., and Ooi, Z. X. (2010). The effect of epoxidized natural rubber (ENR-50) as a compatibilizer on properties of high-density polyethylene/soya powder blends. **Polymer - Plastics Technology and Engineering**. 49: 688-693.
- John, M. J., and Thomas, S. (2008). Biofibres and biocomposites. **Carbohydrate Polymers**. 71: 343-364.
- Joseph, K., Thomas, S., and Pavithran, C. (1996). Effect of chemical treatment on the tensile properties of short sisal fibre-reinforced polyethylene composites. **Polymer**. 37: 5139-5149.

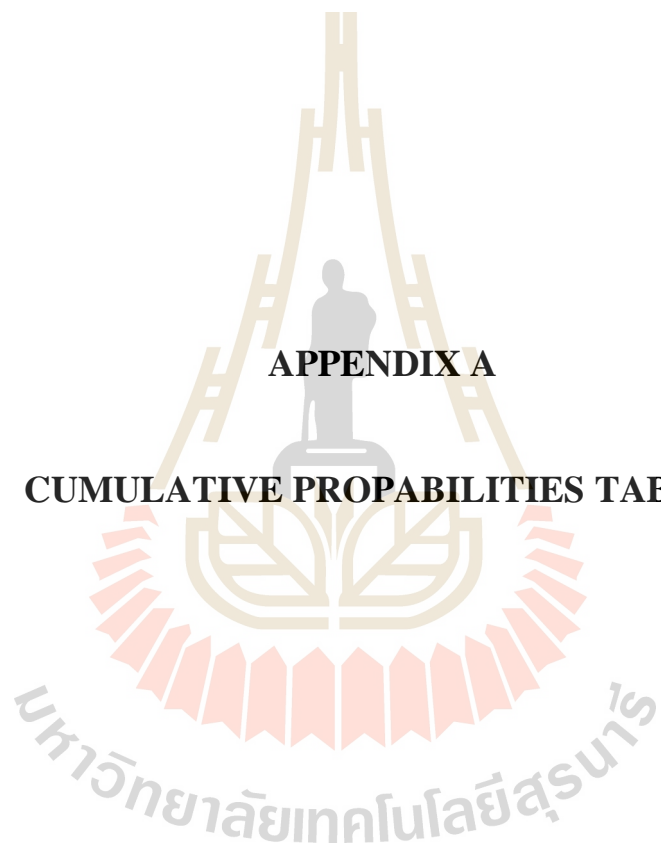
- Kamath, M.G., Bhat, G. S., Parikh, D. V., and Mueller, D. (2005). Cotton fiber nonwovens for automotive composites. **Materials Science and Engineering**. 34-40
- Khalid, M., Ratnam, C. T., Chuah, T. G., Ali, S., and Choong, T. S. Y. (2008). Comparative study of polypropylene composites reinforced with oil palm empty fruit bunch fiber and oil palm derived cellulose. **Materials and Design**. 29: 173-178.
- Khan, R. A., Parsons, A. J., Jones, I. A., Walker, G. S., and Rudd, C. D. (2010). Degradation and interfacial properties of iron phosphate glass fiber-reinforced PCL-based composite for synthetic bone replacement materials. **Polymer-Plastics Technology and Engineering**. 49: 1265-1274.
- Kim, S.-J., Moon, J.-B., Kim, G.-H., and Ha, C.-S. (2008). Mechanical properties of polypropylene/natural fiber composites: Comparison of wood fiber and cotton fiber. **Polymer Testing**. 27: 801-806.
- Kuan, C.-F., Kuan, H.-C., Ma, C.-C. M., and Huang, C.-M. (2006). Mechanical, thermal and morphological properties of water-crosslinked wood flour reinforced linear low-density polyethylene composites. **Composites Part A: Applied Science and Manufacturing**. 37: 1696-1707.
- Lapcik, L., Jindrova, P., Lapcikova, B., Tamblyn, R., Greenwood, R., and Rowson, N. (2008). Effect of the talc filler content on the mechanical properties of polypropylene composites. **Journal of Applied Polymer Science**. 110: 2742-2747.

- Lee, B. H., Kim, H. S., Lee, S., Kim, H. J., and Dorgan, J. R. (2009). Bio-composites of kenaf fibers in polylactide: Role of improved interfacial adhesion in the carding process. **Composites Science and Technology**. 69: 2573-2579.
- Lee, S-H., and Wang, S. (2006). Biodegradable polymers/bamboo fiber biocomposite with bio-based coupling agent. **Composites Part A: Applied Science and Manufacturing**. 37: 80-91.
- Manikandan Nair, K. C., Thomas, S., and Groeninckx, G. (2001). Thermal and dynamic mechanical analysis of polystyrene composites reinforced with short sisal fibres. **Composites Science and Technology**. 61: 2519-2529.
- Meekum, U. (2009). **The development of green composite from natural fibers reinforced poly(lactic acid)**. PTT Co.,Ltd. (Unpublished manuscript).
- Mwaikambo, L. Y., Martuscelli, E., and Avella, M. (2000). Kapok/cotton fabric-polypropylene composites. **Polymer Testing**. 19: 905-918.
- Neppalli, R., Marega, C., Marigo, A., Bajgai, M. P., Kim, H. Y., and Causin, V. (2010). Poly(ϵ -caprolactone) filled with electrospun nylon fibres: A model for a facile composite fabrication. **European Polymer Journal**. 46: 968-976.
- Nyambo, C., Mohanty, A. K., and Misra, M. (2010). Polylactide-based renewable green composites from agricultural residues and their hybrids. **Biomacromolecule**. 11: 1654-1660.
- Parsons, A. J., Ahmed, I., Haque, P., Fitzpatrick, B., Niazi, M. I. K., and Walker, G. S. (2009). Phosphate glass fibre composites for bone repair. **Journal of Bionic Engineering**. 6: 318-323.

- Phinyocheep, P., Saelao, J., and Buzaré, J. Y. (2007). Mechanical properties, morphology and molecular characteristics of poly(ethylene terephthalate) toughened by natural rubber. **Polymer**. 48: 5702-5712.
- Raghu, H., Bose, S., and Mahanwar, P.A. (2006). Effect of particle size of filler on coloration and properties of high density polyethylene. **Journal of Minerals and Materials Characterization and Engineering**. 5: 87-100.
- Ratnam, C. T., Raju, G., and Yunus, W. M. Z. W. (2007). Oil palm empty fruit bunch (OPEFB) fiber reinforced PVC/ENR blend-electron beam irradiation. **Nuclear Instruments and Methods in Physics Research Section B: Beam Interactions with Materials and Atoms**. 265: 510-514.
- Rowell, R.M., Hun, J.S., and Rowell, J.S. (2000). Characterization and factors effecting fiber properties. **Natural Polymers and Agrofibers Composites**. 115-134.
- Rozman, H., Lai, C., Ismail, H., and Ishak, Z. M. (2000). The effect of coupling agents on the mechanical and physical properties of oil palm empty fruit bunch–polypropylene composites. **Polymer International**. 49: 1273-1278.
- Rozman, H. D., Saad, M. J., and Ishak, Z. M. (2003). Flexural and impact properties of oil palm empty fruit bunch (EFB) polypropylene composites the effect of maleic anhydride chemical modification of EFB. **Polymer Testing**. 22: 335-341.
- Rozman, H. D., Tay, G. S., Kumar, R. N., Abusamah, A., Ismail, H., and Mohd, Z. A. (2001). Polypropylene-oil palm empty fruit bunch-glass fibre hybrid composites: a preliminary study on the flexural and tensile properties. **European Polymer Journal**. 37: 1283-1291.

- Rusche, H. (1973). Thermal degradation of wood at temperatures up to 200°C-part I: Strength properties of dried wood after heat treatment. **Holz Roh Werkstoff**. 31: 273-281.
- Schuh, T.G. (2004). **Renewable materials for automotive applications** [On-line]. Available: www.ienica.net/fibresseminar/schuh.html.
- Singh, S., Mohanty, A. K., and Misra, M. (2010). Hybrid bio-composite from talc, wood fiber and bioplastic: Fabrication and characterization. **Composites Part A: Applied Science and Manufacturing**. 41: 304-312.
- Sirisinha, K., and Meksawat, D. (2004). Changes in properties of silane-water crosslinked metallocene ethylene-octene copolymer after prolonged crosslinking time. **Journal of Applied Polymer Science**. 93: 901-906.
- Shelesh-Nezhad, K., and Taghizadeh, A. (2007). Shrinkage behavior and mechanical performances of injection molded polypropylene/talc composites. **Polymer Engineering and Science**. 47: 2124-2128.
- Taylor, J. (2004). **Agricultural fibres for product design and development** [On-line]. Available: <http://jasont.media.mit.edu/papers.html>
- Van Den Oever, M. J. A., Beck, B., and Mëssig, J. (2010). Agrofibre reinforced poly(lactic acid) composites: Effect of moisture on degradation and mechanical properties. **Composites Part A: Applied Science and Manufacturing**. 41: 1628-1635.
- Wan, Y. Z., Wang, Y. L., Li, Q. Y., and Dong, X. H. (2001). Influence of surface treatment of carbon fibers on interfacial adhesion strength and mechanical properties of PLA-based composites. **Journal of Applied Polymer Science**. 80: 367-376.

- Yang, S.-L., Wu, Z.-H., Yang, W., and Yang, M.-B. (2008). Thermal and mechanical properties of chemical crosslinked polylactide (PLA). **Polymer Testing**. 27: 957-963.
- Yu, T., Ren, J., Li, S., Yuan, H., and Li, Y. (2010). Effect of fiber surface-treatments on the properties of poly(lactic acid)/ramie composites. **Composites Part A: Applied Science and Manufacturing**. 41: 499-505.
- Yussuf, A., Massoumi, I., and Hassan, A. (2010). Comparison of polylactic acid/kenaf and Polylactic acid/rise husk composites: The influence of the natural fibers on the mechanical, thermal and biodegradability properties. **Journal of Polymers and the Environment**. 18: 422-429.
- Zhao, Y.-Q., Cheung, H.-Y., Lau, K.-T., Xu, C.-L., Zhao, D.-D., and Li, H.-L. (2008). Silkworm silk/poly(lactic acid) biocomposites: Dynamic mechanical, thermal and biodegradable properties. **Polymer Degradation and Stability**. 95: 1978-1987.
- Zhou, S., Wang, Z., and Hu, Y. (2009). Melt grafting of vinyltrimethoxysilane and water crosslinking of polypropylene/ethylene-propylene diene terpolymer blends. **Journal of Polymer Research**. 16: 173-181.



APPENDIX A

CUMULATIVE PROBABILITIES TABLES

Table A.1 Cumulative probabilities for negative Z-values table.

Z	0.09	0.08	0.07	0.06	0.05	0.04	0.03	0.02	0.01	0
-3.0	0.0010	0.0010	0.0011	0.0011	0.0011	0.0012	0.0012	0.0013	0.0013	0.0013
-2.9	0.0014	0.0014	0.0015	0.0015	0.0016	0.0016	0.0017	0.0018	0.0018	0.0019
-2.8	0.0019	0.002	0.0021	0.0021	0.0022	0.0023	0.0023	0.0024	0.0025	0.0026
-2.7	0.0026	0.0027	0.0028	0.0029	0.0030	0.0031	0.0032	0.0033	0.0034	0.0035
-2.6	0.0036	0.0037	0.0038	0.0039	0.004	0.0041	0.0043	0.0044	0.0045	0.0047
-2.5	0.0048	0.0049	0.0051	0.0052	0.0054	0.0055	0.0057	0.0059	0.0060	0.0062
-2.4	0.0064	0.0066	0.0068	0.0069	0.0071	0.0073	0.0075	0.0078	0.008	0.0082
-2.3	0.0084	0.0087	0.0089	0.0091	0.0094	0.0096	0.0099	0.0102	0.0104	0.0107
-2.2	0.0110	0.0113	0.0116	0.0119	0.0122	0.0125	0.0129	0.0132	0.0136	0.0139
-2.1	0.0143	0.0146	0.0150	0.0154	0.0158	0.0162	0.0166	0.017	0.0174	0.0179
-2.0	0.0183	0.0188	0.0192	0.0197	0.0202	0.0207	0.0212	0.0217	0.0222	0.0228
-1.9	0.0233	0.0239	0.0244	0.0250	0.0256	0.0262	0.0268	0.0274	0.0281	0.0287
-1.8	0.0294	0.0301	0.0307	0.0314	0.0322	0.0329	0.0336	0.0344	0.0351	0.0359

Table A.1 Cumulative probabilities for negative Z-values table (continued).

Z	0.09	0.08	0.07	0.06	0.05	0.04	0.03	0.02	0.01	0
-1.7	0.0367	0.0375	0.0384	0.0392	0.0401	0.0409	0.0418	0.0427	0.0436	0.0446
-1.6	0.0455	0.0465	0.0475	0.0485	0.0495	0.0505	0.0516	0.0526	0.0537	0.0548
-1.5	0.0559	0.0571	0.0582	0.0594	0.0606	0.0618	0.063	0.0643	0.0655	0.0668
-1.4	0.0681	0.0694	0.0708	0.0721	0.0735	0.0749	0.0764	0.0778	0.0793	0.0808
-1.3	0.0823	0.0838	0.0853	0.0869	0.0885	0.0901	0.0918	0.0934	0.0951	0.0968
-1.2	0.0985	0.1003	0.1020	0.1038	0.1056	0.1075	0.1093	0.1112	0.1131	0.1151
-1.1	0.1170	0.1190	0.1210	0.1230	0.1251	0.1271	0.1292	0.1314	0.1335	0.1357
-1.0	0.1379	0.1401	0.1423	0.1446	0.1469	0.1492	0.1515	0.1539	0.1562	0.1587
-0.9	0.1611	0.1635	0.1660	0.1685	0.1711	0.1736	0.1762	0.1788	0.1814	0.1841
-0.8	0.1867	0.1894	0.1922	0.1949	0.1977	0.2005	0.2033	0.2061	0.2090	0.2119
-0.7	0.2148	0.2177	0.2206	0.2236	0.2266	0.2296	0.2327	0.2358	0.2389	0.2420
-0.6	0.2451	0.2483	0.2514	0.2546	0.2578	0.2611	0.2643	0.2676	0.2709	0.2743
-0.5	0.2776	0.281	0.2843	0.2877	0.2912	0.2946	0.2981	0.3015	0.305	0.3085

Table A.1 Cumulative probabilities for negative Z-values table (continued).

Z	0.09	0.08	0.07	0.06	0.05	0.04	0.03	0.02	0.01	0
-0.4	0.3121	0.3156	0.3192	0.3228	0.3264	0.3300	0.3336	0.3372	0.3409	0.3446
-0.3	0.3483	0.352	0.3557	0.3594	0.3632	0.3669	0.3707	0.3745	0.3783	0.3821
-0.2	0.3859	0.3897	0.3936	0.3974	0.4013	0.4052	0.4090	0.4129	0.4168	0.4207
-0.1	0.4247	0.4286	0.4325	0.4364	0.4404	0.4443	0.4483	0.4522	0.4562	0.4602
-0.0	0.4641	0.4681	0.4721	0.4761	0.4801	0.4840	0.4880	0.4920	0.4960	0.5000



Table A.2 Cumulative probabilities for positive Z-values table.

Z	0	0.01	0.02	0.03	0.04	0.05	0.06	0.07	0.08	0.09
0.0	0.5000	0.5040	0.5080	0.5120	0.5160	0.5199	0.5239	0.5279	0.5319	0.5359
0.1	0.5398	0.5438	0.5478	0.5517	0.5557	0.5596	0.5636	0.5675	0.5714	0.5753
0.2	0.5793	0.5832	0.5871	0.5910	0.5948	0.5987	0.6026	0.6064	0.6103	0.6141
0.3	0.6179	0.6217	0.6255	0.6293	0.6331	0.6368	0.6406	0.6443	0.6480	0.6517
0.4	0.6554	0.6591	0.6628	0.6664	0.6700	0.6736	0.6772	0.6808	0.6844	0.6879
0.5	0.6915	0.6950	0.6985	0.7019	0.7054	0.7088	0.7123	0.7157	0.7190	0.7224
0.6	0.7257	0.7291	0.7324	0.7357	0.7389	0.7422	0.7454	0.7486	0.7517	0.7549
0.7	0.7580	0.7611	0.7642	0.7673	0.7704	0.7734	0.7764	0.7794	0.7823	0.7852
0.8	0.7881	0.7910	0.7939	0.7967	0.7995	0.8023	0.8051	0.8078	0.8106	0.8133
0.9	0.8159	0.8186	0.8212	0.8238	0.8264	0.8289	0.8315	0.8340	0.8365	0.8389
1.0	0.8413	0.8438	0.8461	0.8485	0.8508	0.8531	0.8554	0.8577	0.8599	0.8621
1.1	0.8643	0.8665	0.8686	0.8708	0.8729	0.8749	0.8770	0.8790	0.8810	0.8830
1.2	0.8849	0.8869	0.8888	0.8907	0.8925	0.8944	0.8962	0.898	0.8997	0.9015

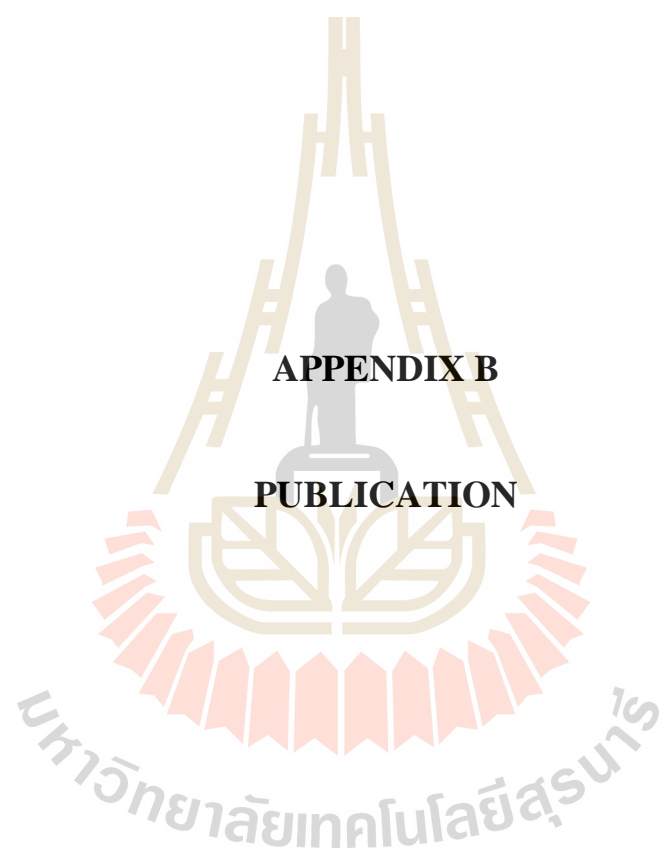
Table A.2 Cumulative probabilities for positive Z-values table (continued).

Z	0	0.01	0.02	0.03	0.04	0.05	0.06	0.07	0.08	0.09
1.3	0.9032	0.9049	0.9066	0.9082	0.9099	0.9115	0.9131	0.9147	0.9162	0.9177
1.4	0.9192	0.9207	0.9222	0.9236	0.9251	0.9265	0.9279	0.9292	0.9306	0.9319
1.5	0.9332	0.9345	0.9357	0.9370	0.9382	0.9394	0.9406	0.9418	0.9429	0.9441
1.6	0.9452	0.9463	0.9474	0.9484	0.9495	0.9505	0.9515	0.9525	0.9535	0.9545
1.7	0.9554	0.9564	0.9573	0.9582	0.9591	0.9599	0.9608	0.9616	0.9625	0.9633
1.8	0.9641	0.9649	0.9656	0.9664	0.9671	0.9678	0.9686	0.9693	0.9699	0.9706
1.9	0.9713	0.9719	0.9726	0.9732	0.9738	0.9744	0.9750	0.9756	0.9761	0.9767
2.0	0.9772	0.9778	0.9783	0.9788	0.9793	0.9798	0.9803	0.9808	0.9812	0.9817
2.1	0.9821	0.9826	0.9830	0.9834	0.9838	0.9842	0.9846	0.985	0.9854	0.9857
2.2	0.9861	0.9864	0.9868	0.9871	0.9875	0.9878	0.9881	0.9884	0.9887	0.989
2.3	0.9893	0.9896	0.9898	0.9901	0.9904	0.9906	0.9909	0.9911	0.9913	0.9916
2.4	0.9918	0.9920	0.9922	0.9925	0.9927	0.9929	0.9931	0.9932	0.9934	0.9936
2.5	0.9938	0.9940	0.9941	0.9943	0.9945	0.9946	0.9948	0.9949	0.9951	0.9952

Table A.2 Cumulative probabilities for positive Z-values table (continued).

Z	0	0.01	0.02	0.03	0.04	0.05	0.06	0.07	0.08	0.09
2.6	0.9953	0.9955	0.9956	0.9957	0.9959	0.9960	0.9961	0.9962	0.9963	0.9964
2.7	0.9965	0.9966	0.9967	0.9968	0.9969	0.9970	0.9971	0.9972	0.9973	0.9974
2.8	0.9974	0.9975	0.9976	0.9977	0.9977	0.9978	0.9979	0.9979	0.998	0.9981
2.9	0.9981	0.9982	0.9982	0.9983	0.9984	0.9984	0.9985	0.9985	0.9986	0.9986
3.0	0.9987	0.9987	0.9987	0.9988	0.9988	0.9989	0.9989	0.9989	0.9990	0.9990





APPENDIX B

PUBLICATION

มหาวิทยาลัยเทคโนโลยีสุรนารี

Publication

Kingchang, P., and Meekum, U. (2011). Design of experiment: Poly(lactic acid) and oil palm empty fruit bunch biocomposite. In **Proceeding of 2nd Research Symposium on Petroleum, Petrochemicals, and Advanced Materials and The 17th PPC Symposium on Petroleum, Petrochemicals, and Polymers.** Bangkok, Thailand.



DESIGN OF EXPERIMENT: POLY(LACTIC ACID) AND OIL PALM EMPTY FRUIT BUNCH BIOCOMPOSITE

Pantip Kingchang^a, Utai Meekum^{a,b}*

^{a)} School of Polymer Engineering, Suranaree University of Technology, Nakhon Rachasima, Thailand
^{b)} Centre for Petroleum, Petrochemical, and Advanced Materials, Bangkok, Thailand

ABSTRACT

Poly(lactic acid) reinforced by oil palm empty fruit bunch(EFB) fiber to form biocomposite was explored. The 2^k design of experiment was used to optimize and quantify the amount of the composite constituents. The affects of material compositions was statistically evaluated. Three parameters, $k = 3$, consisted of EFB fiber(A), silane coupling agent(B) and solid epoxy(C) contents were assigned. The biocomposite samples were compounded on co-rotating twin screw extruder and then test specimen was prepared by injection molding. The specimens were divided into two categories of test samples; original and sauna cured samples. The originals were conducted by annealing at room temperature. The later was achieved by incubating the samples in the moisture saturated oven at 60°C for 12 hrs in order to competition of silane/water crosslink reaction. The flexural properties, impact strength and heat deflection temperature(HDT) were tested and given as the design responds. The morphology was also observed by scanning electron microscopy(SEM). Statistical analysis approach using ANOVA testing showed that the fiber had generally positive effect on HDT. However, silane and solid epoxy showed negative effect on the mechanical properties of composites for samples without sauna healed. However, the mechanical properties were improved after silane/water crosslink in sauna oven. It indicated that the chemical bridging between polymer matrix and fiber via the condensation reaction enhanced the reinforcement/matrix adhesion.

*joom_pantip@hotmail.com

INTRODUCTION

In recent years, as a result of growing environmental awareness, natural fibers have been increasingly used as reinforcement in thermoplastic composite materials because natural fibers have many advantages such as low weight, locally abundant, biodegradable and low cost. Thermoplastic polymers derived from petroleum based, such as PP, HDPE and LDPE are commonly used. However, these polymers do not easily degrade under landfill, resulting in various forms of environmental pollution. PLA is a biodegradable polymer obtained from renewable agricultural raw material, which are initially fermented into lactic acid and then polymerized into long chain molecule[1]. It is degraded by micro organism and it is a thermoplastic polymer with modulate mechanical properties. But commercial application of pure PLA is limited because of its inherent weakness, such as high brittleness and low heat resistance. In this study, the biocomposite based on oil palm empty fruit bunch(EFB) reinforcement and PLA matrix was explored. EFB fibers consist of about 65-77 %wt of cellulose[2, 3]. The EFB fiber is the by-product of oil palm industry and it is dramatically increased as the consumption of oil palm as biodiesel rapidly increased. Thus, considerable research and development efforts have to be undertaken to find usefulness applications for the EFB. However, the main obstacle to be resolved is the compatibility between natural fibers and PLA. To overcome this incompetency, silane was employed as coupling agent to improve the adhesion between the reinforcements and the matrix material, and also moisture crosslink agent via condensation

reaction. Epoxy as compatibilizer was also attempted to enhance the compatibility between reinforcement and matrix phase. The statistical approach by mean of design of experiment(DOE) was constructed to resolve the optimal amount of the constituents used for producing superior properties of biocomposite.

EXPERIMENTAL

A. Material

Poly(lactic acid) grade 2002D was purchased from Nature Works[®] and used as the polymer matrix. The *gamma*-aminopropyltriethoxysilane(A-1100) from Crompton Corporation was used as coupling agents. The solid epoxy, Epotec YD-019, was obtained from Thai Epoxy & Allied Products Co., Ltd. and used as reactive compatibilizer. The epoxidized natural rubber(ENR) having 50% by mol of epoxidation, was supplied by San-Thap International Co.,Ltd and used as composite toughener. Blend of Irganox 1076 and Irgafos 168, supplied from Ciba specialty chemicals, at weight ratio of 1:1 were added as thermal/processing stabilizer. The oil palm empty fruit bunch(EFB) fiber from local palm oil refinery was alkaline and thermal treated in the same manner as described elsewhere[4]. All the chemicals were used as received.

B. Design of experiment

The 2^k factorial design of experiment was elected to optimize and quantify the amount of the composite constitutes. Three parameters, k = 3, consisted of EFB fiber(A), silane(B) and solid epoxy(C) contents were assigned. Each parameter was divided into two levels; high(+1) and low(-1), respectively. In each level, it was also split into two sub levels as shown in table 1. All eight compositions for preparation the biocomposite as the design matrix or the test run were shown in table 2. The statistical analysis, at 95% degree of confidential, was assisted and performed by using commercial available software, Design Expert[™].

Table 1. The parameter and level of DOE.

Parameters	Low level(-1)		High level(+1)	
	Silane(phr)	1.0	3.5	4.0
EFB fiber(phr)	10	25	40	65
Solid epoxy(phr)	0.5	1.5	2.0	3.0

Table 2. Factorial design matrix.

Run	PLA	ENR	Stabilizer	Fiber(A)	Silane(B)	Solid epoxy(C)
1	100	20	2	40(+1)	4.0(+1)	2.0(+1)
2	100	20	2	65(+1)	7.0(+1)	0.5(-1)
3	100	20	2	40(+1)	1.0(-1)	3.0(+1)
4	100	20	2	65(+1)	3.5(-1)	1.5(-1)
5	100	20	2	10(-1)	7.0(+1)	3.0(+1)
6	100	20	2	25(-1)	4.0(+1)	1.5(-1)
7	100	20	2	10(-1)	1.0(-1)	2.0(+1)
8	100	20	2	25(-1)	3.5(-1)	0.5(-1)

C. Fibers preparation

The fiber was soaked in water for overnight. After that, fiber was compressed to remove excess water and then transferred into internal mixer chamber, Haake Rheomix 3000P, at 170°C and ground by using Banbury rotors at the rotors speed of 100 rpm for 15 minutes. The heat treated fiber then was mercerized by constantly boiling in 3%w/v sodium hydroxide solution for

4 hrs. Then the chemical treated fiber was then flooded with water several time until the neutral pH was detected. The heat/chemical treated fiber was finally dried in oven at 80°C until there is no damp moisture detected. Moisture depleted oil palm EBF fibers was eventually treated with silane before used to prepare the composite material. The treatment process was performed by reacting the silane and fiber in the internal mixer at 120°C and rotor speed of 100 rpm for 6 minutes, respectively. The treated fiber was sealed in plastic bag and allowed to rest at room temperature overnight.

D. Composites preparation

The ENR was plasticated on two roll mill and then the solid epoxy was gradually incorporated. After that, the treated fiber was slowly added into the rubber mixture. The rubber/fiber mixture was kneaded until the well mixed ingredient was visualized. The rubber compound was stored at temperature below 0°C in freezer for overnight. Then, solid hard rubber/fiber compound was immediately crushed into small pieces by using motor driven crusher. The self-wiping co-rotating intermeshing twin screw extruder from Brabender model PL2100 was established as mixing equipment. PLA and ground rubber/fiber compound pellets were evacuated in the oven at 80°C for 2 hrs prior to mix. The dried PLA and rubber/fiber were dried blend with heat/processing stabilizer powder in mixing bowl. The pre blended materials was constantly fed into twin screw mixer through the pre calibrated single screw feeder. The biocomposite was obtained by melt mixing at screw speed of 12 rpm and barrel temperature from 150, 160, 170, 180 and 190°C from feeding zone to die zone, respectively. The composite strand was then cooled and coarse ground in motor driven crusher. The test specimen was prepared by injection molding, Tederic, model TRX60c. The injection conditions were achieved at 190°C. The composite test specimens were divided into 2 categories of sample; (i) allowed to annealing at room temperature for overnight and (ii) incubated at 60°C in sealed and moisture saturated oven for 12 hrs. The former was called original and the later called sauna cured sample, respectively

E. Properties measurement and testing

Melt flow index(MFI) of composite was obtained at 2.16/190 according to ASTM D1238. For the flexural properties, they were performed according to ASTM D790 using Instron universal testing machine, model 5565. Notched and unnotched impact strength testing was done in accordance with ASTM D256. Both flexural and impact properties were conducted at room temperature. The ASTM D648 testing with the standard load of 0.455 MPa was followed to measure the heat deflection temperature(HDT) of the sample. Morphology of the fractured surface from the impact test was examined by scanning electron microscope(SEM). The test mentioned test results were used as the statistical responds and analysed by the DOE.

RESULTS AND DISCUSSION

A. DOE analysis

MFI, HDT, flexural and impacts test results and also as responds for DOE are summarized in table 3. It is clearly seen that silane/water reaction via sauna incubation mostly show the better properties than the annealed samples. The observation suggests that the condensation reaction might cause the macro crosslinking in polymer chain or the bridging between fiber and matrix phase to enhance the interfacial bonding. This evidence will be strengthen by the SEM examination later on. Closer investigation by mean of statistical calculation using the DOE

method as described above in order to verifying the main effect of the parameters used on the properties of composite. Begin with the flexural strength as respond, the normal probability against the standardized effects plot is shown in figure 1(a) and 1(b), for original and sauna cured samples, respectively. The plot displays that fiber content(A) and solid epoxy(C) are the greatest negatively(-) and positively(+), effect on flexural strength of both composite samples, respectively. Either or not these parameters are the significant effects on the flexural. They are confirmed by ANOVA testing. The result shows that the designed model with in the assigned parameter levels is significant. Moreover, the fiber content(-A) is significant effects. On the after hand, the epoxy content(C) is not significant effects on the flexural of both origin and sauna cured sample. The outcome indicates that preparing composite at high level of fiber content would give rise to the less stiffness composite than the lower level. Adding epoxy into the compound would enhance the bending strength but with no substantial impact.

Table 3. Result data of original and sauna cured samples.

Run	MFI g/10min	Flexural strength		Flexural modulus		Notched impact		Unnotched		HDT (°C)	
		original	cured	original	cured	original	cured	original	cured	original	cured
1	49.91	42.84	47.33	2.28	2.65	4.27	5.00	10.24	9.19	55.00	59.33
2	38.48	31.72	33.04	2.56	2.50	3.85	4.09	5.94	8.51	53.50	60.67
3	20.84	55.72	52.54	2.54	2.71	4.20	4.96	11.49	13.02	54.00	58.00
4	21.27	42.12	47.37	2.65	2.66	4.60	4.88	10.55	12.49	55.50	65.33
5	79.02	66.69	66.76	2.49	2.45	5.20	6.47	15.62	15.21	55.00	54.00
6	69.81	59.34	60.01	2.52	2.49	5.39	6.13	13.99	12.74	56.17	55.00
7	49.79	66.67	67.58	2.54	2.41	4.60	6.09	12.25	16.17	54.33	53.00
8	45.53	59.09	58.63	2.55	2.49	5.49	6.18	12.30	14.99	54.67	55.67

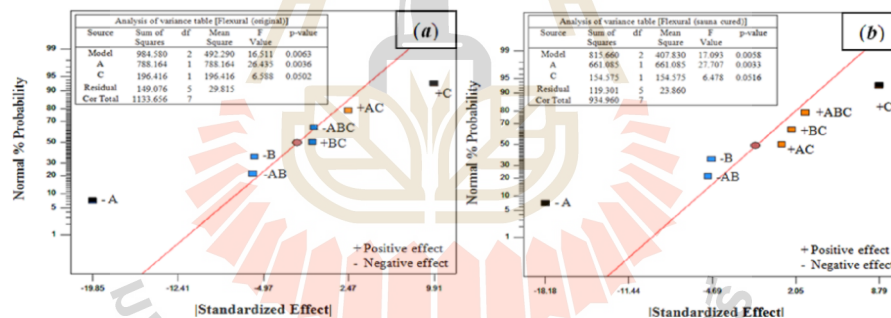


Figure 1. Normal probability plots of flexural strength; (a) original and (b) sauna cured.

Again, for the unnotched impact respond of origin and cured sample analysis, the plots are given in figure 2(a) and 2(b). The original sample result seen that -A and interaction -AB are out of the linear trend line. Similarly, -A and -B are noticed for cured sample. They are possibly indicated as significant parameter for the unnotched impact property. ANOVA testing concludes that the designed models are found to be significant and also the observed parameters except for -B on cured sample. The result strengthen that EFB fiber content play the important role, depressive, on the toughness of composite. Adding silane at low level(-B) onto the fiber does probably help the impact strength of original sample to increase the toughness, (-A)X(-B) = +AB. The exact manner was applied onto the rest of the responds and the significant parameter(s) that effect(s) to

the properties were also concluded. Not only the effect values analysis, the predicted equation, called regressed model, as the function between the respond and significantly designed parameters can also be obtained from the DOE method. Table 4 summarizes the regressed model derived from the design. The given relationships can be roughly used to predict the composite properties that manufactured from the designed parameters at the designed range of levels. Within this study, it is seen that EFB fiber, silane and epoxy do not have the significant effect on flexural modulus and HDT of original composite sample prepared.

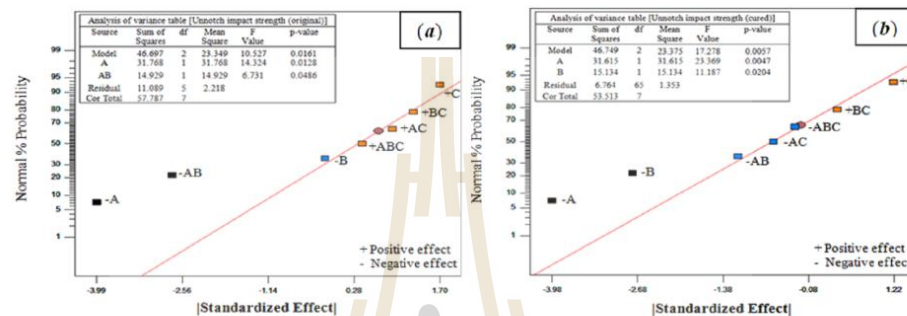


Figure 2. Normal probability plots of unnotched impact strength; (a) original and (b) sauna cured.

Table 4. The predicted regression model of biocomposite derived from ANOVA testing.

	Properties	Regressed models
Original	MFI	$46.83-14.21(A)+12.47(B)$
	Flexural strength	$53.02-9.93(A)+4.96(C)$
	Flexural modulus	No significant model
	Notched impact strength	$4.7-0.47(A)$
	Unnotched impact strength	$11.55-1.99(A)-1.37(AB)$
	HDT	No significant model
Sauna cured	Flexural strength	$54.16-9.09(A)+4.40(C)$
	Flexural modulus	$2.54+0.085(A)-0.023(B)-0.032(AB)+0.038(AC)$
	Notched impact strength	$5.47-0.74(A)$
	Unnotched impact strength	$12.79-1.99(A)-1.38(B)$
	HDT	$57.63+3.21(A)-1.54(C)+0.96(BC)+0.54(ABC)$

B. Scanning electron microscopy(SEM)

The fractured surface SEM photographs obtained from notched specimens of Run#2 and Run#5 are shown in figure 3(a)-3(d) for the original and sauna cured, respectively. Composite derived from Run#2 formula, at high fiber and silane but low epoxy contents, shown the relatively lowest test values. However Run#5, at low fiber and high silane and epoxy contents, manifested the highest test value, especially impact properties. Figure 3(a) illustrates large hole on the matrix surface which is the evidence of fiber pull-out, indicated inferior in interface bonding, that lead to lower the toughness of the sample. Sauna curing of the sample, as seen in figure 3(b), can increase the adhesion between fiber and matrix via the silane/water condensation reaction. That give rise to the marginally increase in the fracture toughness. By decreasing the fiber content but increasing in silane and epoxy as seen in figure 3(c) to 3(d), there is an evidence for fiber

debonding, better interfacial strength, and also higher in impact strengths for both original and cured samples, respectively. The SEM results review that increasing in silane coupling/crosslink agent and epoxy compatibilizer could enhance the surface adhesion between fiber and matrix. However, by mean of statistical data, these two parameters do not guarantee that the toughness of the composite do increase in the same manner. It is because the fiber content plays the major and significant role in the mechanical properties of the biocomposite. The further investigation for fine tuning the parameters and also modifying the composite constituent are unavoidably.

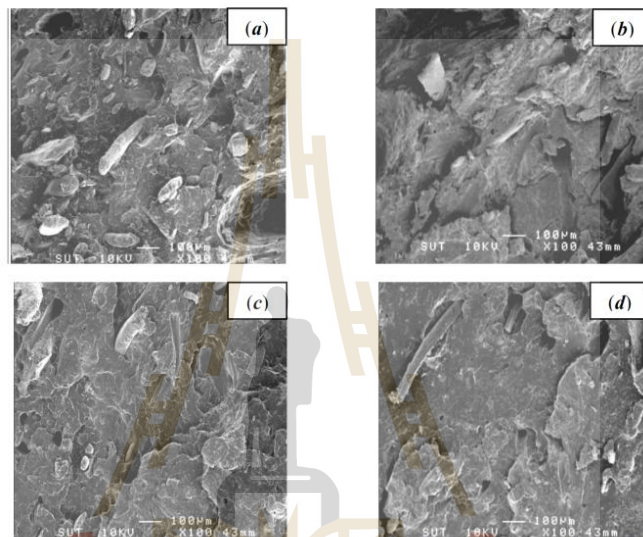


Figure 3. SEM micrograph of biocomposite (a) Run#2(original), (b) Run#2(cured), (c) Run#5(original) and (d) Run#5(cured) at X100.

CONCLUSIONS

Biocomposite from PLA and EFB palm fiber adding as silane as coupling agent and solid epoxy as compatibilizer was manufactured. It found that sauna cured via silane/water reaction does fractionally improved the thermal and mechanical properties of the composite via the enhancement of interfacial adhesion between PLA matrix and fiber. The statistical method by mean of DOE reviewed that fiber content had importantly and significantly effect on the respond properties. Adding too high content would lower the properties. Silane does not clearly has great influence on the performance of the material. Further investigations are required.

REFERENCES

- [1] Cheng, S. et al. (2009) Composites Part B.40, 650-654.
- [2] Khalid, M. et al. (2008) Materials and Design. 29, 173-178.
- [3] Rozman, H. et al. (2000) Polymer International. 49, 1273-1278.
- [4] Ahmad, A. et al. (2009) Composites Part B. 40, 601-606.

BIOGRAPHY

Miss. Pantip Kingchang was born on January 11, 1986 in Chaiyaphum, Thailand. She finished high school from Satri Chaiyaphum School in 2004. She earned her undergraduate degree in Chemical Engineering at King Mongkut Institute's Technology of Ladkrabang (KMITL) in 2008, before attended her Master's degree in Polymer Engineering at School of Polymer Engineering, Suranaree University of Technology (SUT). During her graduate study, she got a research assistant scholarship from Center of Excellence on Petrochemical and Materials Technology. Her research was about oil palm empty fruit bunch/cotton hybrid fibers reinforced poly(lactic acid) composites. In the period of her study, she presented one poster presentation entitle: "Design of experiment: poly(lactic acid) and oil palm empty fruit bunch biocomposite" at 2nd Research Symposium on Petroleum, Petrochemicals, and Advanced Materials and The 17th PPC Symposium on Petroleum, Petrochemicals, and Polymers in Bangkok, Thailand.